"IN-SILICO AND MOLECULAR CHARACTERIZATION OF YSL1 GENE IN WHEAT"

BY

SOURAV PANIGRAHI

Master of Science (Agriculture)

In

Agricultural Biotechnology

DEPARTMENT OF AGRICULTURAL BIOTECHNOLOGY & MOLECULAR BIOLOGY

DR. RAJENDRA PRASAD CENTRAL AGRICULTURAL UNIVERSITY
PUSA (SAMASTIPUR) – 848125, INDIA

2019

Reg. No. – M/AB/201/2017-18

"IN-SILICO AND MOLECULAR CHARACTERIZATION OF YSL1 GENE IN WHEAT"

BY

SOURAV PANIGRAHI

A THESIS SUBMITTED TO THE DR. RAJENDRA PRASAD CENTRAL AGRICULTURAL UNIVERSITY, PUSA IN PARTIAL FULFILLMENT OF THE REQUREMENTS FOR THE AWARD OF THE DEGREE OF

Master of Science (Agriculture)

In

Agricultural Biotechnology

DEPARTMENT OF AGRICULTURAL BIOTECHNOLOGY & MOLECULAR BIOLOGY

DR.RAJENDRA PRASAD CENTRAL AGRICULTURAL UNIVERITY PUSA (SAMASTIPUR) – 848125, INDIA

2019

Reg. No. – M/AB/201/2017-18

Dedicated to Science

✍... *Sourav Panigrahi*

DEPARTMENT OF AGRICULTURAL BIOTECHNOLOGY & MOLECULAR BIOLOGY
COLLEGE OF BASIC SCIENCES & HUMANITIES
DR. RAJENDRA PRASAD CENTRAL AGRICULTURAL UNIVERSITY
PUSA (SAMASTIPUR) - 848125, INDIA

Dr. RAJEEV KUMAR
Assoc. Prof. -cum-Sr. Scientist

Dated..27./..12./..2019.

Certificate

This is to certify that the thesis entitled **"In-Silico and Molecular Characterization of YSL1 gene in Wheat"** submitted by **Mr. SOURAV PANIGRAHI** in the partial fulfillment of the requirements for the award of the degree of **MASTER OF SCIENCE (AGRICULTURE) IN AGRICULTURAL BIOTECHNOLOGY** of Dr.Rajendra Prasad Central Agricultural University, Pusa (Samastipur), Bihar is a record of **bona fide** research work carried by him under my supervision and guidance.

The results embodied in this thesis have not been submitted to any other university or institute for the award of any degree or diploma. The assistance, facilities and sources of information have been duly acknowledged.

Rajeev Kumar
27/12/2019.

(Dr. RAJEEV KUMAR)
Major Advisor & Chairman
Advisory Committee

ENDORSED

10.01.2020.

(Dr. HARSH KUMAR)
(Head)
Department of AB & MB
R.P.C.A.U. Pusa, Samastipur

Certificate

We, the undersigned members of Advisory Committee of **Mr. SOURAV PANIGRAHI**, a candidate for the degree of **MASTER OF SCIENCE (AGRICULTURE) IN AGRICULTURAL BIOTECHNOLOGY**, have gone through the manuscript of the thesis and agree that the thesis entitled **"IN-SILICO AND MOLECULAR CHARACTERIZATION OF YSL1 GENE IN WHEAT"** may be submitted in the partial fulfillment of the requirements for the degree.

Rajeev Kumar 27/12/2019.

(Dr. RAJEEV KUMAR)
Associate Professor -cum- Sr. Scientist
Department of AB & MB
Chairman Advisory committee

MEMBERS OF THE ADVISORY COMMITTEE:

1. Harsh Ku 27.12.19.
(Dr. HARSH KUMAR)
Professor & Head
Department of AB & MB

2. 27/12/2019
(Dr. SATISH KUMAR SINGH)
Associate Professor -cum- Sr. Scientist
Department of PB&G

3. 27/12/2019
(Dr. MAHESH KUMAR)
Assistant Professor -cum- Scientist
Department of SMCA

4. Santosh Kr Singh 27/12/19
(Dr. SANTOSH KUMAR SINGH)
Assistant Professor -cum- Scientist
Department of Soil Science

5. SP Singh 27/12/19
(Dr. S.P. SINGH)
Professor & Head
Department of Entomology
(Nominee of Director of Education)

Certificate

This is to certify that this thesis entitled **"IN-SILICO AND MOLECULAR CHARACTERIZATION OF YSL1 GENE IN WHEAT"** submitted by **Mr. SOURAV PANIGRAHI** in partial fulfillment of requirements of the degree of **MASTER OF SCIENCE (AGRICULTURE) IN AGRICULTURAL BIOTECHNOLOGY** of Dr. Rajendra Prasad Central Agricultural University, Pusa (Samastipur) has been examined and approved on ..12../..03./2020

EXTERNAL EXAMINER

Rajeev Kumar 12/03/2020

(Dr. RAJEEV KUMAR)
Associate Professor -cum- Sr. Scientist
Department of AB & MB
Chairman Advisory committee

MEMBERS OF THE ADVISORY COMMITTEE:

12.03.2020

1. **(Dr. HARSH KUMAR)**
Professor & Head
Department of AB & MB

12/03/2020

2. **(Dr. SATISH KUMAR SINGH)**
Associate Professor -cum- Sr. Scientist
Department of PB&G

12/03/2020

3. **(Dr. MAHESH KUMAR)**
Assistant Professor -cum- Scientist
Department of SMCA

12/03/2020

4. **(Dr. S. P. SINGH)**
Assistant Professor -cum- Scientist
Department of Soil Science

12/03/2020

5. **(Dr. A. K. MISHRA)**
Professor & Head
Department of Entomology
(Nominee of Director of Education)

12.03.2020

(Dr. HARSH KUMAR)
(Head)
Department of AB & MB

Acknowledgement

I express my immense gratitude to my major advisor Dr. Rajeev Kumar, Assoc. Professor (Dept. of AB&MB), Faculty of Basic Sciences and Humanities, for his guidance, parental care, and valuable suggestion. He gave me a good direction to start work and to complete my research and providing me with opportunities to develop skills and techniques in molecular biology with his knowledge, long experience, and attentive teaching. He has helped me all throughout the period of my work in more ways than any advisor could do. I am greatly indebted for receiving his kindness and concern.

It gives me immense pleasure to convey my sincere gratitude towards the esteemed members of my advisory committee: Dr. Harsh Kumar, University Professor, Head of Dept. (AB&MB), Dr. Satish Kumar, Assist Professor (Dept. of PBG), Dr. Santosh Kumar Singh, Asst. Professor (Dept. of Soil Science), Dr. Mahesh Kumar (Dept. of SMCA) and Dr. S.P. Singh, University Professor cum Senior Scientist, Nominee of Director of Education (Dept. of Entomology) for their valuable suggestions and guidance rendered throughout the course of this investigation.

I would like to thank Dr. S. R. Choudhary, Dean of Faculty of Basic Sciences and Humanities, for letting me work till well after closing time and staying back with Rajeev sir just to let me complete my research work every day.

I am highly thankful to Dr. M. Kumar, Uni. Professor (Dept. of AB&MB) and Dr. V.K. Sharma, Assoc. Professor (Dept. of AB&MB) for their sincere guidance valuable suggestions. Heartiest thanks to the faculties of the Department of Agricultural Biotechnology and Molecular Biology for their timely help and willing cooperation.

I am also thankful to all the non-teaching staff members especially, Jai Shankar Ji, Mahto Ji, Deepak Bhaiya, Rupak Bhaiya, Pappu Bhaiya of the Dept. of AB & MB for their immense help during research work. I would also like to extend my heartfelt gratitude to Vipul sir and Shweta ma'am for lending me a helping hand and most needed advices during my period of work in the Genetic Transformation Laboratory.

I am deeply indebted to all my batch mates- Rahul, Praphull, Kanchan, Anant, and Mahi, seniors and juniors for their cooperation, moral support, help, continued affection and unending encouragement and providing a congenial atmosphere in the laboratory during the course of this research work. I will always cherish the moments I shared with them.

A special thanks to my family. Words cannot express how grateful I am to my father, my mother and my cousins for all of the sacrifices that you have made on my behalf. Your prayer for me was what sustained me thus far. I would never be able to pay back the love and affection showered upon by my parents.

I would also like to extend my heartfelt gratitude to the Doctors of TMH, Mumbai and Sparsh Hospital, Bhubaneswar for enabling me to live my life as I am today and allowing me the opportunity to work while in the process of treatment.

Place: ***Pusa***

Date: 27.12.2019

Sourav Panigrahi

(Sourav Panigrahi)

◈◈◈

DR. RAJENDRA PRASAD CENTRAL AGRICULTURAL UNIVERSITY, PUSA (SAMASTIPUR), BIHAR - 848125

Name of the student	:	**Sourav Panigrahi**
Admission No. / Registration No.	:	**M/AB/201/2017-18**
Major Advisor	:	Dr. Rajeev Kumar
Degree to be awarded	:	M.Sc. (Ag) Agricultural Biotechnology
Major subject	:	Agricultural Biotechnology
Minor subject	:	Plant Breeding & Genetics
Year	:	2019
Total number of pages of Thesis	:	78+i-x (Bibliography)
Title of the Research	:	**"In-Silico and Molecular Characterization of YSL1 gene in Wheat"**

ABSTRACT

Wheat is the staple food for the majority of people in the world and thus forms an important component of human nutrition and hence its bio-fortification concerning mineral nutrients is a major concern in the scientific world. In this study, the biofortification of wheat with respect to grain Fe and Zn content has been taken into consideration. Twenty-five wheat genotypes were sown under normal and late sown conditions (heat stress). Estimation of Fe and Zn content in wheat grains was done by AAS after wet digestion by Nitric acid: Perchloric acid:: 1:3. The data about Fe and Zn content in grains of wheat sown under normal and late conditions were analyzed statistically and it was found that there was a reduction of Fe and Zn content in the late sown than the normal sown conditions in most of the genotypes under study. Contrarily, 5 genotypes showed increased Fe accumulation and seven genotypes showed increased Zn accumulation in wheat grains under late sown condition, thus exhibiting negative HSI values. This distribution of Fe and Zn content over two dates of sowing was subjected to cluster analysis and were classified into three groups Fe content and 4 groups based on Zn content in seed.

The YSL gene family plays an important role in Fe and Zn homeostasis into the grains. In this study, all 63 members of the YSL gene family were identified in the wheat genome. Out of all the TaYSL genes, TaYSL2, in particular, was characterized in silico and was found to be expressed in the spike and involved directly in metal-NA loading into the seeds. Three homeologous copies of the gene TaYSL2 namely TaYSL2-6A, TaYSL2-6B and TaYSL2-6D, were identified on the 6th chromosome of each of the three genomes. 6 introns and 7 exons were found in each of the homeologous copies of the gene. In-silico expression of TaYSL2-6A increased many folds under prolonged drought conditions, TaYSL2-6B increased many folds under heat stress and combined stress of heat and drought increases the expression of TaYSL2-6B to many folds and TaYSL2-6D significantly. TaYSL2 gene was taken up

for molecular characterization using gene-based genome-specific primers as well as gene-based SSRs primer in 12 genotypes selected from the varied Fe and Zn content data. Amplification was obtained successfully in all the designed primers. A total of 67 alleles including 37 unique alleles, were obtained from all the primers. The PIC value of primers ranged from 0.542 to 0.904. Maximum polymorphism was observed in B genome followed by A and D genomes respectively. Dice's similarity coefficient computed from the molecular data analysis ranged from 0.821 to 0.672. Based on the similarity coefficient, the genotypes were classified into 4 clusters and were successfully correlated with the Fe and Zn content data.

◊◊◊

ABBREVIATIONS

AB&MB :Agricultural Biotechnology& Molecular Biology	NCBI**:** National Centre for Biotechnology Information
a.a. : amino acid	nt: nucleotides
Bp: Base pairs	NaCl**:** Sodium chloride
BLAST: Basic local alignment search tool	OPT : Oligopeptide Transporter
CBS & H**:** College of Basic Sciences and Humanities	% : Percentage
CDS **:** Coding Sequence	pH: Power of Hydrogen
CTAB: Cetyl tri-methyl ammonium bromide	PCR **:** Polymerase Chain Reaction
DNA : Deoxyribonucleic acid	PHYRE : Protein Homology/AnalogY Recognition Engine
dNTP : Deoxyribonucleotide triphosphate	RPKM : Reads Per Kilobase of transcript, per Million mapped reads
DRPCAU **:** Dr**.** Rajendra Prasad Central Agricultural University	rpm **:** Revolution per minute
° C: Degree Celsius	RNase A**:** Ribonuclease A
et al. **:** Et alli	R: Reverse
EDTA**:** Ethylene di-amine tetra acetic acid	i.e.: That is
EtBr: Ethidium Bromide	TAE: Tris Acetic EDTA
Fig. **:** Figure	TE: Tris EDTA
e.g. **:** For example	TBE**:** Tris-Borate EDTA
F: Forward	Tris**:** Tris (hydroxymethyl) Aminomethane
FPKM : Fragments Per Kilobase of transcript per Million mapped reads	Tm: Melting temperature
GTL: Genetic Transformation Lab	µg : Microgram
HCl: Hydrochloric acid	µl: Micro-litre
HD : Heading	U. V.**:** Ultraviolet
IWGSC : International Wheat Genome Sequencing Consortium	U/ µl: Unit per micro litre
J: Journal	v/ w: volume per weight
Kb: Kilo base pairs	w/ v: weight per volume
mins.**:** Minutes	YASARA : Yet Another Scientific Artificial Reality Application
$MgCl_2$: Magnesium Chloride	YSL: Yellow stripe 1 like

CONTENTS

LIST OF TABLES

LIST OF FIGURES

CHAPTER - I

INTRODUCTION

I INTRODUCTION

Bread wheat (*Triticum aestivum* L.) is hexaploid with three genomes A, B, and D. The haploid DNA content of hexaploid wheat (n=3x=21, ABD) is $1.7x10^{10}$ bps (Amuruganathan and Earle, 1991). Wheat is one of the most important cereals crops originated from southwest Asia but now cultivated worldwide. It belongs to the genus Triticum of the family Poaceae (Gramineae). It is cultivated as a staple crop in the greater part of the world. World wheat production stands at 771.7 million tonnes in a global area of 218.5 million ha for the year 2017 (FAOSTAT, 2018). India stands at 2nd position in wheat production in the world, and in the year 2017, wheat production was 98.51 Million Tonnes. (Directorate of Economics & Statistics). The world's major bread wheat-producing areas include northern China, northern India, Northern USA, Southern Canada, Europe, Russia, Latin America and Africa (Kole,2006).

Fe plays a key role in electron transfer in both photosynthetic and respiratory reactions in chloroplasts and mitochondria. Although abundant mineral in soils, Fe is sparingly soluble under aerobic conditions at high soil pH and exists mainly as oxidized insoluble Fe(III) compounds. Consequently, plants grown on calcareous soils often exhibit severe chlorosis due to Fe deficiency, which results in reduced crop yields (Marschner, 1995). Zn plays an important role in plant metabolism by stabilization of ribosomal fractions, synthesis of cytochrome, activation of enzymes involved in carbohydrate metabolism, protein synthesis, maintenance of cellular membrane integrity, influencing auxin synthesis, and pollen formation. The regulation and maintenance of the gene expression required for the tolerance against environmental stresses in plants such as the capacity for water uptake and transport are Zn dependent. It seems to reduce the adverse effects of heat and salt stress for short periods.

Iron (Fe) and Zink (Zn) are vital for human health. About 60-70% of Fe in our body is present in haemoglobin and found in circulating erythrocytes whereas another 10% is present in the form of myoglobin, cytochromes, and iron-containing enzymes. The remaining 20-30% of surplus Fe is stored as ferritins and hemosiderin in hepatocytes and reticuloendothelial macrophages in healthy individuals. Zn is needed for the proper working of the defense (immune) system, plays an important role in

cell division, cell growth, wound healing, and the breakdown of carbohydrates. Zn also protects the prostate gland from prostatitis and prostatic hypertrophy in males. It helps in maintaining sperm count and mobility and normal levels of serum testosterone.

Thus, mineral nutrition is one of the most critical aspects of nutrition security. More than 3 billion people worldwide are affected by Zn deficiency. More than 47% of pre-school children globally show various symptoms related to Fe deficiency, such as impaired physical growth, mental growth, and learning capabilities. Micronutrients Fe and Zn deficiency result from the low amount of available micronutrients in various plant products such as cereals, pulses, etc., which form a part of the staple diet for the people. Wheat is the staple food for more than half of the population of the world.

For improving the mineral content in food, we must know the mechanisms involved in its uptake and storage of micronutrients in seeds. Under normal conditions, most of the Fe and Zn are absorbed and transported into the plants by mass flow under low pH. According to the mechanisms of metal (especially Fe) take up in plants, particularly under stress conditions, the plants are divided into two categories:

- Strategy I plants
- Strategy II plants

All higher plants, except for the graminaceous group, involve the expression of IRT and FRO genes in roots by transcription factor FER. They take up Fe using ferric-chelate reductases (FROs) to reduce Fe(III) to Fe(II), which is subsequently taken up by ferrous Fe transporters (IRTs). For these events to occur, the soil must have low pH, which is achieved by an H^+ATPase coded by the HA-1 gene. (Eide *et al.*, 1996; Vert *et al.*, 2002; Robinson *et al.*, 1999).

Alternatively, graminaceous plants Involve expression of PS (IDS2) and their release into the soil. The roots secrete Fe chelators of mugineic acid family phytosiderophores (MAs) from their roots via Transporter of MAs (TOM1) to solubilize Fe in the rhizosphere (Takagi, 1976; Mori, 1999). Graminaceous plants then take up Fe and Zn as Fe(III)–PS and Zn-PS complexes from the rhizosphere through the action of Yellow Stripe 1 (YS1) transporters and Fe and Zn transporters

IRTs and ZRTs at the plasma membrane (Mihashi *et al.* 1989). These are controlled by transcription factors like IRO2, IDEF-1&2. As an exception, Rice can transport minerals into the plant body by both strategies.

Zn uptake by the plants has been less studied than that of Fe uptake. Nevertheless, it has been seen that Zn and Cd are transported throughout the plant xylem and into the phloem in mineral form in the same mechanism. ZIP genes are expressed in the roots which take up the Zn from the rhizosphere. Various members of the ZIP family and HMA genes of the P^+ ATPase family, as well as a few members of the IRT family, are expressed in various parts of the plant shoots and have been shown involved in the translocation of Zn in the plant shoots. Although, in recent years, the discovery of various mineral chelators such as NA, which is a precursor of phytosiderophores, has shed light on the deposition of minerals such as Fe, Zn, Mn, etc., into the seed. This loading of micronutrient-chelates into the seeds is carried out by the YSL genes.

Discovered in Maize and subsequently in other plants such as rice, arabidopsis, barley, etc., the orthologs of the gene YS1 are present all over the plant metal transport system and are involved in metal homeostasis in plants. They form a family of genes called YSL genes. The loading of minerals Fe, Zn, and Cu into the seeds is by remobilization of the minerals from senescent leaves to the developing seeds in wheat (Hill, 1980; Hocking, 1994).

In Arabidopsis, 8 AtYSL genes have been reported. Out of which, 5 have been well characterized with respect to their nucleotide and protein sequence, tissue and developmental stage-specific expression profiling. Further, functional analysis of the genes was done by cloning them in the yeast and introducing mutations in the genes rendering them non-functional. The investigations above have made them the best-studied YSL genes suitable for the classification of various YSL genes and to find orthologues in various other crops, in this case, wheat.

AtYSL4 and 6 are expressed in vacuoles and are responsible for the storage of micronutrients and making them available to the embryo during germination. Whereas, AtYSL1, AtYSL2 & AtYSL3 code for plasma membrane protein and are responsible for the loading of micronutrients into the seed. Metal-NA transporters

YSL1 and YSL3 were found to be essential in the remobilization of minerals from senescent leaves towards seed development (Waters *et al.*, 2006).

YSL1 appears to be expressed preferentially in xylem parenchyma cells, whereas YSL3 expresses in phloem companion cells. Their expression help in loading meta-chelates from senescent leaf to xylem and then from xylem to phloem. Such a xylem-to-phloem exchange would reconcile a xylem-associated expression with the observed phloem-associated phenotype, which may be due to lack of remobilization from senescent tissue or defect in seed filling (Le Jean *et al.*, 2005). AtYSL1 is highly expressed in the anther filament. After anther dehiscence, AtYSL1 promoter activity increases in senescing stamens (Le Jean *et al.*, 2005), indicates the remobilization of metals involving AtYSL1.

In seeds, AtYSL1 and AtYSL3 are required to maintain the amount of Fe, Zn and Cu as well as NA (Le Jean *et al.*, 2005; Waters *et al.*, 2006), which supports the view that these metals are delivered to the seeds or absorbed by the developing embryo as NA–metal complexes. It is supposed that for the filling of seeds, the xylem path is interrupted in favour of a symplastic movement. It has been proposed that these genes play an important role in circulating metals from the xylem to the phloem, i.e., from an apoplastic to a symplastic path.

Rice, belonging to the Poaceae family, is more closely related to wheat than arabidopsis. In rice, 18 OsYSL genes have been reported, out of which 5 genes, namely, OsYSL2, OsYSL9, OsYSL15, OsYSL16 & OsYSL18, have been well characterized which codes for plasma membrane proteins responsible for uptake and transport of minerals throughout the plant. OsYSL15 is involved in Fe uptake and distribution throughout the plant, but it is not preferentially expressed only in seeds. OsYSL16 & OsYSL18 are expressed only in roots. Most of the OsYSLs are yet to be well characterized, and thus, their tissue-specific expression, particularly in the reproductive organs, is not yet known. Among the well-characterized OsYSLs, the most suitable candidates to be considered for their retrieval in wheat are OsYSL2 & OsYSL9.

OsYSL9 expresses more specifically in the aleurone layer, whereas OsYSL2, which is expressed in phloem near spike, is directly responsible for metal-NA loading into the seed. OsYSL9 is considered to be involved in Fe and Zn translocation inside

the seed during germination to provide nutrition to the embryo. Therefore, OsYSL2 was selected as the reference gene for finding its ortholog(s) in wheat.

Considering the above facts present study **"In-Silico and Molecular Characterization of YSL1 gene in Wheat**" has been proposed with the following objectives.

I. In-Silico identification of YSL gene(s) using reported gene homologs.

II. Molecular characterization of YSL1 gene.

III. Quantification of Fe and Zn content in seeds of various genotypes.

Note: The present thesis-research work was proposed on the assumption that YSL1 from Arabidopsis, which plays a crucial role in the loading of the Fe, Zn and other nutrients in the seed, will be used as a reference gene to retrieve it in the wheat crop undertaken for the present study. However, the orthologue for the same could not be retrieved. Therefore the YSL2 gene from the rice which has a similar function, was taken for the current study. As per the convention, the name of the gene in the new study should remain the same. Hence YSL1 gene which was proposed in the thesis title and the objective, is the YSL2 gene as per the orthologue used.

◈◈◈

CHAPTER - II

REVIEW OF LITERATURE

II REVIEW OF LITERATURE

Seeds are considered as the foundation for flourishing agriculture on which the food and nutritional security human and their pet are dependent. This very reason necessitates the development of the quality seed. Biofortification has become an integral part of quality seed development as it helps in tackling the micronutrient malnourishment prevailing in the millions of humans in underdeveloped and developing countries like India. Fe and Zn are the critical micronutrients for sustaining good human health. The genetic makeup of the maternal plant along with environmental factors is the primary determining component for their accumulation in the seed. Knowledge of factors that control the flow of nutrition to the developing seeds can help in developing better-biofortified varieties that can increase the pool of essential micronutrients in seed and withstand the adverse environments to a certain extent.

In developing countries, the food plate of the common men is usually rich with items from the plant source. Studies confirm that the nutritional pool of the food from animal sources is far better than that of plant sources, as most developing countries suffer from malnutrition. Therefore there is an urgency to produce seeds that are richer in micronutrients and also favorable for adverse environmental conditions(Cakmak, 2008; white *et al.*,2009). Because of the reasons cited above, the main focus should be drawn to improve the staple food sources such as rice (*Oryza sativa*), wheat (*Triticum aestivum* or *T. durum*), and maize (*Zea mays*), as well as common bean (*Phaseolus vulgaris*) and other legumes i.e., Biofortification (Pfeiffer *et al.*,2007). The micro-nutritional pool mainly depends on the absorption from the rhizosphere, translocation to the xylem, translocation to other tissues, and then to the seeds through the phloem.

The Zn aids the animal as well as supplement human nutrition. It makes Zn a very important micronutrient in the plants and its deficiency in calcareous soils causing abiotic stress in countries like China, India, Australia and Turkey (Hansen *et al.,* 1996). Cereals like wheat and rice usually suffer from Zn deficiency which reduces the yield up to 80% (Fageria *et al.,* 2002). The deficiency of Zn has a substantial impact on countries with predominating cereal-based diets. Plants growing

on Zn deficient soils accumulate heavy metals increasing the potential human health hazard.

2.1 Fe and Zn uptake and distribution in plants

Zinc concentration in the plants depends on a large number of abiotic factors such as the soil and environmental conditions, as well as biotic factors like the genotype of the plant, level of expression of genes which are involved in uptake of zinc from rhizosphere to root, transport through the plant body, deposition in various vegetative organs and remobilization into reproductive organs (Eide, 1996; Korshunova, 1999; Schaaf, 2006). Several genes have been identified to be potentially involved in Zinc homeostasis in cereal crops (Bughio *et al.*, 2002; Gross *et al.*, 2003; Ramesh *et al.*, 2003; Koike *et al.*, 2004). Some of the identified potential candidate genes include members of the ZIP family, NRAMP transporters, NAS genes and YSL transporter family.

Earth's crust is rich in Fe, but the amount is scanty if the rhizosphere is considered, which means the roots have limited access to the absorption of Fe. Soil redox potential and the pH determine the Fe availability. Higher pH and aerobic conditions favor the oxidation of Fe which turns into insoluble ferric oxide. Lower pH keeps the Fe in the elemental form, which favors the absorption of Fe by the roots. Because 30 % of the world's cropland is alkaline, favoring plant growth but resulting in Fe deficiency(Marschner 1995; Takahashi *et al.*, 2001).

Seeing the necessity of Fe and also the toxicity, the plant has evolved its suitable pathways to control the uptake of Fe. Fe concentration in the seeds ultimately affects human nutrition, which therefore draws attention that, why the uptake mechanisms of Fe are important for the biofortification process(Walker *et al.*,2008).

Garcia et al, 1977, used the radioisotope Zn 65 to endogenously label corn plants via nutrient media for Zn bioavailability studies in various parts of plants, especially during ear development. They reported that over 27% of the radioactive Zn was translocated into kernels. They also compared the data of radioactive Zn 65 with non-radioactive Zn in the plant parts and found similar results.

Knight, 1977, developed a method for long term culturing of plants for producing radioisotope labeled plant materials. He used ^{65}Zn for chemical

composition analysis experiments, ^{22}Na and ^{36}Cl for plant physiological ionic studies, ^{59}Fe for human metabolic studies, ^{45}Ca for germination and calcium distribution in seedling roots, and ^{14}C for production of humic substances.

Starks and Johnson, 1985, 1986, conducted a series of experiments using various techniques to incorporate radioactively labeled Zn65 and Cu 65 into wheat plants. The techniques used include foliar application, stem injection, their combination and hydroponics with radioactive isotopes of the minerals. They evaluated the bioavailability of the Zn 65 and Cu 65 in the wheat grains, flour and distribution into 4 protein fractions- albumins, globulins, glutenins and gliadins. They concluded that the methods of incorporation for radioactive minerals were the same as the natural method of mineral nutrition in plants and also utilized in the same ratios in wheat.

Mori and Nishizawa, 1987, reported that Fe deficiency induces the synthesis of Mugineic acid. Siderophores synthesized by microbes also help in the chelation process. Phytosiderophores (PS) are organic substances (such as nicotianamine, mugineic acids (MAs) and avenic acid etc) produced by plants under Fe-deficient conditions, which can form organic complexes or chelates with Fe3+, and increase the movement of iron in soil (Ueno *et al.*, 2007). Chemically it is nonproteinaceous low molecular weight acids that are released by the graminaceous species under the iron (Wallace, 1991) and Zn deficiency stress. The mobilization of micronutrients Fe, Zn, Mn and Cu from the soils is carried out by PS to plant in deficient condition (Takagi *et al.*, 1984). Fe deficiency results in modification of root morphology (Marschner,1995) and upregulates the genes involved in the Iron uptake (Dinneny *et al.*,2008; Colangelo *et al.*,2004). Research depicts in *Arabidopsis thaliana*, 85% of the genes explicitly regulated by Fe were expressed in a particular part of the roots in response to the Fe deficiency (Dinneny *et al.*,2008).

Birnbaum *et al.*,2005, conducted the transcriptome analysis by isolating the cells from specific root layers that expressed GFP under the control of cell-specific promoters via fluorescence-activated cell sorting analysis. This experiment concluded that the genes that were regulating chelation and metal transport were upregulated in the epidermis, whereas genes responsible for hair morphogenesis were

downregulated. The study also indicated that the up-regulation of the genes associated with signaling and stress response occurred in the stele.

Walker *et al.*, 2008, wrote a review on uptake and distribution of Fe under Fe deficiency conditions. Where, he highlighted various genes responsible for taking up of Fe from the rhizosphere, methods of their uptake, the various signaling mechanisms in case of nutrient deficiency in the rhizosphere. He mentioned various transcription factors belonging to the basic helix–loop–helix, ABI3/VP1(B3), and NAC families are involved directly and indirectly in the upregulation of genes responsible for iron deficiency responses.

In Nongraminaceous plants, membrane-bound reductase reduces Ferric ion for the uptake by Ferrous ion transporter. In graminaceous plants, an enzyme phytosiderophore binds with Ferric ion and the Fe-PS complex then transported to the roots.

Elements in reduction strategy are best described in Arabidopsis among the nongraminaceous species (Eckhardt *et al.*,2001; Li *et al.*,2004; Romheld *et al.*,1983). Fe deficiency causes the release of protons into rhizosphere by the enzyme AHA H+-ATPases (Schmidt *et al.*,2003; Santi *et al.*,2005) Lowering of the soil pH makes the Fe more soluble and upregulates the AHA1, AHA2, and AHA7 in the root epidermis (Dinneny *et al.*,2008; Colangelo *et al.*,2004). As the expression of the AHA2 gene was the highest among the three, which makes it the primary root H+-ATPase in the Fe deficiency response (Santi *et al.*,2009).

The NADPH-dependent ferric chelate reductase, AtFRO2, then reduces Fe3+ to Fe2+. Electrons are transferred from NADH+ across four heme groups to Fe in the rhizosphere (Robinson *et al.*,1999). This appears to be the rate-limiting step in Fe uptake in Arabidopsis (Connolly *et al.*,2003). The transgenic overexpression of ferric chelate reductases in the roots of rice, tobacco and soybeans has been successful in increasing tolerance to Fe-limiting conditions(Ishimaru *et al.*,2007; Vasconcelos *et al.*,2006; Oki *et al.*,2004).

Once reduced, Fe (II) can then be transported into the root epidermal cells by the divalent metal transporter AtIRT1(Henriques *et al.*, 2002; Vert *et al.*, 2002; Varotto *et al.*,2002). AtIRT1 also transports Zn, Mn, Cd, Co,(Eide *et al.*,1996; Korshunova *et al.*,1999) and Ni (Schaaf *et al.*,2006). Additional root epidermal

transporters for these metals have not been yet identified; but in the irt1-1 loss of function mutant, shoot accumulation of Fe, Mn, Zn, and Co decreases significantly, and the plants become Cd tolerant,(Vert *et al.*,2002; Connolly *et al.*,2002) suggesting that AtIRT1 is a primary transporter for these metals under Fe deficiency. A similarly broad range of metals was found to be transported by the tomato orthologs LeIRT1 and LeIRT2, which complement yeast mutants defective in the uptake of Fe, Zn, Mn, and Cu. Thus, the Fe deficiency response also leads to the uptake of metals other than Fe, all of which are potentially toxic.

The second type of metal uptake mechanisms is seen in members of graminaceous families such as rice, wheat, corn, etc. Fe chelating substances and Mugineic acids synthesized and secreted by the graminaceous species roots dissolve sparingly soluble Fe compounds in the rhizosphere (Marschner *et al.*, 1986) and affected by soil bacteria (Chattopadhyay, 2006; Dipanwita and Chattopadhyay, 2013). Iron is then transported back to the roots as a complex of PS- Fe+3 through a specific transport system without prior reduction.

Ishimaru *et al.*, 2006, conducted an expression analysis of OsIRTs and found that they were expressed in membranes of root cells when introduced in onion. PETIS analysis conducted, also showed that rice plants could take up iron from the rhizosphere both as Fe2+ directly and Fe3+-phytosiderophore complex.

Hill *et al.*,1980, published a review depicting the movement of mineral nutrients inside the plants as mobile, immobile and nutrients of variable mobility in the phloem. He reviewed various forms of mineral uptake and the forms in which they were distributed throughout the plant body. He also described various physiological and environmental factors such as sink size, nutrient supply, etc. involved in the distribution and deposition of minerals in plant parts. He also discussed the relation of leaf senescence to remobilization of nutrients from leaves and its importance in the loading of nutrients into the seeds.

Hocking, 1994, made a field study of the various seasonal changes in the distribution of nutrients in various plant parts. He found that most of the nutrient uptake was over by anthesis and phloem soluble minerals are transported to the grain via the phloem post-anthesis. It was seen that 29% of the grain dry matter was provided by the redistribution of dry matter from the leaves and stem. It was also

found that about 15-51 % of the total grain Zn was redistributed from the leaves. He concluded that the redistribution of mineral nutrients from vegetative to reproductive parts was a valuable trait in wheat, more so when the nutrient uptake is severely restricted in the post-anthesis period.

Pearson and Rengel, 1994, conducted an experiment to find out the mobility of Mn and Zn in wheat. They grew plants in soil with Zn and Mn deficit conditions, adequate conditions, followed by transfer into a chelate buffered nutrient solution to monitor the remobilization of Zn and Mn in the plant. They found that a large amount of Mn and Zn depleted from the root and stem, during grain development. It was concluded that although there was no remobilization of Mn from the leaves of the plants to the grain, Zn was remobilized to the grains from the flag leaves.

Herren and Feller, 1994, 1996, studied the transfer of Zn from leaves to the grains and found that though Zn is mainly transported through the xylem. Before loading into the seed, it has to be loaded into the phloem first at the peduncle. This fact was proved by feeding radiolabeled Zn to the Xylem in healthy plants and in plants devoid of a healthy phloem. They also pointed out that most of the grain Zn content was from the Zn present in the flag leaf which was redistributed post-anthesis into the grains.

Garnett *et al.*, 2005, investigated the uptake and distribution of Fe and Cu in wheat grown at a low and adequate level of availability of both the elements in sand cultures by using ICP-OES. They found that about 77% of the total shoot Fe content was redistributed to the grain at maturity. The above-ground parts did not take up much Fe post-anthesis. The remobilization of Fe and Cu was found to be higher than that of Zn.

Peleg *et al.*, 2009, discovered and mapped a total of 82 QTLs for 10 minerals, including Zn and Fe by using the RIL population developed from a cross between durum wheat and wild emmer wheat. 14 pairs of QTLs were mapped to seemingly homeologous positions over A and B genomes. They also got a significant positive correlation between QTLs of GPC, Fe, Zn and Cu content supported by overlaps between the QTLs, suggesting a common pathway for distribution of these minerals in the plants.

2.2 Estimation of Fe and Zn content in plant tissues

Zasoski and Burau, 1977 worked on quantitative digestion of both plant and animal tissues and developed a procedure for multi-element analysis of tissue digested with the nitric perchloric acid mixture.

Novozamsky and Houba, 1993 used the wet digestion method to determine total element contents in plant material. They performed sequential digestion with hydrogen fluoride, nitric acid and hydrogen peroxide followed by atomic spectrometry.

Anzano *et al.*, 1995 treated feedstuffs with concentrated sulphuric acid and hydrogen peroxide to determine elements at both 1% level and the trace level. For the estimation they used flame and electrothermal atomic absorption spectrometry.

Srivastava *et al.*, 2008 collected plant tissue of rice and wheat and wet ashed it in a di-acid mixture of nitric acid and perchloric acid on sand bath at 200^0C. The samples were analysed for calcium, iron and molybdenum using double beam atomic absorption spectrophotometry.

Pathak and Agrawal, 2014 estimated micronutrients such as calcium, iron, zinc, magnesium and copper from seeds of fenugreek genotypes using atomic absorption spectrophotometry.

Paula *et al.*, 2014 explained Atomic Absorption Spectroscopy (AAS) as a handy tool for determining the concentration of the specific mineral in a sample as the mineral content was estimated by computing the absorbance displayed by the sample when exposed to UV light of specific wavelengths.

Palma *et al.*, 2015 conducted an experiment by digesting various samples with different concentrations of nitric: perchloric acid ratios and concluded that in plant samples, a 4:1 ratio is ideal for digestion in a single step.

Uddin *et al.*, 2016 compared the efficiency of digestion by 3 different wet digestion methods, i.e., nitric: perchloric acid (2:1), only nitric acid and mixture of nitric, hydrochloric acids (1:3). He concluded that the third method was the most efficient in the extraction of minerals based on observation in AAS.

2.3 In-silico characterization of gene and gene family

In silico characterization of the gene or the gene family under study includes the use of various bioinformatics tools like the identification of the gene sequence on the ref seq, finding homologs of a gene in the different organism if not yet reported, expression analysis using prior data and probable protein structure prediction.

Marchler-Bauer, 2004, 2011, 2015, 2017, developed the database of protein functional domains, conserved domains, and built software to find the reported domains present in the sequence of an unknown protein by alignment in NCBI, i.e., the CDD search tool. He further developed it so that the architecture of the family and subfamily of any unknown protein with a known sequence may be known by it.

Malviya *et al.*, 2014 carried out in silico characterization of the Dof gene family in pigeon pea (*Cajanus cajan*). They identified and classified the 38 genes of the Dof gene family into 3 major clusters based on the phylogenetic analysis. They also performed in-silico cis-regulatory analysis, thus finding the various function and expression patterns of the genes. They also studied the duplication events and compared the results with that of other plants such as 30 genes of rice, 36 genes of arabidopsis, 78 genes of soybean, and prepared phylogenetic tree based on their sequences, which revealed 7 major clusters.

Liu *et al.*, 2016 identified the 42 genes of the expansin superfamily in *Medicago truncatula*. By phylogenetic analysis, they grouped the proteins encoded the genes into 4 major clades. They identified the cases of gene duplication, and also analyzed the expression pattern of the various genes. A number of cis-acting regulatory elements were also identified in the gene sequences by them.

Mishra *et al.*, 2017 studied the divergence and conservation of the SSIII gene in various monocots and dicot plants. The in-silico analysis was done to study the expression pattern of the gene in different species. Their genomic and protein sequences were compared, length of introns and exons, protein catalytic domains were inferred, and phylogenetic analysis was carried to group the gene in evolutionary clusters. They also compared the 3d structure of catalytic domains of the genes and found it to be superimposed with high confidence.

2.4 Studies on YSL gene family

Phytosiderophores are organic substances (such as nicotinamine, mugineic acids (MAs) and avenic acid, etc) produced by plants (Mori and Nishizawa, 1987) under Fe-deficient conditions, which can form organic complexes or chelates with Fe3+, and increase the movement of iron in soil (Ueno *et al.*, 2007). Chemically it is nonproteinaceous low molecular weight acids released by the graminaceous species under the iron (Wallace, 1991) and Zn deficiency stress. The mobilization of micronutrients Fe, Zn, Mn and Cu from the soils is carried out by PS to plant in deficient conditions (Takagi *et al.*, 1984).

Benes *et al.*, 1983; Anderegg *et al.*, 1989 reported that Nicotianamine forms Stable complexes with manganese (Mn), Fe(II), cobalt (Co), zinc (Zn), nickel (Ni) and copper (Cu), in increasing order of affinity.

Curie *et al.*, 2001 found 8 Yellow stripe1 like genes (YSL) in nongraminaceous plants, i.e., Arabidopsis thaliana responsible for the transport of Fe-NA complexes throughout the plant vascular system. All YSL genes except YSL 4 and YSL 6 were found on plasma membranes.

Curie *et al.*, 2001 discovered YS1 gene in maize. Mutation of the YS1 gene in maize resulted in a decrease in uptake of Fe-chelates in the plants. They cloned the ZmYS1 gene in yeast and found that the mutant yeast growth was restored specifically in Fe-PS containing media. Therefore, they concluded that ZmYS1 is the metal transporter that is involved in the uptake of Fe-PS from the soil. Expression analysis also confirmed that there was an increased expression of the ZmYS1 gene in both root and shoot of maize plants in Fe deficient conditions.

Schaaf *et al.*, 2004 determined the transport activity by using growth complementation of yeast mutants and two-electrode voltage clamp analysis in *Xenopus leavis* oocytes. They found that ZmYS1 transports Fe3+–PS as well as other PS-chelated metals, such as Cu, Zn, Co, and Ni. They also reported that this transport depends on a proton co-transport and the membrane potential of the cell.

Murata *et al.*, 2006 conducted Immuno-histological staining of HvYS1 with an anti-HvYS1 antibody. They also analysed the transient expression of HvYS1 using hvYS1:: GFP fusion and demonstrated that the HvYS1 transporter is located on the plasma membrane of epidermal cells.

Koike *et al.*, 2004 reported 18 putative YS1 like genes, i.e. OsYSLs in rice. They further isolated OsYSL2 and studied its expression pattern using GFP and GUS analysis and found that it was expressed highly in the leaves during low Fe condition post-anthesis. They also reported that its expression was limited to the shoot, more specifically in the leaves and grains. Hence they concluded that it was involved in the translocation of Fe into the grain via the phloem.

Le Jean *et al.*, 2005 reported that YSL1 plays a significant role in the loading of Fe and NA in seed by analyzing the YSL1 mutants. They also found that the YSL1 gene expresses in shoot and not in the root by GUS reporter analysis. Further, they also reported that YSL1 is Fe regulated.

Waters *et al.*, 2006 reported that YSL1 and YSL3 were directly involved in the homeostasis of Fe from senescent leaves towards seed development. He also worked on whole-plant mineral partitioning throughout the life cycle in *Arabidopsis thaliana* ecotypes Columbia, Landsberg erecta, Cape Verde Islands, and the mutant line ysl1ysl3 and reported the location of expression of ysl1 and ysl3 genes throughout the lifecycle of the plant.

Suzuki *et al.*, 2006, 2008, studied the release of MAs in Zinc deficient barley through HPLC analysis. They found that deficiency of Zn led to the expression of various transcription factors involved in the biosynthesis of MAs in the roots of barley plants. There was an increased expression of HvNAAT-B transcription factors in Zn deficient barley roots and not in Fe deficient barley roots. Further analysis by PETIS showed that Zn-MA was absorbed and transported more than Zn2+ in Zn deficient barley roots.

Ueno *et al.*, 2009 carried out further characterization and comparative analysis of ZmYS1 and HvYS1 in terms of the pattern of expression and tissue specificity. They found the difference not only in the expression patterns but also in the tissues in which they were expressed were different. ZmYS1 was expressed in leaves, sheath and seminal roots, whereas HvYS1 expression was restricted to roots and expressed mainly under Fe deficiency. The various analyses led to the conclusion that HvYS1 is mainly involved in the uptake of Fe into roots, whereas ZmYS1 is involved in primary uptake as well as the distribution of Fe in the plant body.

Chu *et al.*, 2010 confirmed that successful reproduction requires the function of Arabidopsis Yellow Stripe-Like1 and Yellow Stripe-Like3 metal-nicotianamine transporters in both vegetative and reproductive structures and that they are responsible for mineral homeostasis via vessels through the plant to be deposited in the seeds.

Ishimaru *et al.*, 2010 isolated OsYSL2 in rice and reported that it was expressed mainly in the phloem tissue in grain. They conducted an experiment using OsYSL overexpressed lines and expression inhibited lines (RNAi) and found that it was also involved in the long-distance transport of Fe and Mn and its accumulation into the seeds. Overexpression of the gene led to 4.4 fold increase in mineral content of polished rice, hence highlighting its importance in biofortification.

◈◈◈

CHAPTER - III

MATERIALS AND METHODS

III MATERIALS AND METHODS

3.1 Plant material:

Wheat (*Triticum aestivum* L.) genotypes maintained at the Department of Agricultural Biotechnology & Molecular Biology; C.B.S &H., R.P.C.A.U., Pusa, were used for the present study. The details of the plant materials used, methods adopted, and various techniques used during this study are described in this chapter.

3.2 Experimental Site:

The materials for the study were planted in the fields of Pusa Farm, Dr. RPCAU, Pusa, Samastipur, Bihar under normal and late sown conditions. The late sown condition was considered as the treatment for heat stress. The geographical location of the site is North latitude of 25.984, East longitude of 85.674, and altitude of 52.20m above mean sea level. Quantification of mineral content in the wheat seeds was carried out in the Micronutrient laboratory, Department of Soil Science, Dr. R.P.C.A.U., Pusa and the in-silico and molecular characterization work was carried out in the genetic transformation laboratory, Department of Agricultural Biotechnology and Molecular Biology, Dr. R.P.C.A.U., Pusa.

Table 3.1: List of genotypes and their pedigree

Sl No.	Cultivar	Pedigree
1.	CRP 07	CNDO/R143//ENTE/MEXICO/3/AEGILOPS SQUARROSA (TAUS)/4/WEAVER/5/PASTOR
2.	CRP 08	MILAN/KAUZ/3/URES/JUN//KAUZ/4/CROC_1/AE.SQUARROSA (224)//OPATA
3.	CRP 15	TILHI
4.	CRP 16	NL 750
5.	CRP 18	W462//VEE/KOEL/3/PEG//MRL/BUC
6.	CRP 20	JUPARE C 2001
7.	CRP 21	ATTILA/3*BCN//BAV92/3/TILHI
8.	CRP 27	VORB/4/D67.2/PARANA66.270//AE.SQUARROSA (320)/3/CUNNINGHAM
9.	CRP 30	CROC_1/AE.SQUARROSA(205)//KAUZ/3/SASIA/4/TROST
10.	CRP 33	PFAU/MILAN//TROST/3/PBW65/2*S ERI.1B
11.	CRP 34	TILHI/PALMERIN F 2004
12.	CRP 37	Youngmy-6
13.	CRP 40	UP2338*2/KKTS*2//YANAC
14.	CRP 42	UP2338*2/KKTS*2//YANAC
15.	CRP 43	MURGA/KRONSTAD F 2004
16.	CRP 45	BAV92//IRENA/KAUZ/3/HUITES/4/FN/2*PASTOR/5/BAV92//IRENA/KAUZ/3/HUITES
17.	CRP 46	BABAX/LR39//BABAX/3/VORB/4/SUNCO/2*PASTOR
18.	CRP 48	WDLL1*2/KURUKU*2/5/REH/HARE//KACHU

19.	CRP 49	#1/4/CROC_1/AE.SQUARROSA (205)//KAUZ/3/SASIA/5/KACHU
20.	CRP 50	SKAUZ*2*FCD'S'//VORB
21.	CRP 51	OPATA//SORA/AE.SQUARROSA (323)
22.	CRP 52	CNDO/R143//ENTE/MEXI_2/3/AEGILOPS SQUARROSA (TAUS)/4/WEAVER/5/TICUS/6/2*PBW65/2*PASTOR
23.	CRP 54	BABAX/KS94U76//BABAX/3/2*SOKOLL
24.	HD 2967	CHECK
25.	PBW 343	CHECK

3.3 Methods:

3.3.1. Quantification of Fe and Zn content in seeds

The seeds of the selected wheat lines were crushed and digested by the wet digestion method (Nitric acid: Perchloric acid::3:1), and their mineral content was calculated using Atomic Absorption Spectrophotometer. The details of the procedure are as follows.

3.3.1.1 Fe and Zn content analysis by wet digestion method / di-acid method

Sample Preparation

- Wheat seeds harvested from the field were collected separately for different genotypes.
- The seeds were then spread on filter paper and dried in the shade.
- The air-dried seed samples were then weighed by the help of a digital balance and 0.5g of each sample was taken.
- Seed samples (0.5g) were crushed in mortar and pestle, and kept in labeled 2 ml Eppendorf's tubes.
- Conical flasks of 100 ml were taken, and crushed samples were transferred to them and labeled.
- The content was pre-digested for 24 hours by adding 10 ml of the di-acid mixture, i.e., nitric acid: perchloric acid (3:1).
- 10 ml di-acid mixture, i.e., nitric acid : perchloric acid (1:3), was added to each flask for digestion and was kept overnight.
- The next day, the conical flasks were kept on a hotplate and allowed to evaporate until the brown fumes disappeared, and about 1-2 ml aliquot was left.

- The flasks containing 1-2 ml aliquots were cooled, and the volume in each sample was made up to 50ml by the addition of distilled water with the help of a volumetric flask.
- Whiteman class A filter paper was used to filter the solution into a plastic bottle.
- Then Fe and Zn content were estimated from the solution using AAS.

Micronutrient estimation in AAS

- The Atomic Absorption Spectrophotometer (AAS) was first standardized by measuring the absorbance of stock solutions of known concentrations. Absorbance to the concentration graph was plotted from the obtained absorbance values.
- The samples were then tested and their absorbance was recorded. Their concentrations were obtained by plotting the absorbance value on the curve.
- The AAS values were multiplied by dilution factor (x100) to get the micronutrient content in the seed in ppm.

3.3.1.2 Analysis of Fe content and Zn content data

The genotypes were planted under RBD in the field with 3 replications. The data were analyzed by running the two-way analysis of variance (ANOVA) using OPSTAT online software for Fe and Zn content data separately. The critical differences for genotypes, DOS, and their interaction were calculated.

3.3.1.3 Calculation of Heat Susceptibility Index

Heat Susceptibility Index was used to evaluate the effect of heat stress on different genotypes based on the variation in Fe and Zn content in seeds over two dates of sowing. The formula for calculating HSI, taken from Fisher & Maurer (1978), is given as,

Heat Susceptible Index (HSI) = $(1-Y/Y_P)/D$

Where, $D = 1-X/X_{P,}$

Y = Mean performance of the genotype under heat stress condition,

Y_P = Mean performance of the genotype under normal condition,

X = Mean performance of all the genotypes under heat stress,

X_P = Mean performance of all the genotypes under normal conditions.

3.3.1.4 Clustering of Genotypes

The data of Fe and Zn content in the seeds for two dates of sowing were used to cluster the 25 genotypes based on Ward's minimum variance method by R software. Dendrograms were prepared from Fe content data and Zn content data separately to represent different clusters of genotypes using R Studio.

3.3.2. In-Silico Identification and Characterization of gene

Methods used for the In-Silico Identification and Characterization of the gene under study are described under the following headings.

1. Finding a well-characterized YSL gene responsible for the transport/loading of micronutrient chelates into the seed in a species.
2. Finding orthologs of the gene in the wheat genome.
3. Designing genome-specific primers for the YSL gene in the A, B & D genomes.
4. Identifying all members of the YSL gene family in wheat and classifying them into different clades based on phylogenetic analysis of their probable proteins.

3.3.2.1 Finding true orthologs of the gene in the wheat genome

Various references were studied thoroughly, and the reported genes for the uptake of Fe and Zn and its deposition into seed were considered. AtYSL1 was first considered suitable for further work as it was expressed in the reproductive structures and was directly involved in the rerouting of Fe and Zn from senescent leaves into the developing seeds.

AtYSL1 genomic sequence was retrieved from the NCBI database. BLASTn was performed on the wheat genome using NCBI BLAST, followed by EnsEMBL and Phytozome. The aligned segments were then compiled together to get a region on the chromosome number II of the A, B & D genomes of wheat. The sequences were then aligned with the location of probable genes annotated by TGACv1.

The probable protein sequence was obtained on UNIPROT, and BLASTx was performed on all plant species. The highest match was obtained with OsYSL9, followed by AtYSL3. All other BLASTn results were similarly processed, and no protein alignment to AtYSL1 was found. As Arabidopsis is a dicot plant, considering wheat is a monocot belonging to Gramineae, it was assumed that the true ortholog to AtYSL 1 was not present on the wheat genome.

Instead of taking the Arabidopsis AtYSL1 gene, YSL genes from the rice was taken as a reference for further study because rice belonging to the Poaceae family, was more closely related to wheat than arabidopsis, even though OsYSLs were not having expression specific to only flowering organs. The most suitable candidates considered for the present study were OsYSL2 & 9. The OsYSL9 expresses in the aleurone layer, and OsYSL2 expresses in phloem near the spike. Hence OsYSL2 was selected as a reference gene for finding the 1st YSL gene in wheat using IWGSC BLAST. The homeologues on other wheat genomes were obtained by using the homeologues tool on EnsEMBL.

3.3.2.2 Marking Intron Exon boundaries

CDS of the homeologous genes of each of the genomes was aligned against the genomic sequence of the respective gene using the Clustal W program and intron-exon boundaries were carefully marked on the sequences of the genes.

3.3.2.3 Designing Genome specific Primers

The genomic sequences of the gene and its homeologues were aligned using ClustalW. They were then analyzed for genome-specific SNP regions. The SNPs present at the 3' end of the sequence was considered while designing genome-specific primers, keeping Tm values at 60-62^{0}C and primer length 17-24 bp. Placing of the primers was distributed in such a way that the probable amplicons were having the overlapping ends to cover the entire gene.

Similarly, reverse primers were designed by taking SNPs at 5' end. The reverse primers were retrieved using Reverse complement tool of Harvard.

As soon as the primers were almost ready, taking the extended flanking regions from EnsEMBL database whose annotations were provided by TGACv1, the database annotations were changed to IWGSC. The gene sequence was taken, and

BLASTn was performed in the new database on EnsEMBL. The sequence location and flanking sequence data aligned perfectly.

The gene sequences were also queried for the presence of Gene based SSRs and their location on the gene using Batch Primer 3 software.

Then genome-specific SSR primers were designed using the same software by setting the Tm to 60-62^{0}C and primer length to 18-24 bp.

3.3.2.4 3D protein structure prediction

The 3D protein structure was computed using the PHYRE2 software, and the probable protein structure was compared with the structures of ZmYS1 and OsYSL2. The steps followed to predict the 3D model of the desired protein from its sequence is described below.

'Normal' mode modeling by Phyre2 was used to produce a set of potential 3D models of the protein, based on alignment with known protein structures. The pipeline of protein structure prediction by PHYRE2 involves:

- Detection of sequence homologues with PSI-Blast.
- Prediction of secondary structure and disorder with Psi-pred and Diso-pred.
- Construction of a hidden Markov model (HMM) of the query sequence based on the homologues detected.
- Scanning the obtained HMM against the library of HMMs of proteins with experimentally solved structures.
- Construction of 3D models of protein, based on the alignments between the HMM of the query sequence and the HMMs of known protein structure.
- Modeling insertions and deletions using a loop library, a fitting procedure (cyclic coordinate descent) and a set of empirical energy terms
- Modeling of amino acid sidechains by using a rotamer library and implementing a fast graph-based approach (R3) to optimize the choice of rotamer for each sidechain while trying to avoid steric clashes.
- Displaying the best model for prediction of binding site by 3DLigandSite.
- Prediction of trans-membrane helix and protein topology by memsat-svm.

This procedure produced accurate models of about 70% of the domains in a typical genome. It is possible because remote homology detection techniques such as profile-profile and HMM-HMM matching can reliably detect and align protein sequences even if they have substantially diverged over evolutionary time. It is common to be able to confidently and correctly detect homology even when sequence identity between a pair of proteins is as low as 15%.

The domain analysis section was used to study, where along the protein sequence matches have been found and color-coded according to their confidence. The matches were ranked by a raw alignment score which is based on the number of aligned residues and the quality of alignment, which, in turn, was based on the similarity of the residue probability distributions for each position, secondary structure similarity and the presence or absence of insertions and deletions.

Each row provided information on the template used for the model and a small graphic indicating where along the protein sequence the match was, color-coded by confidence. The image obtained was a picture of the model constructed for the query sequence based on the template. The Confidence column represented the probability that the match between the query sequence and this template is a true homology.

The output PDB file was analyzed for structural stability by Ramachandran Plot analysis using RAMPAGE software (http://mordred.bioc.cam.ac.uk/~rapper/rampage.php), and all outliers were corrected by using MODLOOP software (https://modbase.compbio.ucsf.edu/modloop/) (Fisher *et al.*, 2000, 2003).

Fig. 3.1: Webpage for PHYRE2 protein structure prediction software

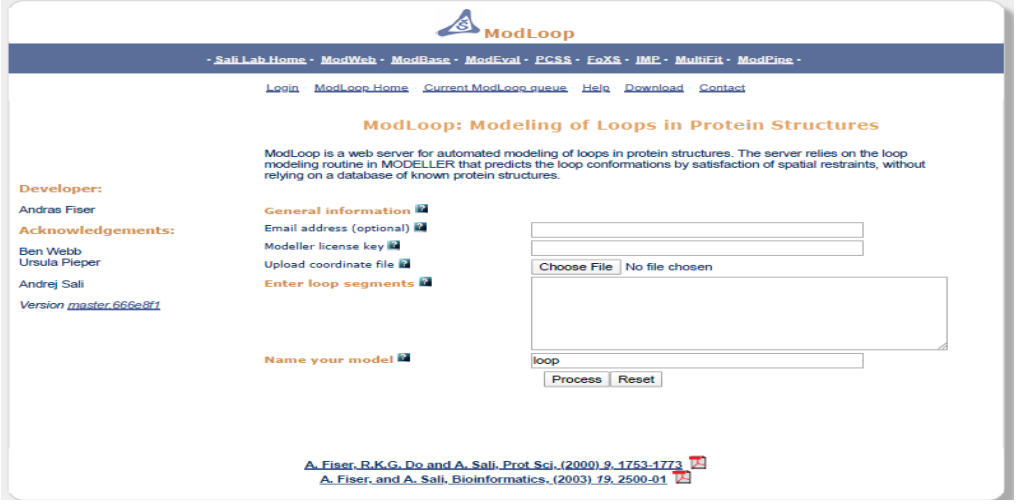

Fig. 3.2: Webpage for MODLOOP loop modification software

The obtained PDB file with all the protein structure and sequence information was then loaded on to YASARA energy minimization software (http://www.yasara.org/index.html), and the corrected model of protein with minimum energy utilization was computed. The results were obtained in the YASARA scene format and were analyzed by using YASARA viewer software.

3.3.2.5 Finding conserved domains in the protein

The Protein sequences were queried for the identification of conserved domains to predict the probable function, the family, and the super-family of the gene by using the Batch CD-search tool in the NCBI database (https://www.ncbi.nlm.nih.gov/Structure/cdd/wrpsb.cgi). Both the nucleotide sequence and protein sequence could be used as a query sequence and thus, were entered in separate windows for checking the accuracy of the prediction of conserved domains in the protein.

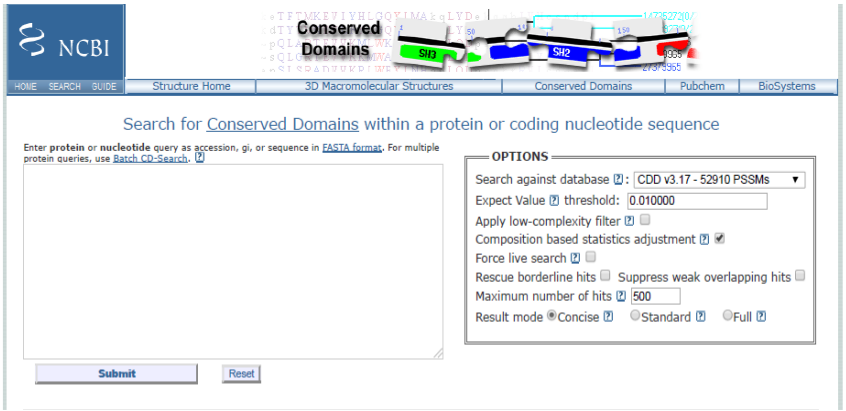

Fig. 3.3: Webpage for searching Conserved domains in NCBI

3.3.2.6 In-Silico Expression analysis

The cDNA sequences of the genes were obtained from the EnsEMBL, and BLASTn was performed on the sequences in the WheatEXP transcriptome database (https://wheat.pw.usda.gov/WheatExp/). The results were analyzed from the graphs and tables of the expression data in various tissues at various points of time in the plant development.

3.3.2.7 Identification of members of the YSL gene family in wheat

The nucleotide sequences of all the YSL genes reported in rice and arabidopsis were retrieved from the NCBI database. Each of these sequences was then used to perform BLASTn on the Wheat genome by using the BLAST tool on EnsEMBL. All BLASTn results with more than one alignment >50bp and having e value below $2x10^{-8}$ were taken under consideration. The overlapping genes annotated with high confidence by IWGSC were retrieved along with their homeologues. Their nucleotide and protein sequences were retrieved and saved as text files separately. The TaYSL genes thus obtained were named according to the maximum alignment with their corresponding OsYSLs by following syntenic order of genes.

3.3.2.8 Phylogenetic analysis and classification of gene family

The nucleotide, as well as protein sequences, were loaded onto MEGA7 software separately in FASTA format, and alignments were made using ClustalW. The alignment files were then processed for the UPGMA tree by using 1000 bootstraps method with Poisson correction and pairwise deletion.

The resulting phylogenetic tree of the TaYSLs proteins was compared with the phylogenetic trees of OsYSL and AtYSLs proteins, and thus, they were classified accordingly.

3.3.3. Molecular Characterization by SSR and Gene-specific markers (Genome specific)

Molecular characterization of the genes under study was done by gene-based SSR and genome-specific primers designed from the retrieved homeologous gene sequences. The steps followed for the characterization are described as follows.

3.3.3.1. Enzymes, buffers, and solutions

- **0.5 M Ethylene diamine tetraacetate (EDTA, Na2 EDTA. $2H_2O$) pH 8.0**

186.12gm Sodium EDTA.$2H_2O$ (MW=372.2) was dissolved in 800ml double distilled water by stirring vigorously, and pH was adjusted to 8.0 with NaOH. The volume was made up to 1 Liter, followed by sterilization by autoclaving.

- **1M Tris-HCl (pH 7.5)**

121.1gm of Tris base was dissolved in 800 ml double-distilled water, and the pH was made up to the desired value (pH 7.5) by adding concentrated HCl. The volume was made up to 1 Liter, followed by sterilization by autoclaving.

- **3M Sodium Acetate (pH 5.5)**

204 gm of sodium acetate (MW=136) was dissolved in 400 ml double-distilled water (H_2O), and the volume was adjusted to 500ml and the solution was sterilized by autoclaving.

- **5M Sodium Chloride (NaCl)**

146.1 gm of NaCl (MW=58.44) was dissolved in 400 ml double-distilled water, and volume was adjusted to 500ml and the solution was sterilized by autoclaving.

- **(24:1,v/v) Chloroform: Isoamyl alcohol (CHCl3: IAA)**

40 ml isoamyl alcohol was added to 960 ml chloroform. The mixture was stored at 4 ºC in dark glass bottles.

- **Ethidium bromide (C21H20BrN3, 10mg/ml)**

1gm ethidium bromide was added to 100 ml double distilled water and stirred vigorously on a magnetic stirrer for several hours to ensure that the dye was dissolved. The container was wrapped in aluminium foil and stored at 4 ºC.

- **(10X) Tris- Borate – EDTA (TBE) buffer**

108.0 gm Tris, 55.0 gm boric acid, and 9.3 g Na2EDTA were added to 900 ml double distilled water (H2O). The volume was made up to 1 liter.

- **76% Ethanol + 0.2 M Sodium Acetate:**

Mix 76ml of absolute ethanol, 6.7ml of 3M sodium acetate, pH 5.5, 17.3 ml of double-distilled water, the volume was made up to 100 ml.

- **76% Ethanol + 10mM Ammonium Acetate :**

Mix 380ml of absolute ethanol, 6.30 ml of 7.5M Ammonia acetate, pH 5.5, 88.7 ml of double-distilled water, the volume was made up to 475 ml.

3.3.3.2 Extraction Buffer for DNA isolation

To extract DNA from fresh leaves, the leaves were ground with liquid Nitrogen using the CTAB extraction buffer**.**

Table 3.2: Composition of2X CTAB extraction buffer

Stock	**200 ml**
dd H2O	92.0 ml
1M Tris pH 7.5	40.0 ml
5M NaCl	56.0 ml
0.5 M EDTA pH 8.0	8.0 ml
CTAB	4.0 g
Beta-mercaptoethanol	4.0 ml

3.3.3.3 Genomic DNA isolation using the CTAB method

The seeds of the genotypes showing performances significantly beyond the mean value +/- SD were considered for molecular characterization study. The DNA was isolated by the CTAB method using the following protocol adopted from Doyle and Doyle, 1987 and Shehzadi *et al.*, 2010.

- The soil was taken from the field, sterilized and filled in open aluminum containers. Wheat seeds of the respective genotypes were obtained from the harvested stock and soaked overnight. The pre-soaked seeds were sown in the sterilized soil containing aluminium containers to obtain 7-10 days seedlings.
- Few leaves (2-3 g) were taken from the 7-10 days old seedlings in a mortar pestle.

- 1000 ul CTAB and 100 ul B-mercaptoethanol were added to the leaves and crushed.
- The crushed sample was taken in an Eppendorf's tube and kept in a water bath for 90 minutes at 65^0 C.
- Then the tubes were taken out of the hot water bath and mixed well. 200 ul of Chloroform: Isoamyl alcohol (24:1) was added to it and mixed well.
- The tubes were then loaded on to Centrifuge and centrifuged at 4000 rpm for 10-15 minutes.
- The tubes were then taken, and the supernatant was transferred into another tube. The residues were discarded. When the supernatant was not adequately pure, the above steps were repeated a few times.
- Ice cold propanol (200-300 ul) was added with the help of micropipette and mixed gently till a white cottony clot was obtained. It was spooled out of the tube into a separate tube, and the liquid was discarded.
- When the cottony clot was not obtained, the tubes were centrifuged at 4000 rpm for 1-2 minutes. The liquid was then discarded and the pellets obtained were taken for purification.
- The pellets were air-dried, and 200-300 ul of Sodium acetate dissolved in 70% ethanol was added to the tube and kept for 10 minutes and then the supernatant was discarded.
- 50 ul of 10 mM Ammonium acetate in 76% ethanol was added to the pellets and left for 10 minutes.
- The supernatant was discarded, and the DNA was stored by dissolving in 30-40 ul 1X TE buffer.

Quantification of the Genomic DNA and its quality study

The quality and quantity of the extracted genomic DNA were measured by the band intensity on ethidium bromide-stained agarose gel and comparison with DNA molecular ladder by following steps-

1. 0.8% Agarose was prepared in 1X TBE buffer, heated in a microwave oven on medium power until boiling and dissolved.

2. 3µl ethidium bromide (10mg/ml) was poured and mixed. Then the gel was poured into the already prepared tray and allowed to set for 30-40 minutes at room temperature.
3. The comb was carefully removed, and the gel plate was placed in the electrophoretic running tank containing 1X TBE buffer.
4. Samples mixed with 6X loading dye were loaded in respective wells and separated along with a 1kb DNA ladder; by running the gel at 80V for 40-50 min.
5. The gel was removed from the casting tray and visualized under Gel-documentation System

Following extraction, the genomic DNA was quantified, purified, and the quality check was performed using a spectrophotometer ratio of OD value at wavelength 260 and 280 nm in 1:1000 dilution of the extract. The concentration of the DNA was calculated as:

Conc. of DNA (µg/µl) = OD260 nm X 50 X Dilution factor / 1000

Where,

Dilution factor = Volume of the diluted sample used for DNA quantification / Volume of the sample used for dilution

OD260 nm = Optical density or absorbance at 260 nm wavelength.

Concentration of dsDNA at 1 unit O.D. at 260 nm = 50µg / ml

The ratio between the readings at 260 nm and 280 nm (OD260 nm / OD280 nm) was used as an estimate of the purity of the DNA samples. If this ratio (A 260/ A 280) is:-

1.8-2.0 = Pure DNA

>2.0 = RNA contamination

<1.8 = Protein and Phenol contamination

A pure preparation of DNA has OD 260 nm / OD 280 nm ratio between 1.8 and 2.0 (Sambrook and Russell, 2001). Computed OD values were used to dilute the DNA samples to working concentrations.

3.3.3.4 Amplification of isolated genomic DNA by PCR

Each polymerase chain reaction (PCR) was performed in a volume of 10 µl in a thermocycler (Biometra, Germany). It has a max ramp rate of 4°C/sec.

The reaction mixture was prepared as given in table 3.3. Then the reaction mixture was mixed well with the help of micropipette or by giving a short spin for a few seconds.

Except for the template DNA, the master mixture was equally distributed to PCR tubes (9µl/tube) to which 1 µl of the template DNA from the respective genotypes was added, making the final volume to 10µl.

Table 3.3: Composition of the reaction mixture for PCR amplification

Stock	Stock Conc.	Working Conc.	1X
Nuclease free water	-	-	5 µl
PCR buffer with 2 mM MgCl2	10 X	1 X	1.0 µl
MgCl2	25 mM	5 µM	1 µl
dNTP	10 mM	2.5 mM	1 µl
Forward Primer	100 µM	5 µM	0.5 µl
Reverse Primer	100 µM	5 µM	0.5 µl
Taq DNA polymerase	5 U / µl	1 U	0.2 µl
Template DNA	-	100-150 ng / µl	0.8 µl
Total	-	-	10 µl

Table 3.4: List of designed primers used for PCR amplification

Primer		Sequence (5' ---> 3')	Length (bp)	T_m (^{0}C)
TaYSL2-6Ai	Forward	ACCGGCGTTGGTCTAAGAC	19	60
	Reverse	CAACTCTGGCCACCTGTGTA	20	62
TaYSL2-6Aii	Forward	TCCTGTGGAGCTTCTTCCAA	20	60
	Reverse	TACTTCCGGTACTTCTGCGT	20	60
TaYSL2-6Aiii	Forward	GACGGGTACTGGAAGGCC	18	60
	Reverse	AACACTCATATTTTCCCATTGG	22	60
TaYSL2-6Bi	Forward	CGTCGGTGTAGGACAAGCC	19	60
	Reverse	CAACTCTGGCCACCTGTGTA	20	62
TaYSL2-6Bii	Forward	TGCAGGTCCGCGGATTCC	18	60
	Reverse	AAGCAAGAAGCAGACAGTTCA	21	60
TaYSL2-6Biii	Forward	CATCGCGCCGTCTACGTTT	19	60
	Reverse	CCTTCGAACACTCATATTTTGT	22	60
TaYSL2-6Di	Forward	GGTGACCGGCGCTTGGTC	18	62
	Reverse	CAACTCTGGCCACCTGTGTA	20	62
TaYSL2-6Dii	Forward	TCTTGGCGATACATGGTGAG	20	60
	Reverse	AACAGACAGCTCGAGGCAG	19	60
TaYSL2-6Diii	Forward	GGCTGCATCGTTGCGCCA	18	60
	Reverse	CATCCTAAATACTCCCATTGC	21	60
TaYSL2-S1	Forward	TTTCGTACAACCTTTAATGTGT	22	58
$(AATT)_3$	Reverse	TCAAATGAAACTGTATCCTCG	21	58
TaYSL2-S2	Forward	TGGCGACCGAGATTGAACG	19	60
$(GGAGCC)_3$	Reverse	CTTGAGGATGATGACGGTGAA	21	62

3.3.3.5 Visualization of amplified DNA

Preparation of 2% agarose gel

- 2g of agarose was taken and dissolved in 100 ml of 1 X TBE buffers, pH 8.0 having
- The agarose suspension was boiled in the microwave oven until the transparent solution was formed.
- 4 µl of ethidium bromide (10mg/ml) was added to the gel before casting. The gel was cast in a casting tray with a comb by avoiding air bubbles formation.
- The gel was cooled for 30- 40 min at room temperature until it solidified.

Electrophoresis and Analysis of Result

The comb was removed carefully, and the gel was kept in running tray having 0.5X TBE buffer (pH 8.0). About 2µl of 6X loading dye (0.03% bromophenol blue and 0.03% xylene cyanol FF) was added to each sample after PCR and before loading the sample into well. The samples were then loaded carefully into the wells of the gel with the help of the micropipette. A 100 bp ladder was loaded in the well adjacent to the wells containing PCR products for comparison of size.

The power supply was set at 100V and was allowed to run for 30-45 minutes, till the dye covered 3/4th of the gel. The gel was taken out after running, and then the amplified product was visualized and photographed under UV light using a Gel Documentation System of Bio-Rad, Berkeley, U.S.A. The bands were then analyzed using QuantityONE software, and band size were determined.

3.3.3.6 Scoring of generated bands

The polymorphism was recorded among the entries based on the presence or absence of the bands in different genotypes. The bands were scored by giving code '1' for the presence and '0' for the absence of the bands and the data were subjected to further analysis.

3.3.3.7 Calculation of PIC and polymorphism percentage

Assessment of allelic diversity and identification of polymorphic and informative markers was accomplished by computation of PIC value of the markers as follows:

$$\mathbf{PIC = 1-\sum_{j-1}^{k} P^2_{ij}}$$

Where K is the total number of alleles detected for a locus of a marker, and P_{ij} is the frequency of the j^{th} allele for i^{th} marker, and summation extends over k alleles.

The polymorphism percent found among the markers was calculated using the following formula.

$$\text{Polymorphism Percent} = \frac{\text{No. of unique alleles}}{\text{Total no. of alleles}} \times 100$$

3.3.3.8 Computation of similarity coefficient

Molecular polymorphism detected by gene-based genome-specific primers was recorded based on variation in the sizes of the amplicons generated in each entry. All the entries were scored for the presence and absence of the particular alleles of the respective primer. Using the binary matrix as discrete variables, genetic similarities (Dice, 1945) among the entries were calculated.

3.3.3.9 Clustering of genotypes based on Similarity coefficient

Cluster analysis was performed using the data on the similarity coefficient. Using sequential agglomerative hierarchical non-overlapping (SAHN) and neighbor-joining clustering based on similarity coefficients as the methods for tree building in the cluster analysis, the dendrogram based on similarity indices was obtained by unweighted paired group method using the arithmetic mean (UPGMA). The analysis was performed with the help of NTSYS-pc software (Rohlf, 1997). Grain Fe and Zn accumulation divergence patterns between the genotypes were assessed by identifying clusters at appropriate phenon levels for all the classification modules used.

◈◈◈

CHAPTER - IV

EXPERIMENTAL FINDINGS

IV EXPERIM ENTAL FINDINGS

4.1 Quantification of Fe and Zn content in seeds

The Fe and Zn content in wheat seeds were analyzed by using AAS. Most of the genotypes showed a reduction in mineral content from 1st DOS to 2nd DOS. The highest Fe accumulation was seen in the case of CRP 7 in 1st DOS at 76 mg/g of seed and CRP 54 in 2nd DOS at 43.9 mg/g of seed. The highest accumulation of Zn was observed in CRP 48 in both dates of sowing as 65.6 mg/g and 55.1 mg/g of seed in 1st and 2nd DOS respectively.

4.1.1 Analysis of Fe content and Zn content data

Two-way mean table, ANOVA, C.D., and S.E. were computed using the OPSTAT (Sheoran *et al.*, 1998). It was found that the variance among the genotypes between the 2 DOS and the interaction between them, based on their Fe and Zn content, was highly significant (**Table No. 4.1 & 4.2**). The C.D. based on Zn content for genotypes was 5.427, and for DOS was 1.535. Overall, C.D. considering the interaction of genotypes with the DOS, was 7.675 (**Table No. 4.4**). Similarly, The C.D. based on Fe content for genotypes was 6.336 and for DOS was 1.792. Overall, C.D. considering the interaction of genotypes with the DOS, was 8.961 (**Table No. 4.5**).

Table 4.1: Analysis of Variance Table for Fe content

Source of Variation	DF	Sum of Squares	Mean Squares	F-Calculated
Replication	2	235.370		
Genotypes	24	14,609.558	608.732**	19.965
Dates of Sowing	1	6,387.061	6,387.061**	209.484
Interaction G X D	24	10,110.235	421.260**	13.817
Error	98	2,987.969	30.489	
Total	149	34,330.193		

Table 4.2: Analysis of Variance Table for Zn content

Source of Variation	DF	Sum of Squares	Mean Squares	F-Calculated
Replication	2	170.349		
Genotypes	24	5,926.069	246.920**	11.038
Dates of Sowing	1	185.188	185.188**	8.279
Interaction G X D	24	3,808.221	158.676**	7.094
Error	98	2,192.163	22.369	
Total	149	12,281.992		

Table 4.3: Table of Two Way Mean and HSI

Sl. No.	Genotypes	Fe content		Mean Fe (Genotypes)	HSI Fe	Zn content		Mean Zn (Genotypes)	HSI Zn
		DOS1	DOS2			DOS1	DOS2		
1	HD 2967	20.467	26.500	23.483	-0.92	25.167	32.633	28.900	-0.50
2	CRP 37	25.600	38.800	32.200	-1.61	31.667	45.933	38.800	-0.76
3	CRP 54	32.167	43.933	38.050	-1.14	30.333	46.000	38.167	-0.87
4	CRP 7	76.067	36.667	56.367	1.62	34.367	25.767	30.067	0.42
5	CRP 34	33.467	20.967	27.217	1.17	35.800	32.800	34.300	0.14
6	CRP 48	56.000	29.233	42.617	1.49	65.600	55.133	60.367	0.27
7	CRP 8	23.467	11.000	17.233	1.66	27.967	34.833	31.400	-0.42
8	CRP 51	34.100	22.500	28.300	1.06	43.167	45.600	44.383	-0.10
9	CRP 49	70.333	36.633	53.483	1.50	48.767	28.133	38.450	0.72
10	CRP 43	31.100	41.500	36.300	-1.05	35.900	39.267	37.583	-0.16
11	CRP 20	30.933	28.967	29.950	0.20	42.000	30.200	36.100	0.48
12	CRP 27	41.200	32.633	36.917	0.65	27.067	38.833	32.950	-0.74
13	CRP 42	62.700	42.400	52.550	1.01	25.633	38.400	32.017	-0.84
14	CRP 50	50.233	21.500	35.867	1.79	38.767	36.267	37.517	0.11
15	CRP 30	31.300	22.633	26.967	0.87	38.267	20.333	29.300	0.79
16	CRP 21	38.200	35.167	36.683	0.25	44.400	29.567	36.983	0.57
17	CRP 18	32.900	30.167	31.533	0.26	37.600	40.000	38.800	-0.11
18	CRP 45	40.867	15.467	28.167	1.94	37.200	36.400	36.800	0.04
19	CRP 33	31.833	25.167	28.500	0.65	44.533	32.900	38.717	0.44
20	CRP 40	27.200	35.667	31.433	-0.97	40.933	31.100	36.017	0.41
21	CRP 46	72.967	26.967	49.967	1.97	41.667	37.967	39.817	0.15
22	CRP 52	34.633	15.000	24.817	1.77	30.100	31.633	30.867	-0.09
23	CRP 16	40.167	31.433	35.800	0.68	38.133	27.533	32.833	0.47
24	CRP 15	32.933	13.000	22.967	1.89	46.267	35.700	40.983	0.39
25	PBW 343	49.500	10.167	29.833	2.48	28.767	31.567	30.167	-0.16
	Mean (DOS)	40.813	27.763	**(Fe)**		37.603	35.380	**(Zn)**	
	C.V.			**16.55812**				**13.31979**	

Table 4.4: Table of C.D. and S.E. of Fe content in wheat

Factors	C.D.	SE(d)	SE(m)
Genotype	6.336	3.188	2.254
DOS	1.792	0.902	0.638
Genotype X DOS	8.961	4.508	3.188

Table 4.5: Table of C.D. and S.E. of Zn content in wheat

Factors	C.D.	SE(d)	SE(m)
Genotype	5.427	2.731	1.931
DOS	1.535	0.772	0.546
Genotype X DOS	7.675	3.862	2.731

4.1.2 Heat Susceptibility Index

HSI was calculated based on the reduction in Fe and Zn content in various genotypes due to heat stress imposed as a result of delayed sowing versus normal sown conditions over the two dates of sowing. It was observed that the HSI for most of the genotypes was positive, i.e. the Fe and Zn accumulation in grains reduced in the late sown conditions from that of the normal sown conditions. However, in few genotypes such as HD 2967, CRP 37, CRP 54, and CRP 43, the HSI for both Fe and Zn content was found negative as the content of two nutrients increased under the late sown conditions. The genotypes CRP 8, CRP 51, CRP 27, CRP 42, CRP 18, CRP 52 and PBW 343 showed negative HSI for Zn and positive for Fe as there was an increase in the content of Zn only under late sown conditions. While for the genotype CRP 40, the HSI was negative for the Fe and positive for the Zn as there was an increase in Fe content only under heat stress (**Fig. 4.1**).

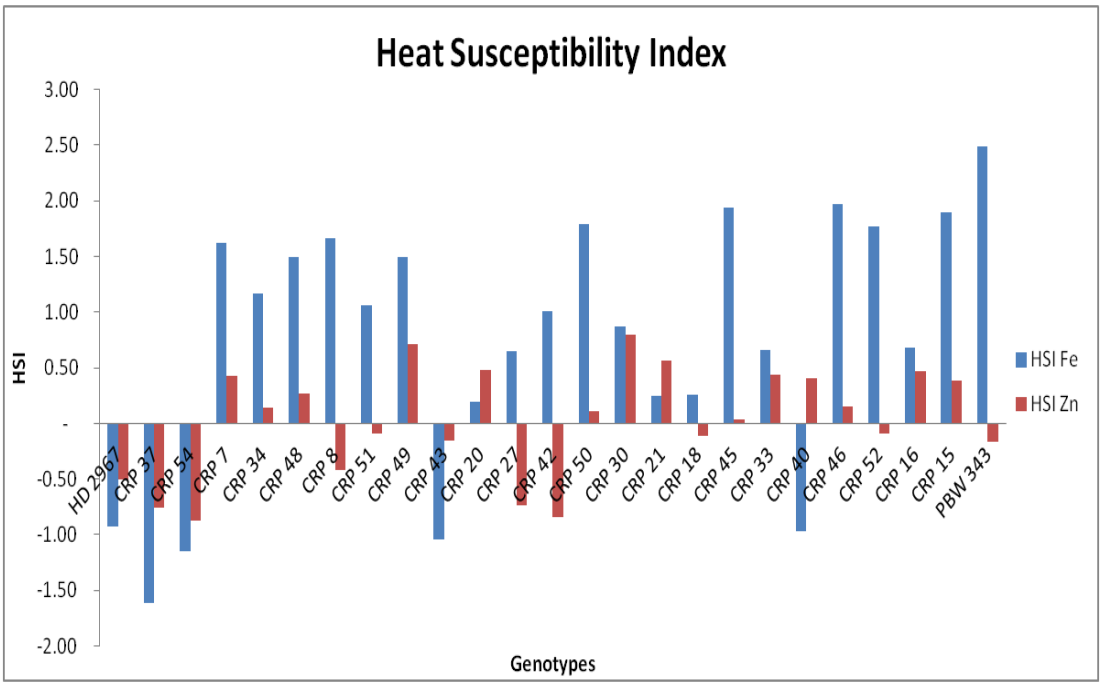

Fig. 4.1: Bar graph showing HSI of the genotypes under study concerning Fe and Zn accumulation in seed under heat stress

4.1.3 Cluster analysis

Fe content data over two dates of sowing were subjected to cluster analysis, and three major clusters were obtained concerning Fe content accumulation and sensitivity of the genotypes understudy for the heat stress over two dates of sowing (**Fig. 4.2**). By comparing the Fe content of the genotypes in various clusters, it was observed that the first cluster consisted of genotypes CRP 42, CRP 50, CRP 7, PBW 343, CRP 46, CRP 49 and CRP 48 which were high Fe accumulators. The second cluster consisted of HD 2967, CRP 20, CRP 18, CRP 34, CRP 51, CRP 30, CRP 33, CRP 45, CRP 52, CRP 15, and CRP 8 which were low Fe accumulators. The rest of the genotypes which were average Fe accumulators fell under 3rd cluster.

On the other hand, four major clusters were observed for the distribution of Zn content data over two dates of sowing in 25 genotypes (**Fig. 4.3**). The first cluster consisted of genotypes CRP 27, CRP 42, CRP 52, CRP 8, PBW 343, and HD 2967. The second cluster consisted of genotypes CRP 37, CRP 54, CRP 51, CRP 43, CRP 18, CRP 46, CRP 50 and CRP45. The genotype CRP 48 which had the highest Zn and Fe accumulation in the grain, formed a monogenotypic cluster. The fourth cluster consisted of the rest of the genotypes.

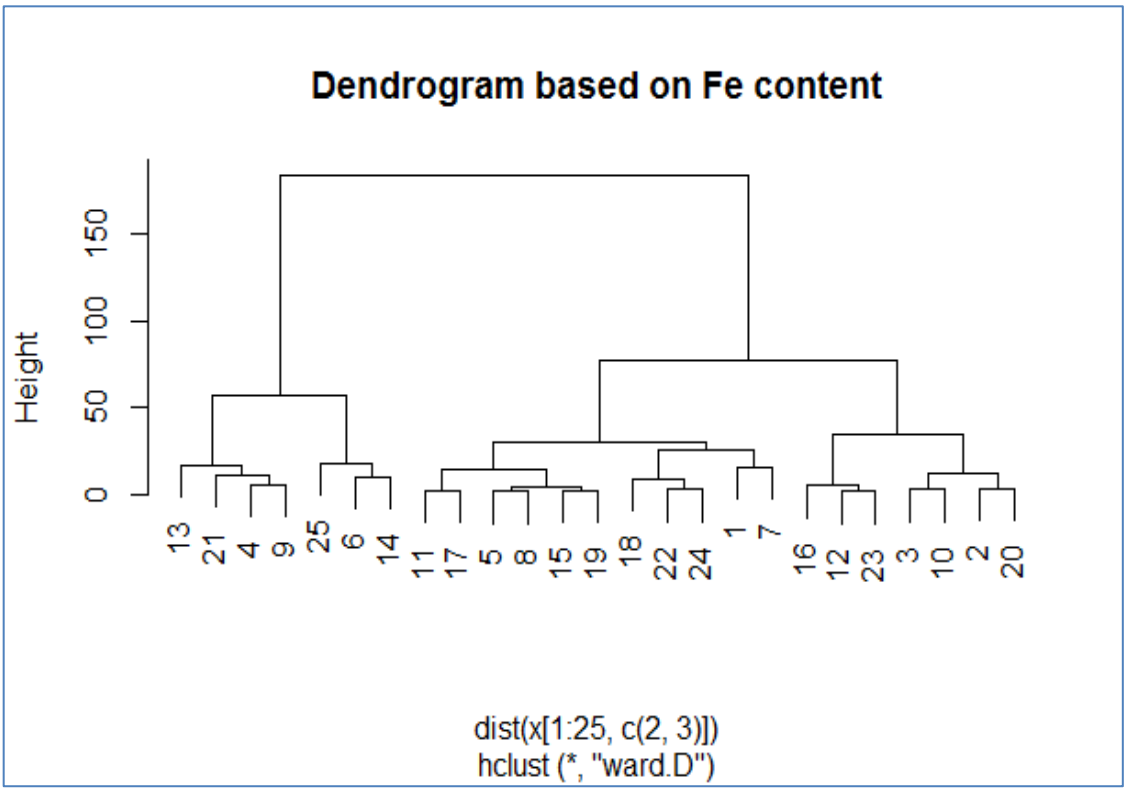

Fig. 4.2: Dendrogram based on Fe content in wheat grain

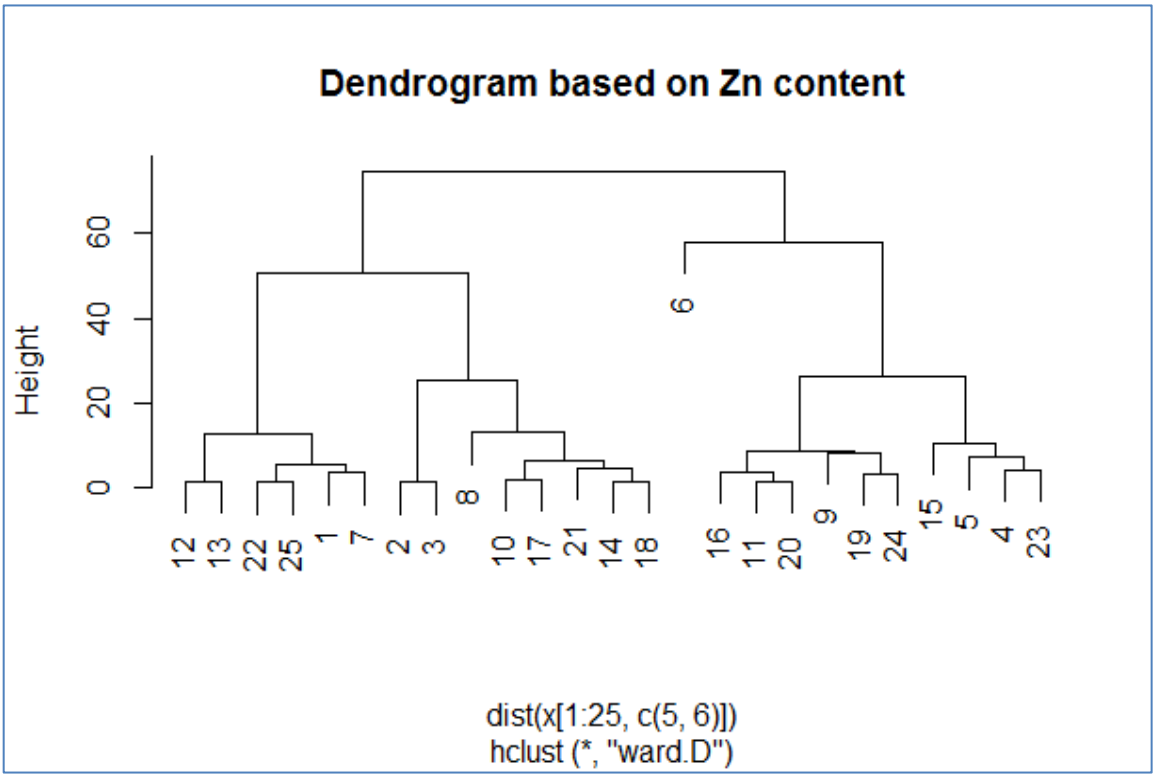

Fig. 4.3: Dendrogram based on Zn content in wheat grain

4.2 In silico analysis

4.2.1 Finding true orthologs of the gene in the wheat genome

First, AtYSL1 was selected as a reference gene as it was directly related to the seed loading of micronutrients and the most characterized among the YSLs. It worked along with AtYSL3 as a pair of membrane transporters involved in the seed loading of micronutrients. Retrieved genomic sequence of the AtYSL1 was used to perform BLASTn on the wheat genome. The aligned segments were compiled together resulting in the specification of a region on the 2nd chromosome of each of the wheat A, B & D genomes. The sequences were then aligned with the location of a probable gene as per TGACv1 Annotation. The obtained aligned region is depicted in **Fig. 4.4**. The obtained length of alignment was very short (50-52 bp) with a high e-value (0.0091 to 0.14).

The probable protein sequences were obtained from EnsEMBL (**Fig. 4.5 to Fig. 4.7**) and BLASTp was performed using UniProtKB on all well characterized YSL proteins. The highest match was obtained with OsYSL9, followed by OsYSL16, OsYSL2 and AtYSL3 (**Fig. 4.8**). It may be assumed that the true ortholog of AtYSL1 was not present on the wheat genome as Arabidopsis is a dicot plant, and wheat a monocot belonging to Poaceae. Considering the facts above AtYSL1 could not be taken as a reference gene.

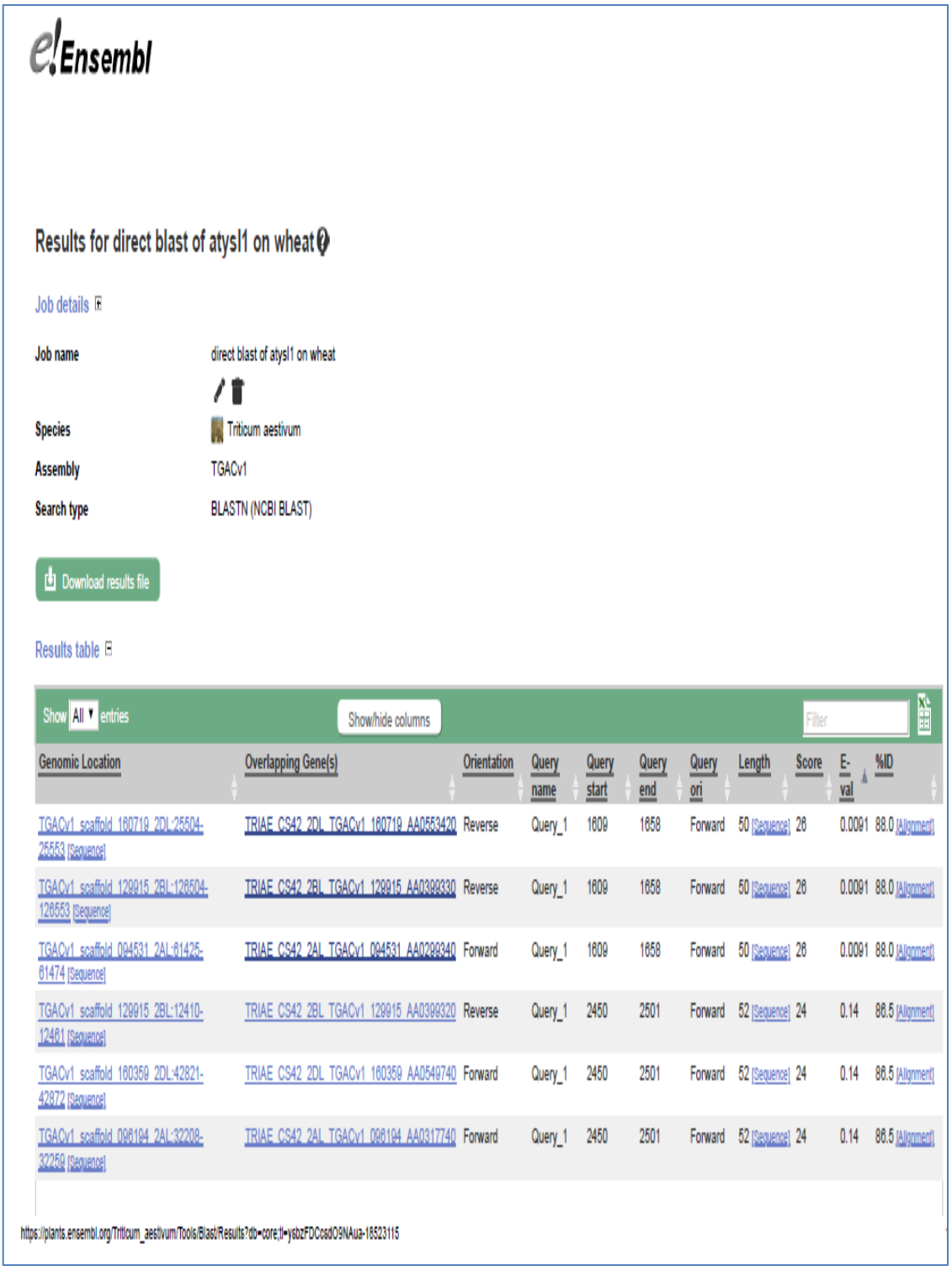

Ensembl

Results for direct blast of atysl1 on wheat

Job details

Job name	direct blast of atysl1 on wheat
Species	Triticum aestivum
Assembly	TGACv1
Search type	BLASTN (NCBI BLAST)

Download results file

Results table

Show All entries | Show/hide columns | Filter

Genomic Location	Overlapping Gene(s)	Orientation	Query name	Query start	Query end	Query ori	Length	Score	E-val	%ID
TGACv1_scaffold_160719_2DL:25504-25553 [Sequence]	TRIAE_CS42_2DL_TGACv1_160719_AA0553420	Reverse	Query_1	1609	1658	Forward	50 [Sequence]	26	0.0091	88.0 [Alignment]
TGACv1_scaffold_129915_2BL:126504-126553 [Sequence]	TRIAE_CS42_2BL_TGACv1_129915_AA0398330	Reverse	Query_1	1609	1658	Forward	50 [Sequence]	26	0.0091	88.0 [Alignment]
TGACv1_scaffold_094531_2AL:61425-61474 [Sequence]	TRIAE_CS42_2AL_TGACv1_094531_AA0298340	Forward	Query_1	1609	1658	Forward	50 [Sequence]	26	0.0091	88.0 [Alignment]
TGACv1_scaffold_129915_2BL:12410-12461 [Sequence]	TRIAE_CS42_2BL_TGACv1_129915_AA0398320	Reverse	Query_1	2450	2501	Forward	52 [Sequence]	24	0.14	86.5 [Alignment]
TGACv1_scaffold_160359_2DL:42821-42872 [Sequence]	TRIAE_CS42_2DL_TGACv1_160359_AA0549740	Forward	Query_1	2450	2501	Forward	52 [Sequence]	24	0.14	86.5 [Alignment]
TGACv1_scaffold_096194_2AL:32208-32259 [Sequence]	TRIAE_CS42_2AL_TGACv1_096194_AA0317740	Forward	Query_1	2450	2501	Forward	52 [Sequence]	24	0.14	86.5 [Alignment]

https://plants.ensembl.org/Triticum_aestivum/Tools/Blast/Results?db=core;tl=ysbzFDCsdO9NAua-18523115

Fig. 4.4: BLASTn result of AtYSL1 genomic sequence on wheat genome

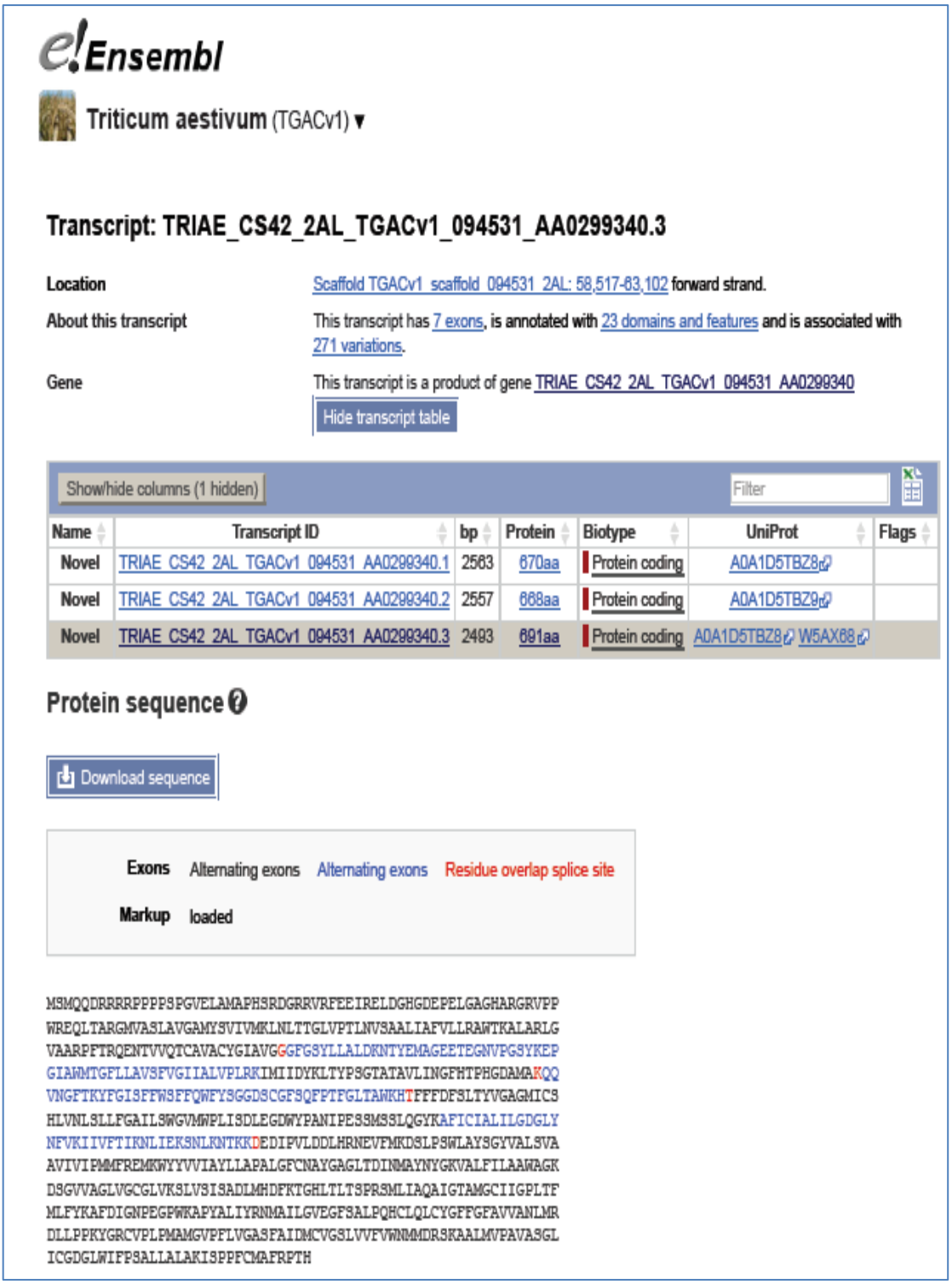

Fig. 4.5: Probable protein sequences of genes from aligned region on 2A chromosome

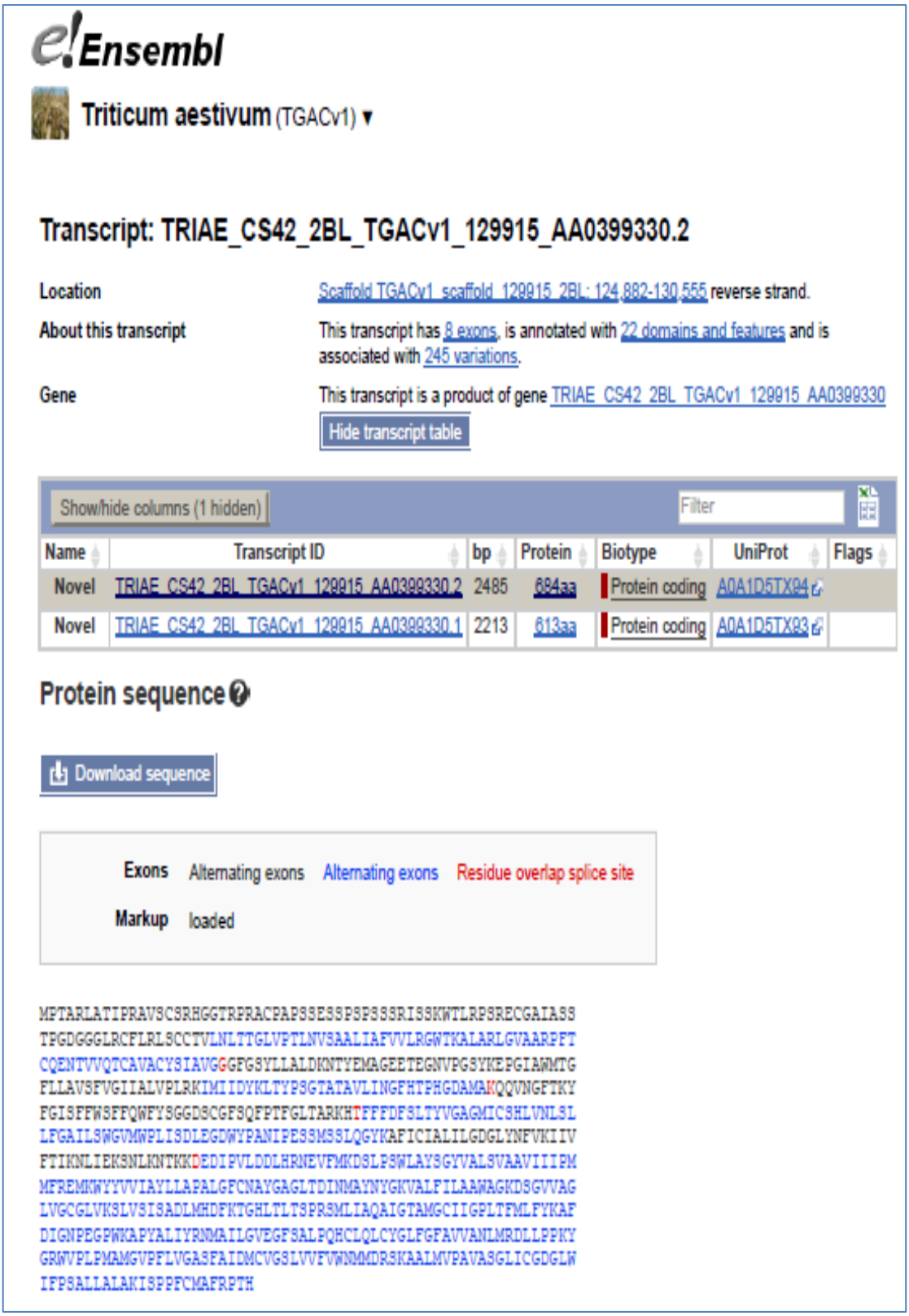

Fig. 4.6: Probable protein sequences of genes from aligned region on 2B chromosome

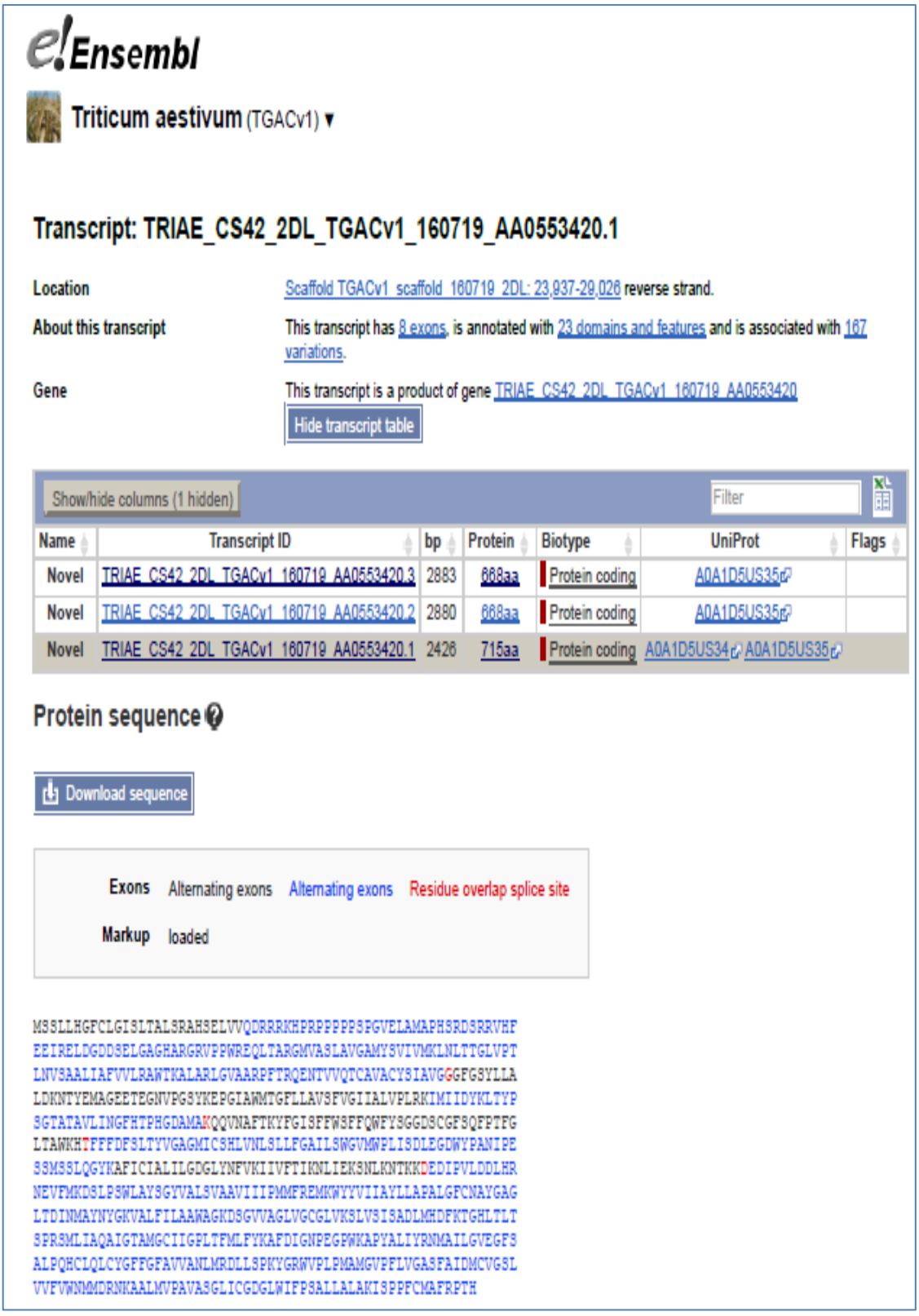

Fig. 4.7: Probable protein sequences of genes from aligned region on 2D chromosome

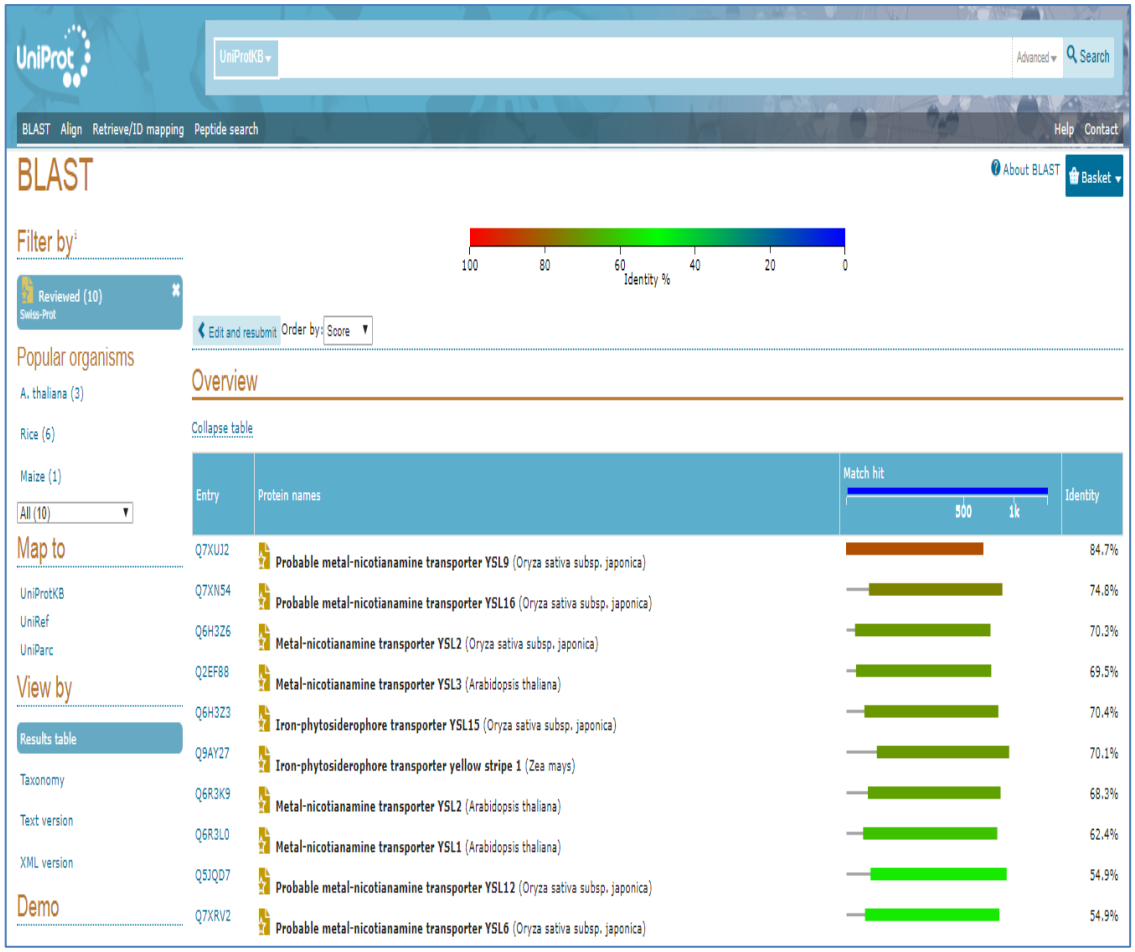

Fig. 4.8: BLASTp of retrieved protein sequence with well characterized proteins

Rice, a monocot, belonging to family Poaceae is relatively more closely related to wheat. Thus its well-characterised YSL genes instead of the arabidopsis genes were taken as reference for further study. Among the well-characterized OsYSLs, the OsYSL2 was selected as the reference gene for finding its ortholog(s) in wheat as it expresses in phloem near spike and is directly responsible for metal-NA loading into the seed. BLAST of the genomic sequence of OsYSL2 on the wheat genome (IWGSC, 2018) revealed various sites of alignment, with the highest alignment (389) and lowest e-value (1.3*e-104) on chromosome 6 of B genome, followed by D and A genome respectively (Table No.4.6). The aligned sequence and the overlapping genes annotated at high confidence by IWGSC were retrieved and saved (**Fig. 4.9**). Then the homeologues of the obtained genes on all the three genomes were retrieved from homeologues tool on EnsEMBL (**Fig. 4.10**). It was found that the three genes with the highest alignment were homeologues of each other.

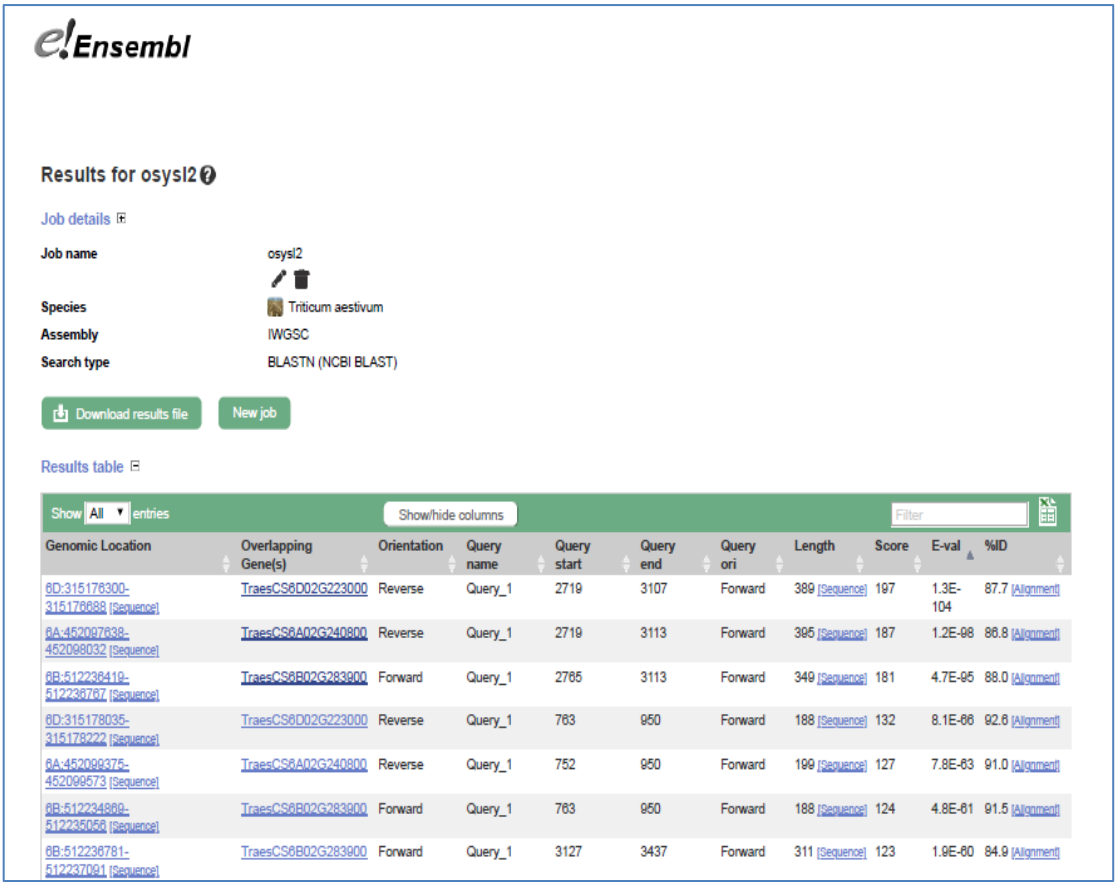

Fig. 4.9: BLASTn result of OsYSL2 genomic sequence on wheat genome

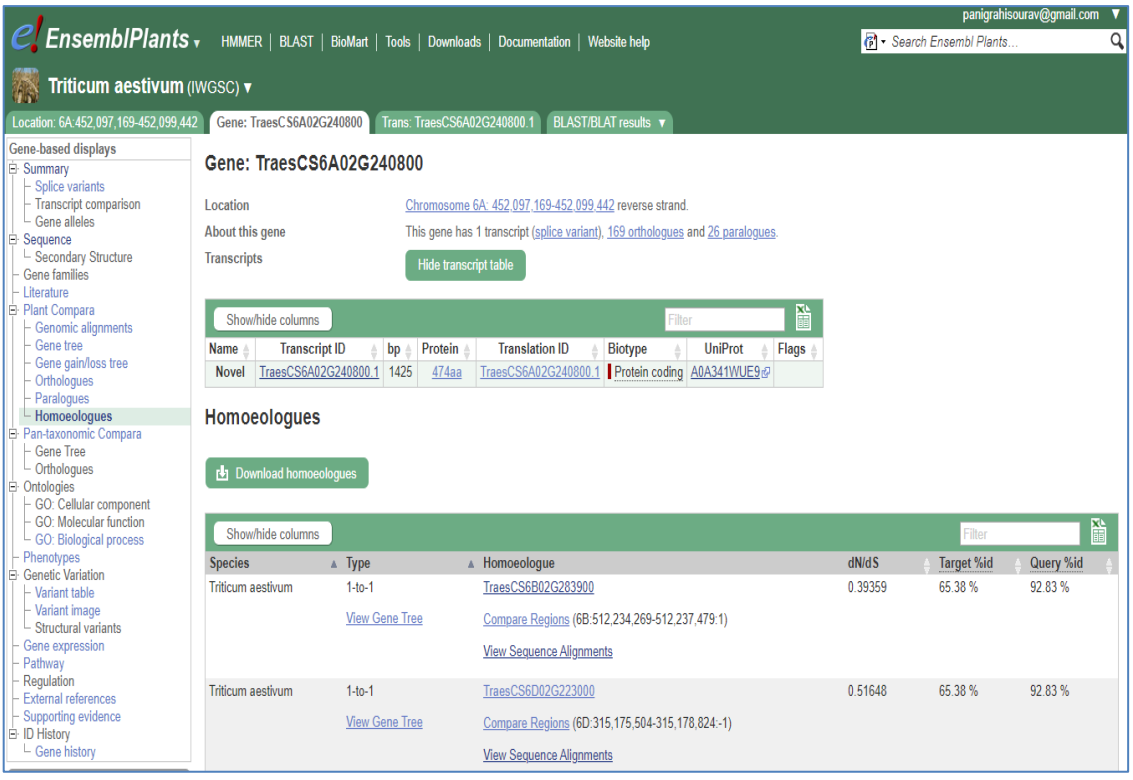

Fig. 4.10: Homeologues of TaYSL2-6A on B and D genome in wheat

Table 4.6: Information of Gene TaYSL2

Gene name	Gene ID (IWGSC)	Gene length (bp)	Length of mRNA	Length of protein	UNIProt ID (functional)	Location on wheat genome
TaYSL2-6A	TraesCS6A02G240800	2274	1425	474	A0A3B6NSL5	Chromosome 6A: 452,097,169-452,099,442 reverse strand
TaYSL2-6B	TraesCS6B02G283900	3211	2381	673	A0A3B6PQ61	Chromosome 6B: 512,234,269-512,237,479 forward strand
TaYSL2-6D	TraesCS6D02G223000	3321	2459	673	A0A3B6QHY3	Chromosome 6D: 315,175,504-315,178,824 reverse strand

The probable protein sequence of the three genes was retrieved (**Fig. 4.11 to Fig. 4.13**) and was used to perform BLASTp. The resulting BLAST result showed the highest score (2,966) and identity (83.4%) to the protein sequence of OsYSL2 (**Fig. 4.14**). Thus, the genes obtained were confirmed to be the true orthologs of OsYSL2 in wheat.

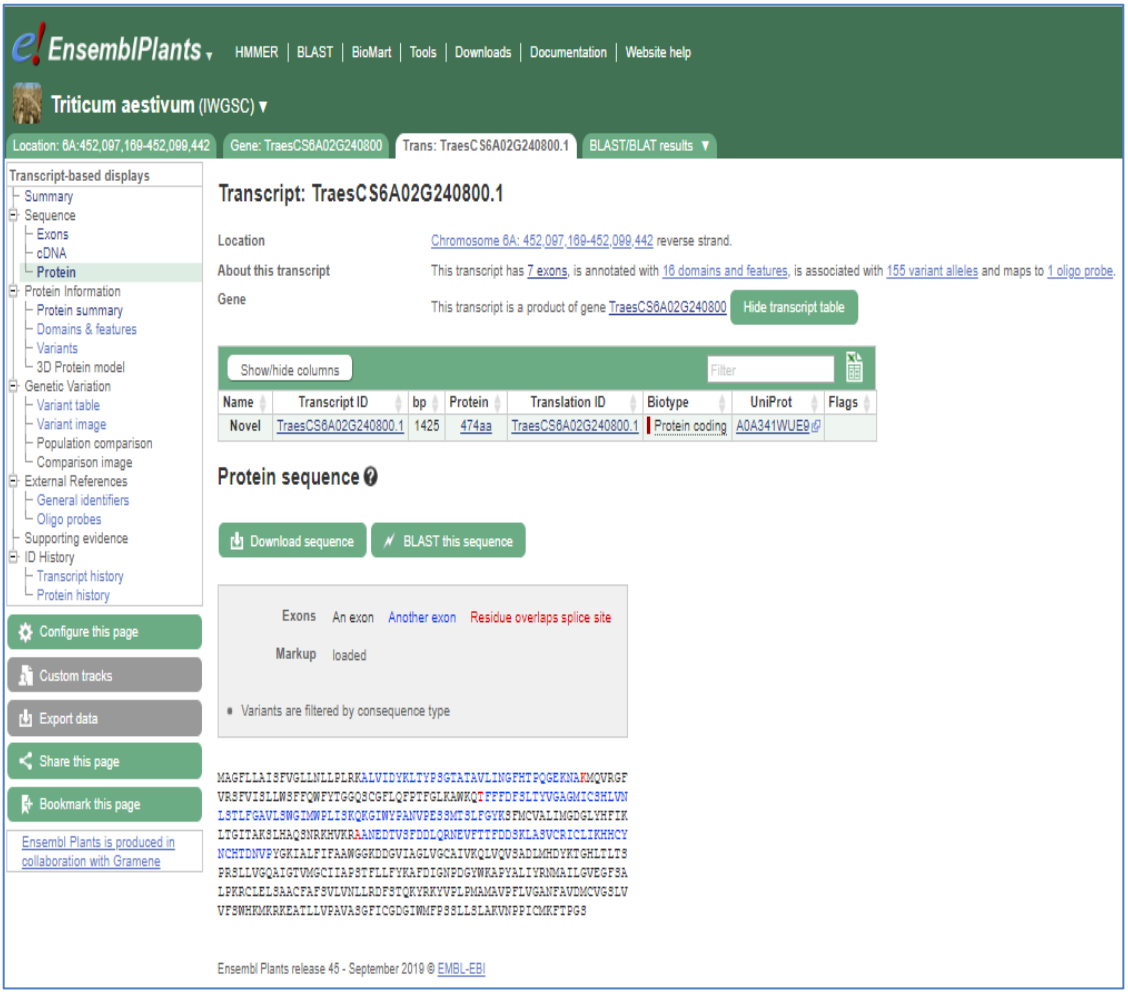

Fig. 4.11: Retrieving protein sequence of TaYSL2-6A

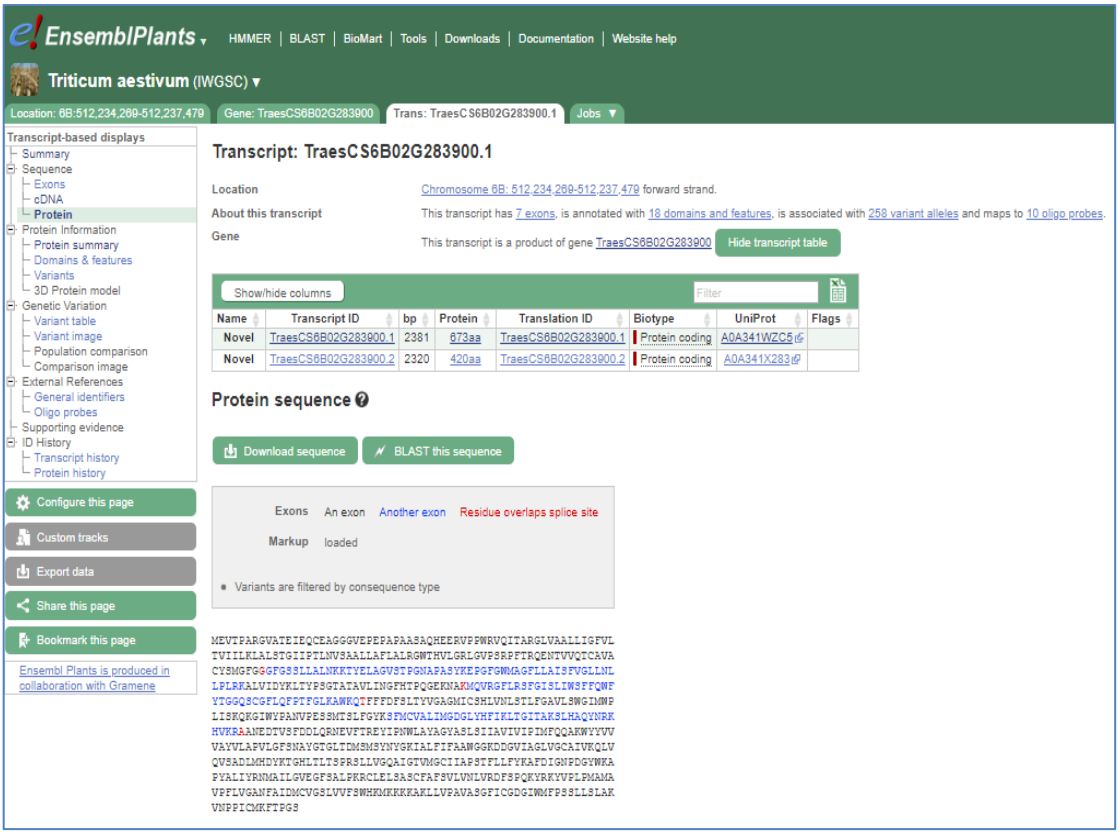

Fig. 4.12: Retrieving protein sequence of TaYSL2-6B

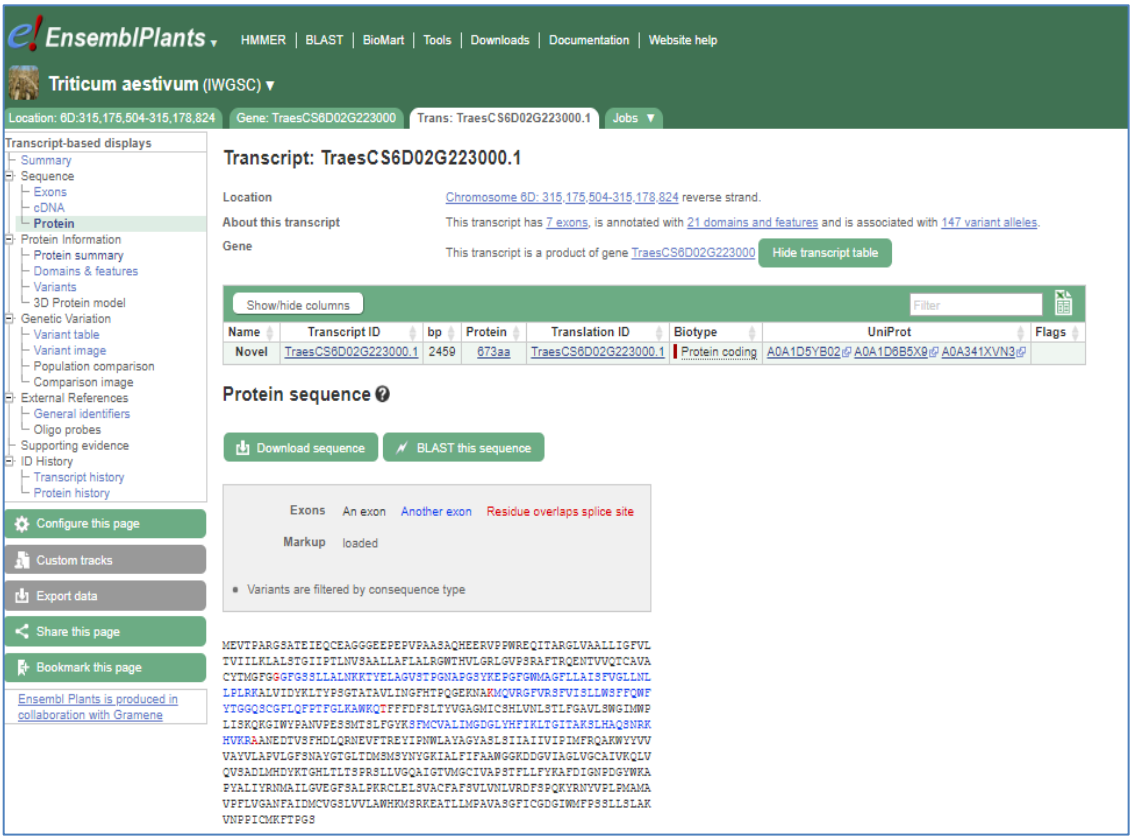

Fig. 4.13: Retrieving protein sequence of TaYSL2-6D

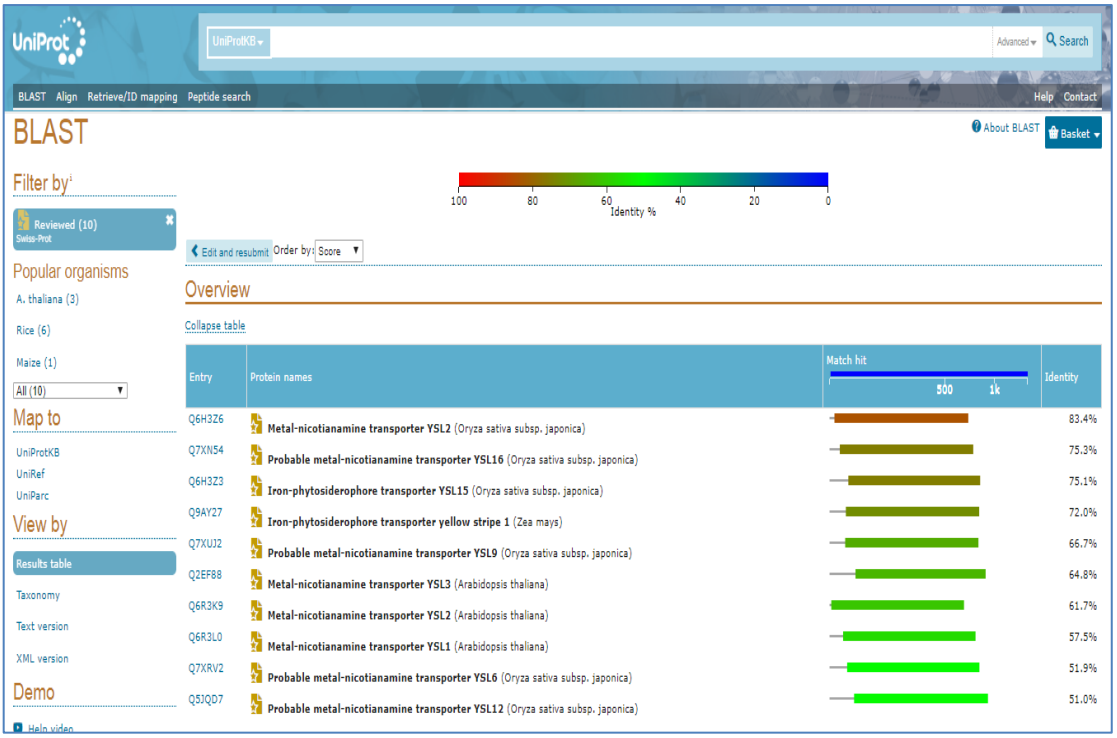

Fig. 4.14: BLASTp of protein sequence of TaYSL2 with well characterized proteins

4.2.2 Marking Intron Exon boundaries

The mRNA transcript sequences and the genomic sequences of the obtained gene and its homeologues i.e., TaYSL2-6A, TaYSL2-6B, and TaYSL2-6D, were retrieved from the EnsEMBL. The genomic sequence of each gene and its mRNA sequence were aligned in ClustalW software, and the alignment showed that there were 6 introns and 7 exons in each of the genes. The number of exons and introns and their length are given in table 4.7 and table 4.8. It was seen that the number of exons and introns did not vary between the homeologues. However, the total length of the transcripts and length of the exons, introns and total length of gene varied considerably (**Table 4.7 & 4.8**; **Fig. 4.15**).

Table 4.7: Comparison of length of exons in the homeologues of TaYSL2

	Exon 1	Exon 2	Exon 3	Exon 4	Exon 5	Exon 6	Exon 7	mRNA
6A	63	98	135	190	115	143	681	1425
6B	498	173	98	135	190	115	1172	2381
6D	498	173	98	135	190	115	1250	2459

Table 4.8: Comparison of length of introns in the homeologues of TaYSL2

	Inton 1	Inton 2	Inton 3	Inton 4	Inton 5	Inton 6
6A	392	91	96	89	75	106
6B	112	360	93	90	89	86
6D	114	395	93	96	89	75

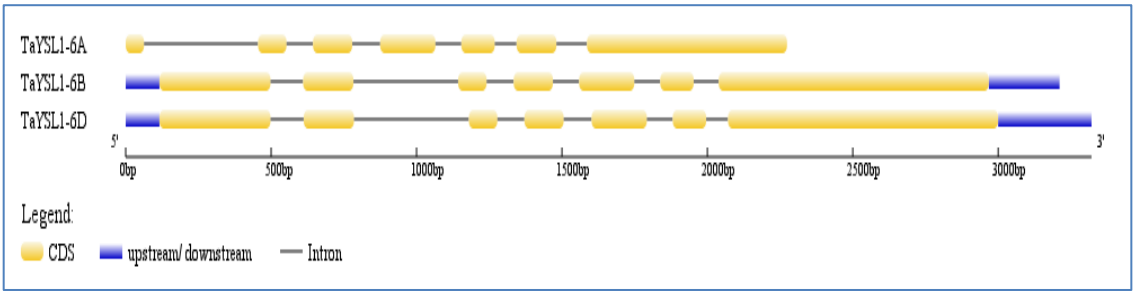

Fig. 4.15: Gene structures of the TaYSL2 gene homeologues

4.2.3 3D protein structure prediction

The protein structures were predicted from PHYRE2 software by the HMM method. The results showed that the C- terminal of the proteins was showing high homology with the structure of folate ecf transporter, a transport protein, and thus the structure was colour coded with high confidence, i.e. 60.1%, from a.a. 364 - 458 in TaYSL2-6A, 58.8% confidence from a.a. 569 - 656 in TaYSL2-6B, 51.7% confidence from a.a. 569 - 656 in TaYSL2-6D. The TaYSL2-6D and TaYSL2-6B sequences were also aligned with a tric trimeric intracellular cation channel2 orthologue from *Rhodobacter sphaeroides* with 53.4% confidence from a.a. 556 - 667 and 46.2% confidence from a.a. 547-667 respectively. While this alignment was absent with TaYSL2-6A. In addition to this, the TaYSL2-6D also showed homology with an uncharacterized structural membrane protein involved in cation exchange with 53.6% confidence from a.a. 565 - 667. However, such homology could not be observed with TaYSL2-6A and TaYSL2-6B protein sequences. The protein structure of TaYSL2-6D also aligned with the reported structure of sll0855 protein, a slow cyanobacterial Cl^- /H^+ antiporter with moderately high confidence, i.e., 47.5%. Whereas, the sll0855 protein exhibited an alignment of 39.4% confidence with the TaYSL2-6A and no homology with the TaYSL2-6B protein (**Fig. 4.17 to Fig. 4.19**).

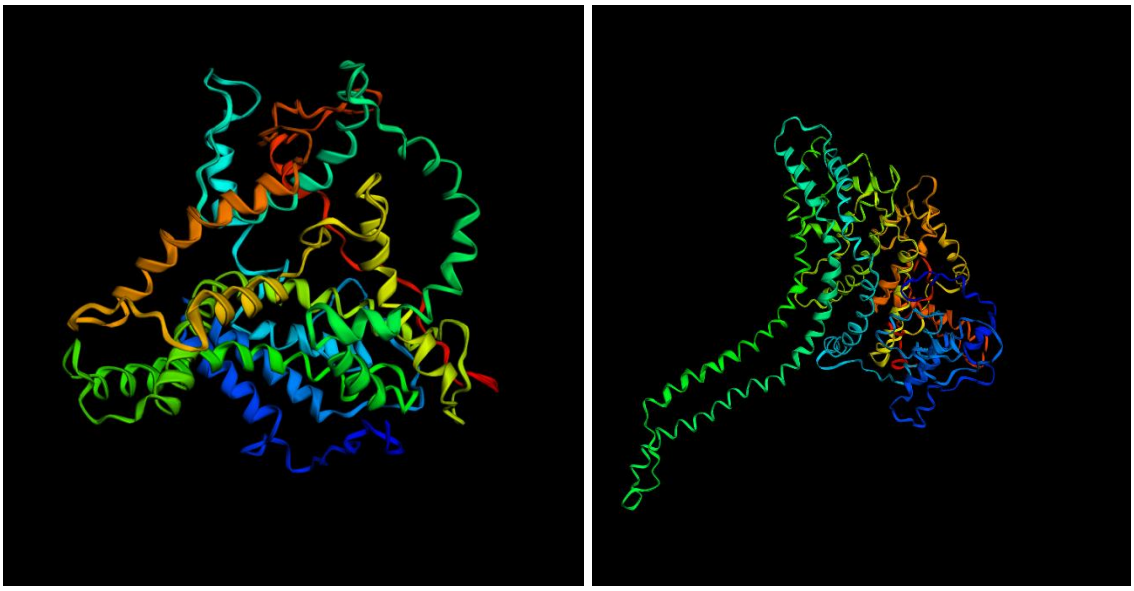

TaYSL2-6A **TaYSL2-6B**

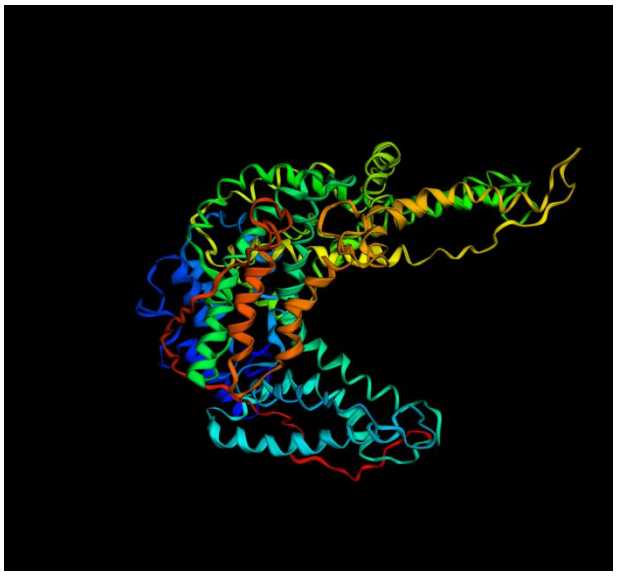

TaYSL2-6D

Fig. 4.16: Predicted protein structures of TaYSL2-6A (1), TaYSL2-6D (2) and TaYSL2-6B (3)

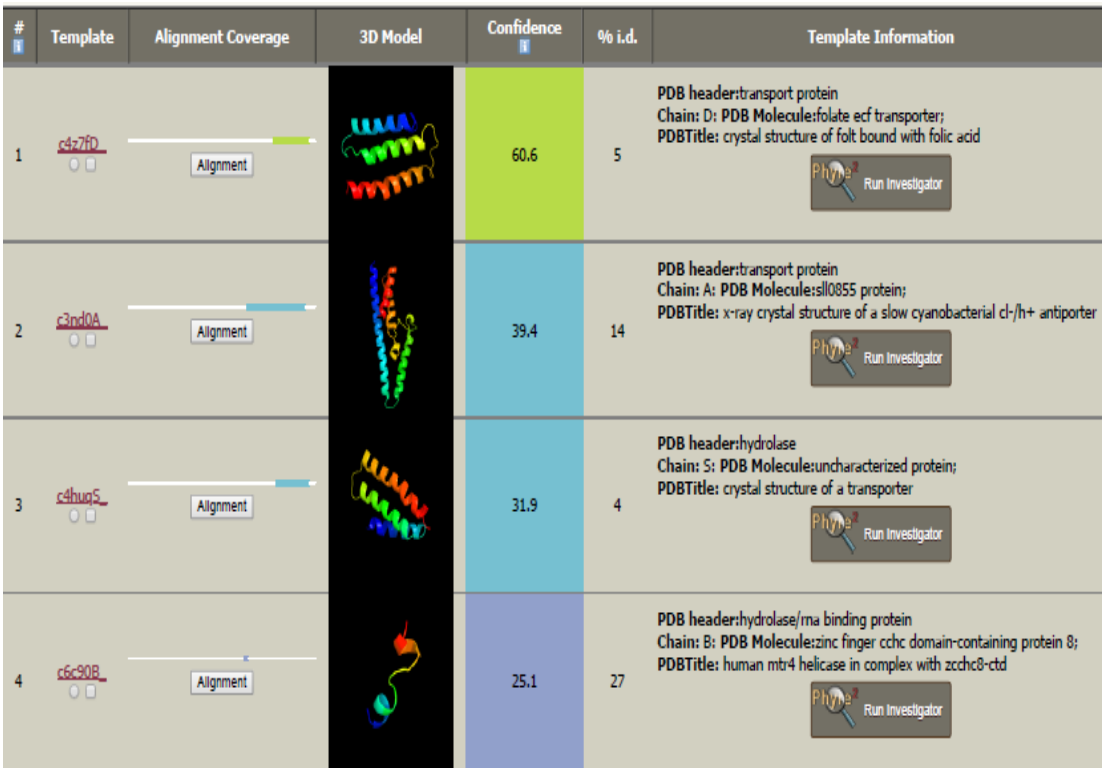

#	Template	Alignment Coverage	3D Model	Confidence	% i.d.	Template Information
1	c4z7fD_	Alignment		60.6	5	**PDB header:**transport protein **Chain:** D: **PDB Molecule:**folate ecf transporter; **PDBTitle:** crystal structure of folt bound with folic acid Run Investigator
2	c3nd0A_	Alignment		39.4	14	**PDB header:**transport protein **Chain:** A: **PDB Molecule:**sll0855 protein; **PDBTitle:** x-ray crystal structure of a slow cyanobacterial cl-/h+ antiporter Run Investigator
3	c4huqS_	Alignment		31.9	4	**PDB header:**hydrolase **Chain:** S: **PDB Molecule:**uncharacterized protein; **PDBTitle:** crystal structure of a transporter Run Investigator
4	c6c90B_	Alignment		25.1	27	**PDB header:**hydrolase/rna binding protein **Chain:** B: **PDB Molecule:**zinc finger cchc domain-containing protein 8; **PDBTitle:** human mtr4 helicase in complex with zcchc8-ctd Run Investigator

Fig. 4.17: Details of major structural protein alignments with TaYSL2-6A

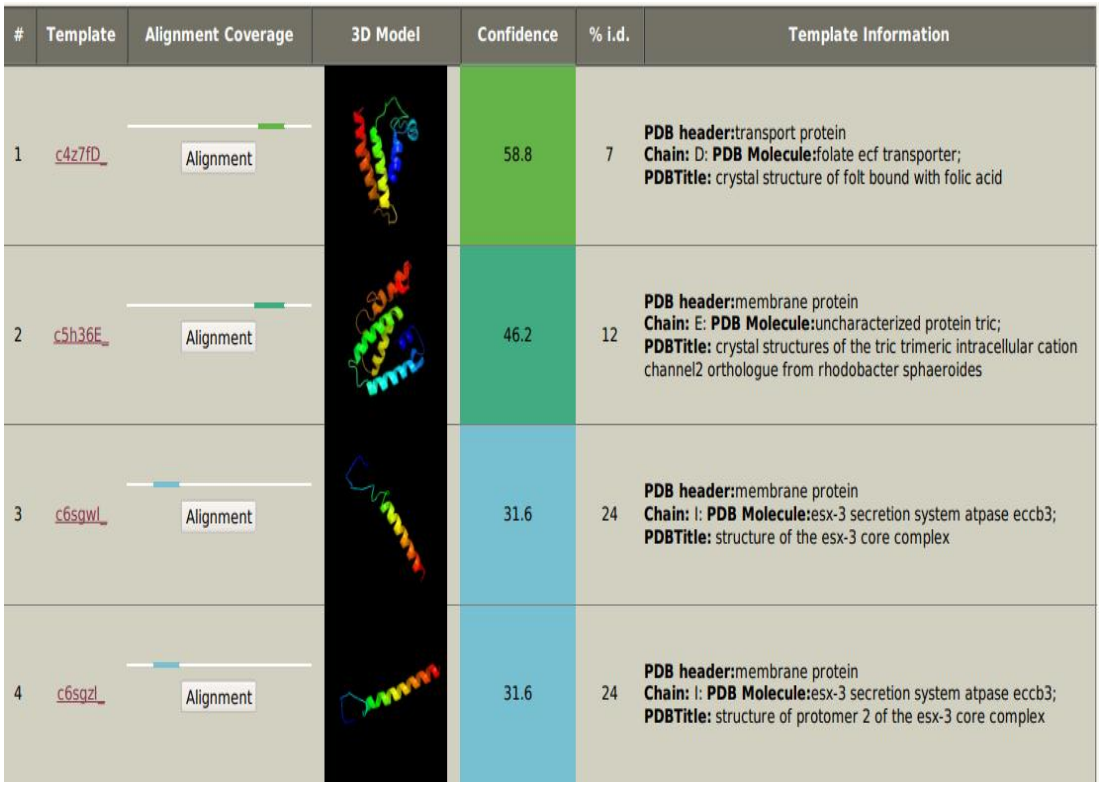

#	Template	Alignment Coverage	3D Model	Confidence	% i.d.	Template Information
1	c4z7fD_	Alignment		58.8	7	**PDB header:**transport protein **Chain:** D: **PDB Molecule:**folate ecf transporter; **PDBTitle:** crystal structure of folt bound with folic acid
2	c5h36E_	Alignment		46.2	12	**PDB header:**membrane protein **Chain:** E: **PDB Molecule:**uncharacterized protein tric; **PDBTitle:** crystal structures of the tric trimeric intracellular cation channel2 orthologue from rhodobacter sphaeroides
3	c6sgwI_	Alignment		31.6	24	**PDB header:**membrane protein **Chain:** I: **PDB Molecule:**esx-3 secretion system atpase eccb3; **PDBTitle:** structure of the esx-3 core complex
4	c6sgzI_	Alignment		31.6	24	**PDB header:**membrane protein **Chain:** I: **PDB Molecule:**esx-3 secretion system atpase eccb3; **PDBTitle:** structure of protomer 2 of the esx-3 core complex

Fig. 4.18: Details of major structural protein alignments with TaYSL2-6B

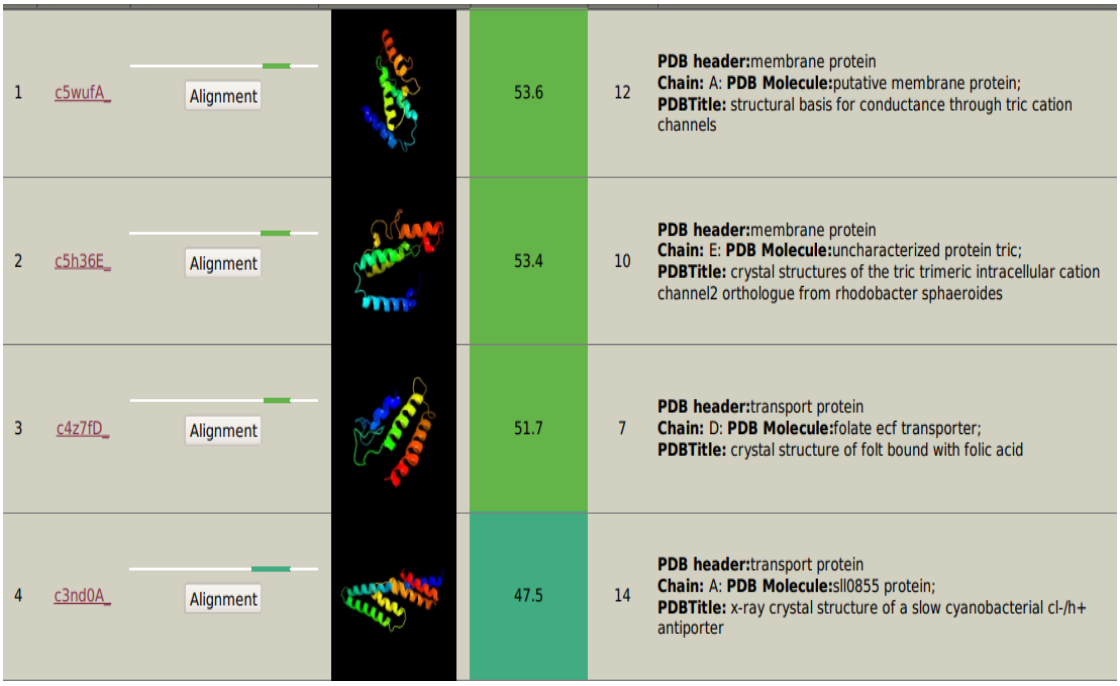

Fig. 4.19: Details of major structural protein alignments with TaYSL2-6D

4.2.4 Conserved domains in the protein

The conserved domain search of the TaYSL2 protein sequences revealed that the proteins belonged to the OPT family in general. OPT transporters are thought to have 12-14 transmembrane domains and contain the SPYxEVRxxVxxxDDP motif. The TaYSL2-6A protein had a Bitscore of 298 and an e-value of 1.04 x e^{-94}. The TaYSL2-6B protein had a Bitscore of 412 and an e-value of 5.99 x e^{-136}. The TaYSL2-6D protein had a Bitscore of 409 and an e-value of 8.88 x e^{-135} (**Table 4.9**). The three proteins were predicted to be highly similar to the protein product of AtYSL3, which is a near homologue of OsYSL2, and is involved loading of NA-chelated metals from phloem to grains.

Table 4.9: Conserved domain analysis of TaYSL2 proteins

	Bitscore	e-value	Domain	Superfamily
TaYSL2-6A	298	1.04 x e^{-94}	OPT	OPT
TaYSL2-6B	412	5.99 x e^{-136}	OPT	OPT
TaYSL2-6D	409	8.88 x e^{-135}	OPT	OPT

4.2.5 In-silico Expression Analysis

Expression of TaYSL2 was observed by transcriptome analysis of five types of tissues at three different points of time during development of the wheat crop, i.e. Z71, Z75, Z85 in grain, Z10, Z23, Z71 in leaf, Z10, Z13, Z39 in root, Z32, Z39, Z65 in spike and Z30, Z32, Z65 in stem. The TaYSL2 was observed to be expressed in very small quantities in leaf, root, spike and stem at any point of time. Its expression was maximum in the grains, especially at Z85 (soft dough stage), i.e., 11.2 FPKM in total. The expression of TaYSL2 increased suddenly at Z65 (half of flowering complete) in the stem and during the period of Z71 (2 DAA) to Z85 in grain (**Fig. 4.20**). The reference for the Zadok scale has been given in **Table 4.11**.

The expression analysis in different tissues of grain revealed that TaYSL2-6B was highly expressed (7.0 to 10.6 RPKM) in comparison to TaYSL2-6A (0.2 to 1.9 RPKM) and TaYSL2-6D (0.9 to 2.3 RPKM). The expression of TaYSL2 was particularly higher in the endosperm as compared to the inner and outer pericarp (**Fig. 4.21**).

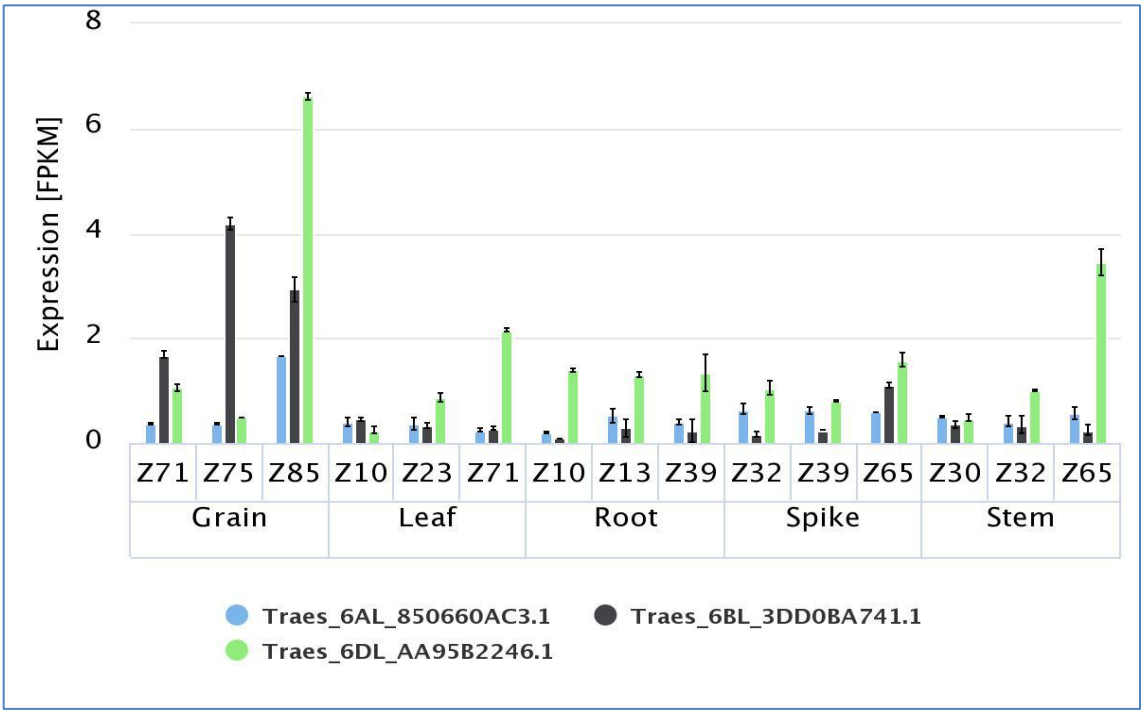

Fig. 4.20: Developmental time course in five tissues expression data graph

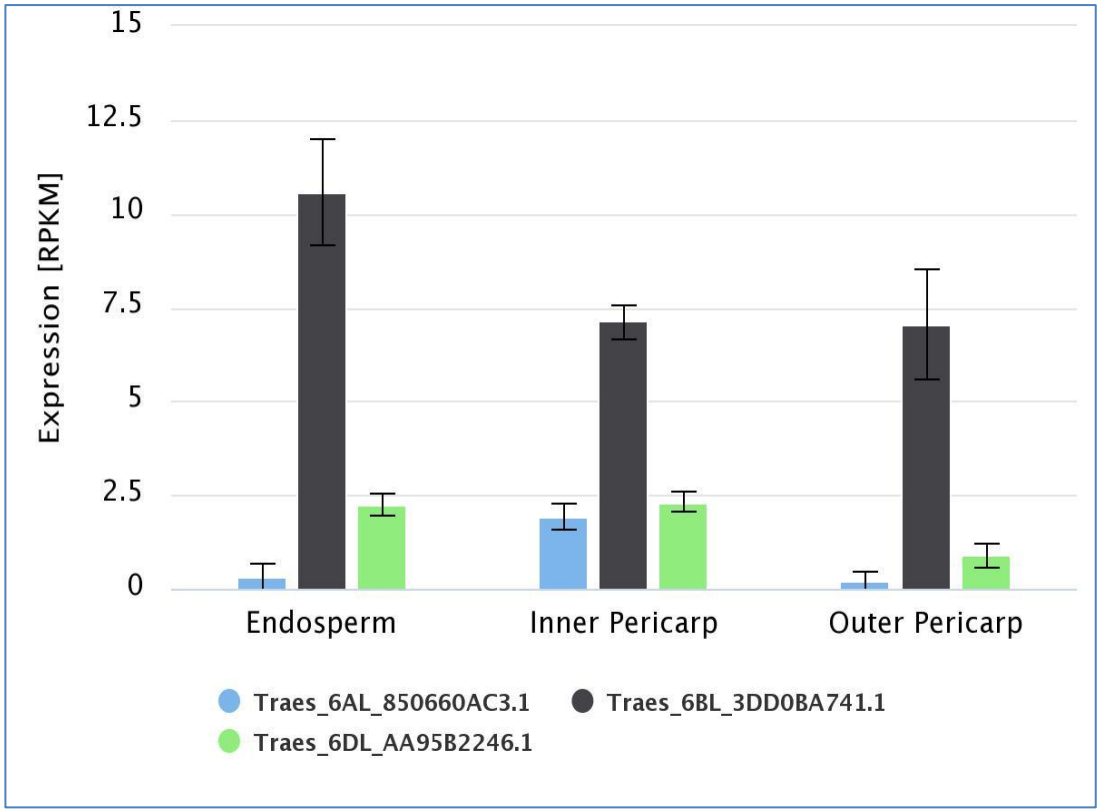

Fig. 4.21: Grain Layers Expression Data Graph

The analysis of the expression of TaYSL2 throughout the developmental stages of grain, i.e., 10 DPA to 30 DPA shows that though the expression was almost consistent in all types of tissues during the period of 10-20 DPA (4.5 to 5.0 FPKM for TaYSL2-6B in endosperm & transfer cells and 2.8 FPKM in Aleuronic layer), the expression among the tissues slightly varied at 30 DPA, with slight increase in expression in aleuronic layer and endosperm (**Fig. 4.22**).

The expression of TaYSL2 was also analyzed in the senescing leaves and it was found that only the TaYSL2-6A and TaYSL-6B were expressed wherein the TaYSL-6B expressing slightly more than TaYSL-6A. The total expression initially increased from a total of 4.1 RPKM to 6 RPKM during the HD stage to 12 DAA and then reduced to 4.1 RPKM by 22 DAA (**Fig. 4.23**).

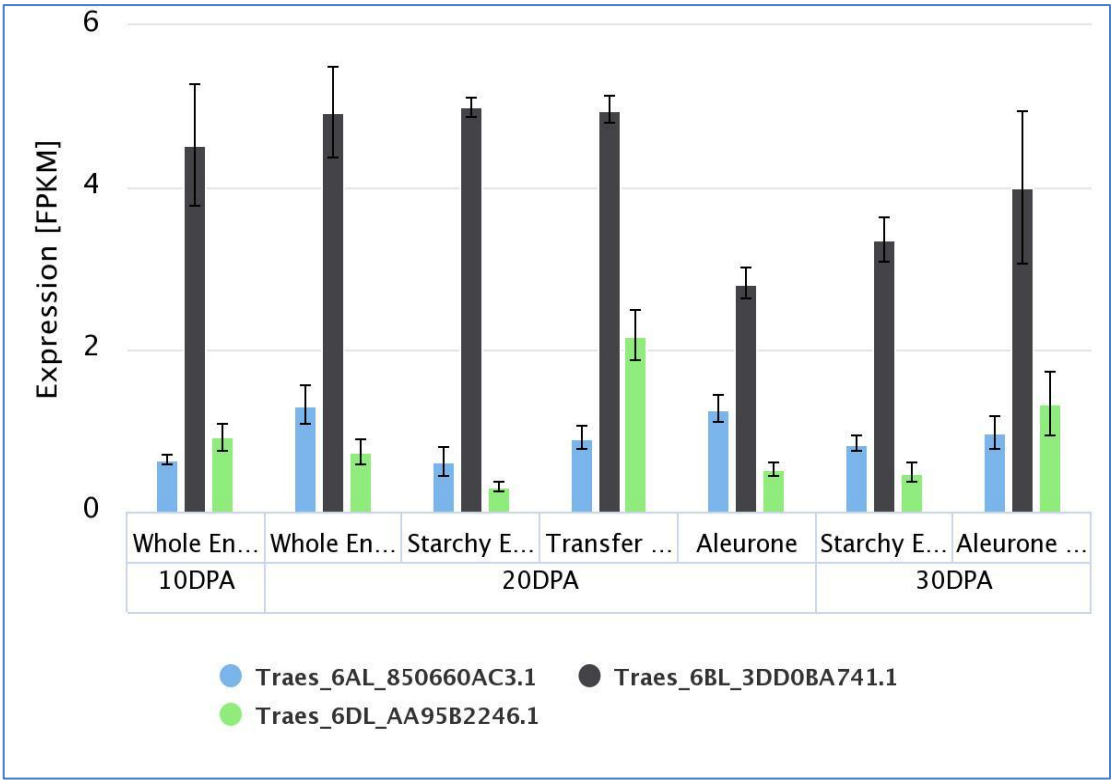

Fig. 4.22: Grain layer developmental time course expression data graph

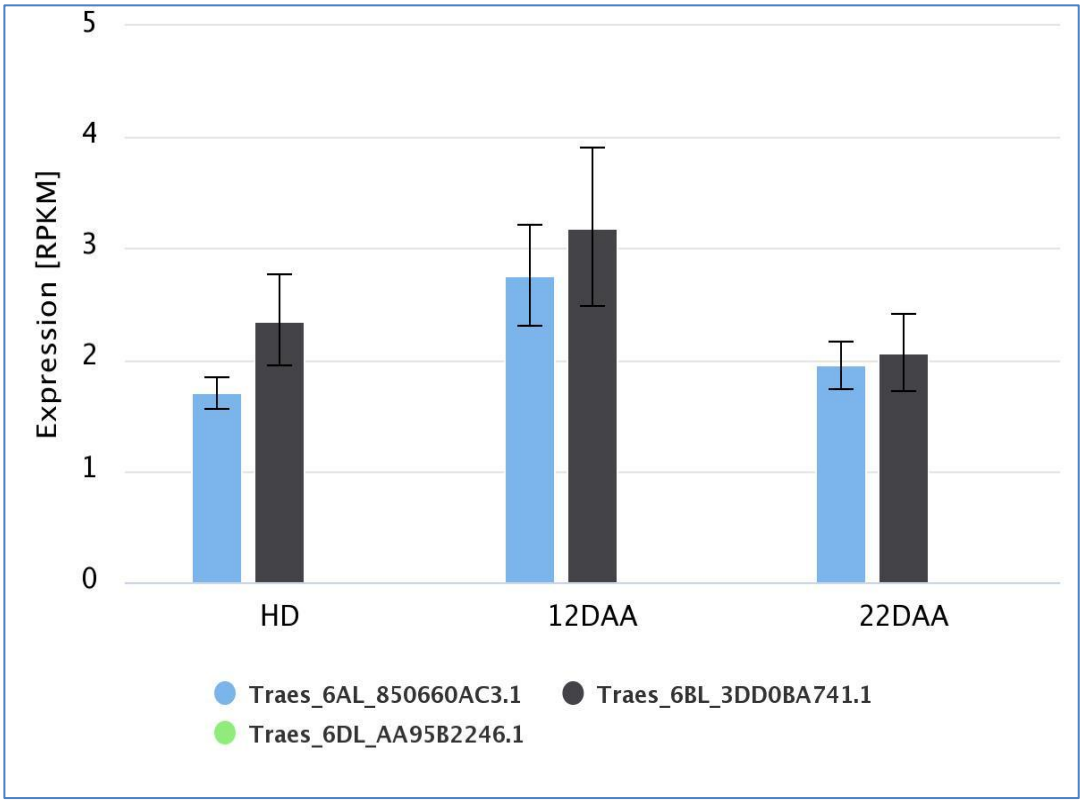

Fig. 4.23: Senescing Leaves time course Expression Data Graph

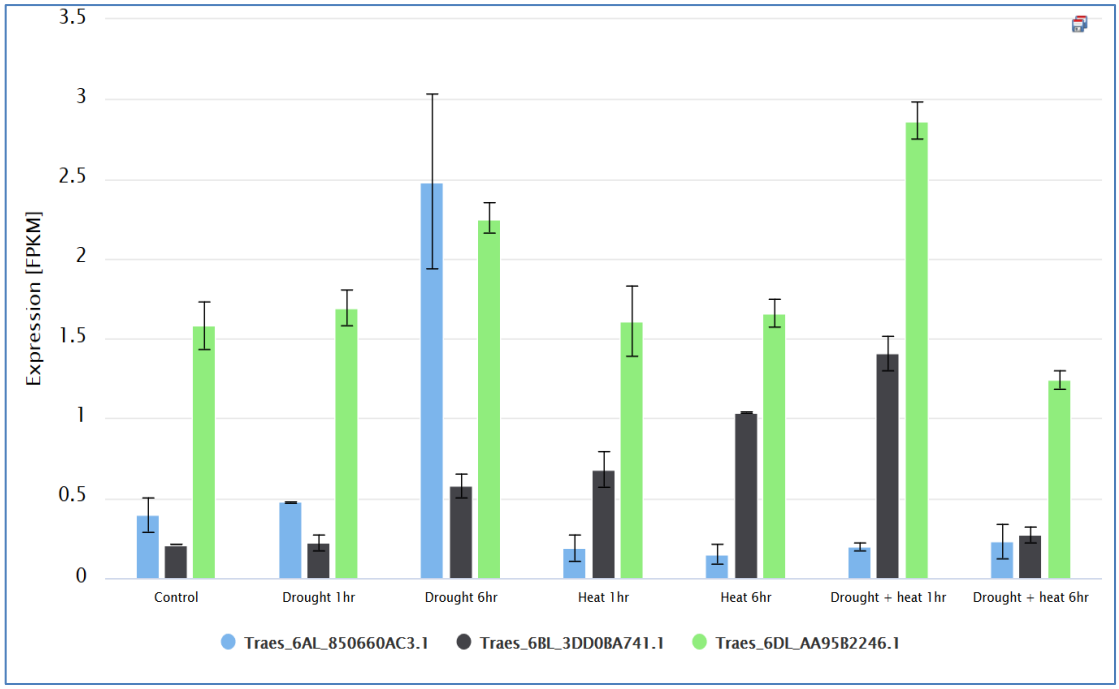

Fig. 4.24: Drought and Heat Stress Expression Data Graph

The expression of TaYSL2 under heat and drought conditions was analysed. It was found that there was almost no change in expression pattern of TaYSL2 after 1 hour drought stress, but after 6 hours of drought stress there was an overall increase in expression of TaYSL2. The expression of TaYSL2-6A increased to about 2.5 FPKM, while expression level of TaYSL2-6B and TaYSL2-6D increased to 0.58 FPKM and 2.25 FPKM respectively. It was observed that under heat stress, there was hardly any change in expression of TaYSL2-6D. In contrast, expression of TaYSL2-6A dropped to 0.19 FPKM and expression of TaYSL2-6B increased to 0.68 FPKM after 1 hour stress and 1.04 FPKM after 6 hours of heat stress. Under combination of heat and drought stress, expression of TaYSL2-6A dropped to about 0.2 FPKM. The expression pattern of TaYSL2-6B and TaYSL2-6D were similar. Expression of TaYSL2-6B increased to 1.41 FPKM after 1 hour stress and reduced to 0.27 FPKM after 6 hours of heat stress while expression of TaYSL2-6D increased to 2.86 FPKM after 1 hour and reduced to 1.24 FPKM after 6 hours of stress condition (**Fig. 4.24**).

The expression data in tabular format has been mentioned in **Appendix A** with the level of expression in different tissues at different periods of time and in different conditions with their error levels.

Table 4.10: Zadoks Scale Table

Stage	Wheat growth stage	Zadoks scale	Leaves	Root	Stem	Spike	Grain
Seedling	First leaf through coleoptile	10	**x**	**x**			
Three leaves	3 leaves unfolded	13		**x**			
Three tillers	Main shoot and 3 tillers	23	**x**				
Spike at 1 cm	Pseudostem erection	30			**x**		
Two nodes	2nd detectable node	32			**x**	**x**	
Meiosis	Flag leaf ligule and collar visible	39		**x**		**x**	
Anthesis	1/2 of flowering complete	65			**x**	**x**	
2 DAA (50°C.days)	Kernel (caryopsis) watery ripe	71	**x**				**x**
14 DAA (350°C.days)	Medium Milk	75					**x**
30 DAA (700°C.days)	Soft dough	85					**x**

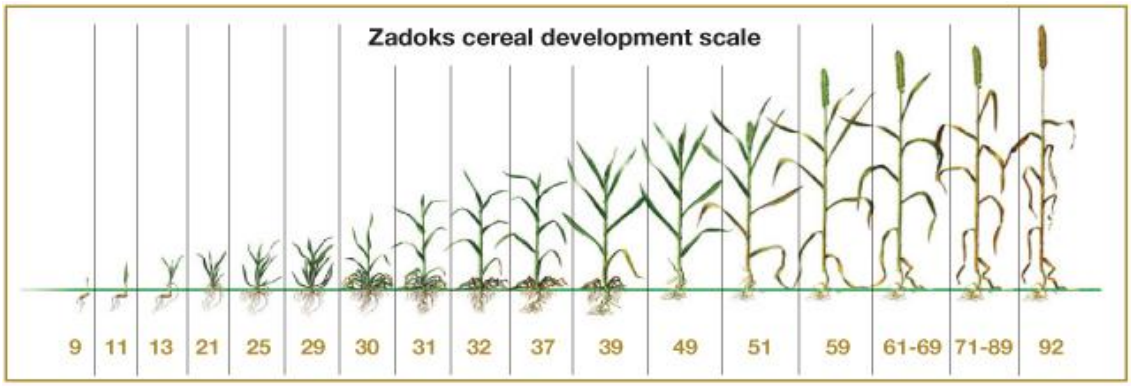

Fig. 4.25: Pictorial illustration of Zadoks cereal development scale

Picture Courtesy: Zadoks JC, Chang TT, Konzak CF. (1974) A decimal code for the growth stages of cereals. Weed Research 14: 415-21.

4.2.6 Identification of members of the YSL gene family in wheat

The BLASTn performed for all the reported OsYSL genes in wheat genome. It resulted in the identification of a total of 63 YSL genes on A, B, and D genomes of wheat. The TaYSLs genes were named according to their corresponding homologues in rice. Their probable protein products were then used for BLASTp on the rice

genome and the results were verified. The genes were further checked for the presence of the YSL specific motif on their probable protein sequence. All the genes with their IWGSC annotation ID, location on the chromosome, length of mRNA, length of protein and orientation have been given in **APPENDIX B.**

4.2.7 Phylogenetic analysis and classification of gene family

The phylogenetic tree based on the neighbor-joining model with Poisson correction and 1000 bootstraps for the proteins of all TaYSL genes revealed that the proteins were divided into 4 major clades. TaYSL2 falls under clade 1 along with TaYSL3, TaYSL9, TaYSL10, TaYSL11, TaYSL19, TaYSL20 & TaYSL21 and some reported YSLs of other crops such as OsYSL2, OsYSL9, OsYSL15, OsYSL16, ZmYS1, AtYSL1 and AtYSL3. The complete Phylogenetic tree has been attached in the **APPENDIX C.** The phylogenetic tree for clade 1 of TaYSLs and OsYSLs has been illustrated in **Fig. 4.26**.

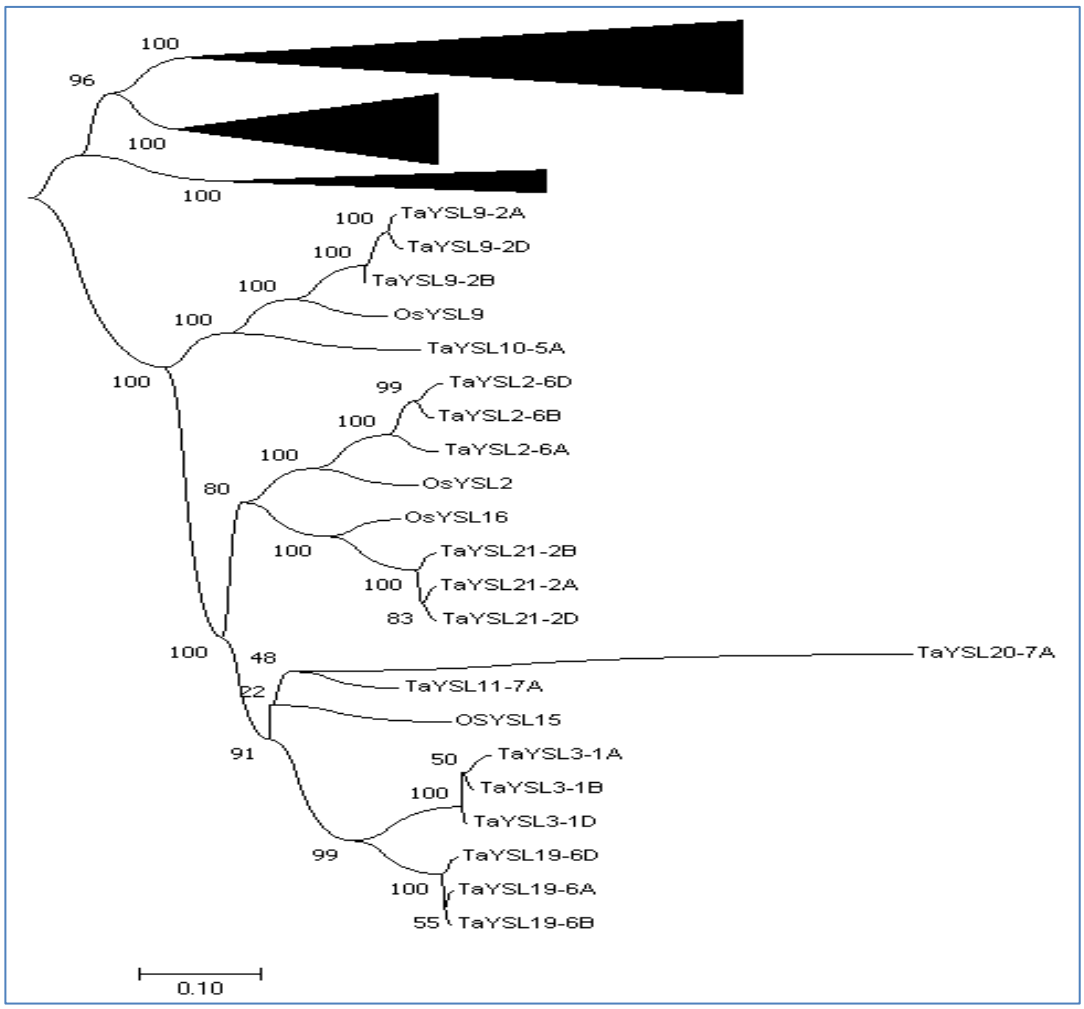

Fig. 4.26: Phylogenetic tree of clade 1 TaYSLs and OsYSLs proteins

4.3 Molecular Analysis

4.3.1 Gene-based Genome specific polymorphism detection within wheat genome

The various primers specific for the TaYSL2 gene present in A, B, and D genomes were used to amplify the gene fragments in various genotypes and were compared for the presence of polymorphism based on the bands.

Amplification by TaYSL2-6Ai primer

The amplification of the 1st segment of TaYSL2-6A gene in all the 12 genotypes taken under study yielded results at Ta 68^{0}C. The band of interest was seen to be present in all the 12 genotypes as a single band with size ranging from approximately 1057 bp (CRP 51, CRP 52) to 1186 bp (CRP 21) (**Fig. 4.27**). The analysis of bands showed that out of the total 6 alleles observed, 2 were unique and 4 were shared. The polymorphism percentage was calculated as 33.3% and The PIC value was calculated to be 0.793 (**Table 4.11**).

Amplification by TaYSL2-6Aii primer

The amplification of the 2nd segment of TaYSL2-6A gene in all the 12 genotypes taken under study yielded results at Ta 60^{0}C. The band of interest was seen to be present in all the 12 genotypes as a single band with size ranging from approximately 1338 bp (CRP 15, CRP 21) to 1455 bp (CRP 51, CRP 52) (**Fig. 4.27**). The analysis of bands showed that out of the total 8 alleles observed, 4 were unique and 4 were shared. The polymorphism percentage was calculated as 50% and The PIC value was calculated to be 0.862 (**Table 4.11**).

Amplification by TaYSL2-6Aiii primer

The amplification of the 3rd segment of the TaYSL2-6A gene in all the 12 genotypes taken under study yielded results at Ta of 58^{0}C. The band of interest was seen to be present in all the 12 genotypes as a single band with size ranging from approximately 698 bp (CRP 7) to 828 bp (CRP 51) (**Fig. 4.27**). The analysis of bands showed that out of the total 5 alleles observed, 2 were unique and 3 were shared. The polymorphism percentage was calculated as 40% and The PIC value was calculated to be 0.737 (**Table 4.11**).

Amplification by TaYSL2-6Bi primer

The amplification of the 1st segment of TaYSL2-6B gene in all the 12 genotypes taken under study yielded results at Ta of 61^0C. The band of interest was seen to be present in all the 12 genotypes as a single band with size ranging from approximately1420 bp (CRP 21, CRP 33) to 1513 bp (CRP 15) (**Fig. 4.28**). The analysis of bands showed that out of the total 5 alleles observed, 2 were unique and 3 were shared. The polymorphism percentage was calculated as 40% and The PIC value was calculated to be 0.75 (**Table 4.11**).

Amplification by TaYSL2-6Bii primer

The amplification of the 2nd segment of the TaYSL2-6B gene in all the 12 genotypes taken under study yielded results at the Ta of 62^0C. The band of interest was seen to be present in all 12 genotypes as a single band with size ranging from approximately 1285 bp (CRP 52) to 1411 bp (CRP 18) (**Fig. 4.28**). The analysis of bands showed that out of the total 7 alleles observed, 4 were unique and 3 were shared. The polymorphism percentage was calculated as 57.1% and The PIC value was calculated to be 0.82 (**Table 4.11**).

Amplification by TaYSL2-6Biii primer

The amplification of the 3rd segment of the TaYSL2-6B gene in all the 12 genotypes taken under study yielded results at the Ta of 58^0C. The band of interest was seen to be present in all the 12 genotypes as a single band with size ranging from approximately 753 bp (CRP 7) to 805 bp (CRP 45, CRP 46) (**Fig. 4.28**). The analysis of bands showed that out of the total 6 alleles observed, 2 were unique and 4 were shared. The polymorphism percentage was calculated as 33.3% and The PIC value was calculated to be 0.806 (**Table 4.11**).

Amplification by TaYSL2-6Di primer

The amplification of the 1st segment of the TaYSL2-6D gene in all the 12 genotypes taken under study yielded results at the Ta of 68^0C. The band of interest was seen to be present in all the 12 genotypes as a single band with size ranging from approximately 1382 bp (CRP 7, CRP 15) to 1456 bp (CRP 51, CRP 52) (**Fig. 4.29**). The analysis of bands showed that out of the total 7 alleles observed, 2 were unique

and 5 were shared. The polymorphism percentage was calculated as 28.6% and The PIC value was calculated to be 0.904 (**Table 4.11**)

Amplification by TaYSL2-6Dii primer

The amplification of the 2nd segment of the TaYSL2-6D gene in all the 12 genotypes taken under study yielded results at the Ta of 62^0C. The band of interest was seen to be present in all the 12 genotypes as a single band with size ranging from approximately 1244 bp (CRP 52) to 1366 bp (CRP 37) (**Fig. 4.29**). The analysis of bands showed that out of the total 4 alleles observed, 2 were unique and 2 were shared. The polymorphism percentage was calculated as 50% and The PIC value was calculated to be 0.625 (**Table 4.11**).

Amplification by TaYSL2-6Diii primer

The amplification of the 3rd segment of the TaYSL2-6D gene in all the 12 genotypes taken under study yielded results at the Ta of 65^0C. The band of interest was seen to be present in all the 12 genotypes as a single band with size ranging from approximately 629 bp (CRP 7) to 651 bp (CRP 33, CRP 37, CRP 45, CRP 46, CRP 48, CRP 50, CRP 52) (**Fig. 4.29**). The analysis of bands showed that out of the total 3 alleles observed, 1 was unique and 2 were shared. The polymorphism percentage was calculated as 33.3% and The PIC value was calculated to be 0.542 (**Table 4.11**).

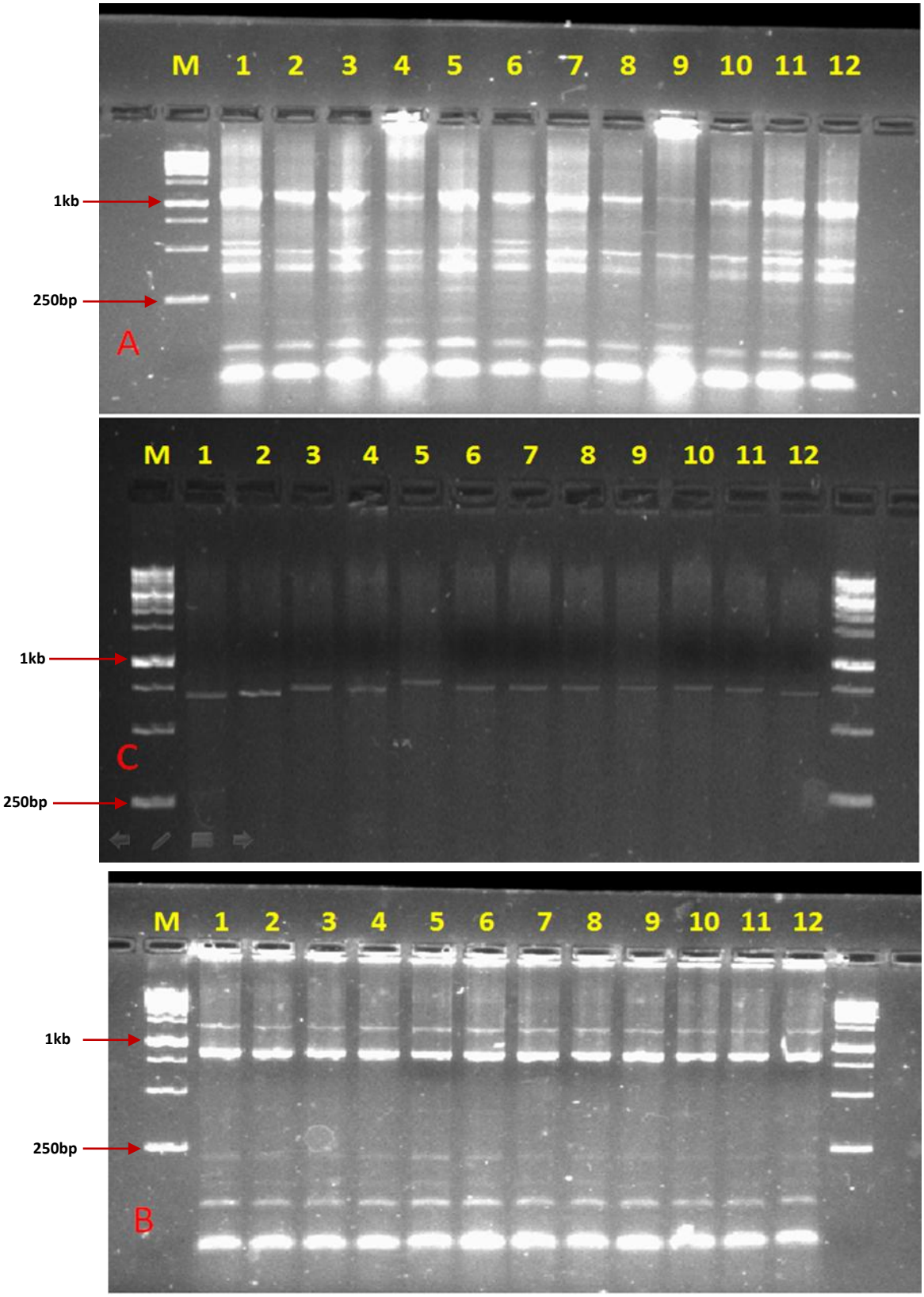

Fig. 4.27: Amplification of Primer TaYSL2-6Ai (A), TaYSL2-6Aii (B) & TaYSL2-6Aiii (D) in Genotypes CRP7, CRP15, CRP18, CRP21, CRP33, CRP37, CRP45, CRP46, CRP48, CRP50, CRP51 & CRP52 in wells 1-12 respectively.
M= 1 Kb DNA ladder

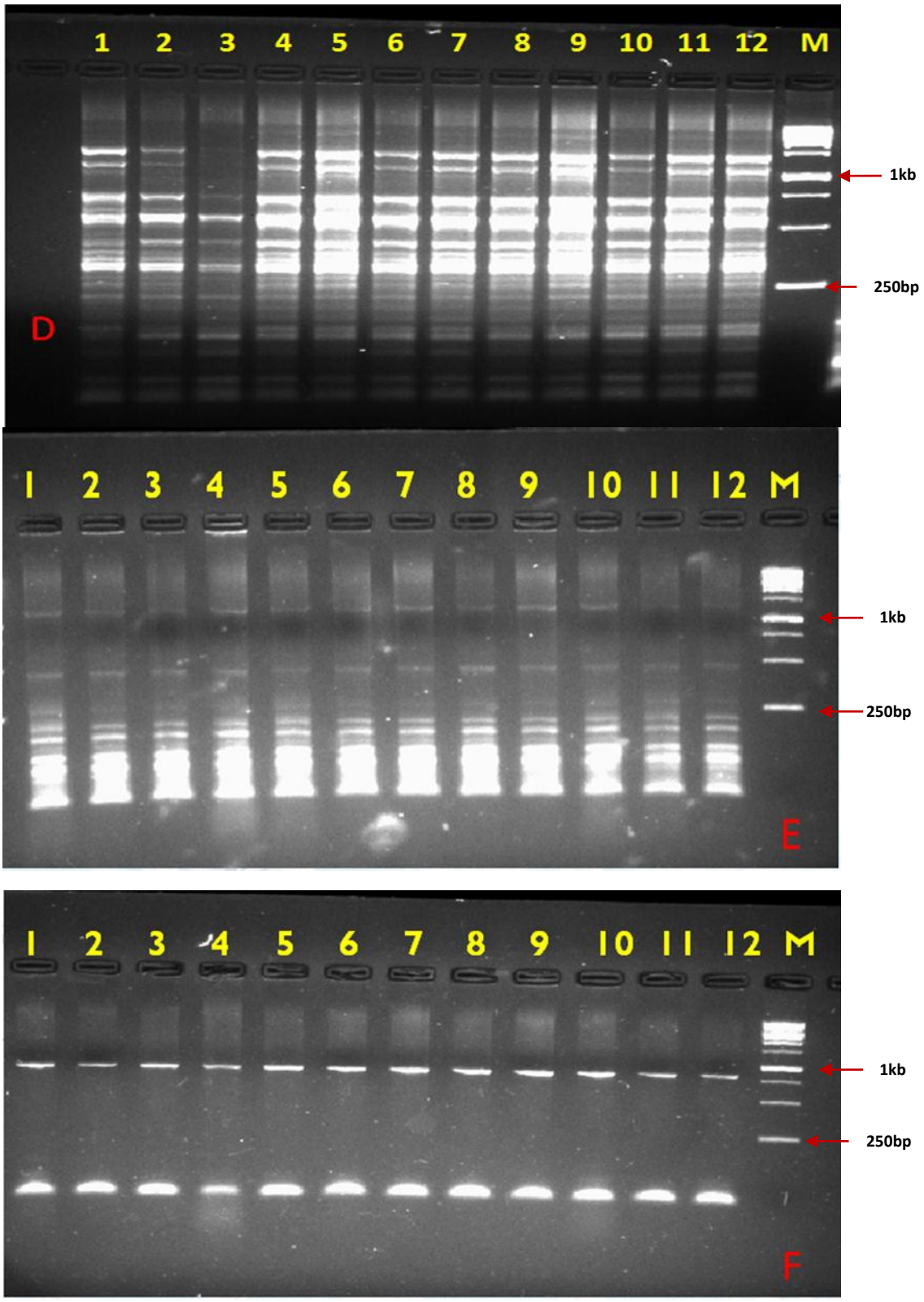

Fig. 4.28: Amplification of Primer TaYSL2-6Bi (D), TaYSL2-6Bii (E) & TaYSL2-6Biii (F) in Genotypes CRP7, CRP15, CRP18, CRP21, CRP33, CRP37, CRP45, CRP46, CRP48, CRP50, CRP51 & CRP52 in wells 1-12 respectively.
M= 1 Kb DNA ladder

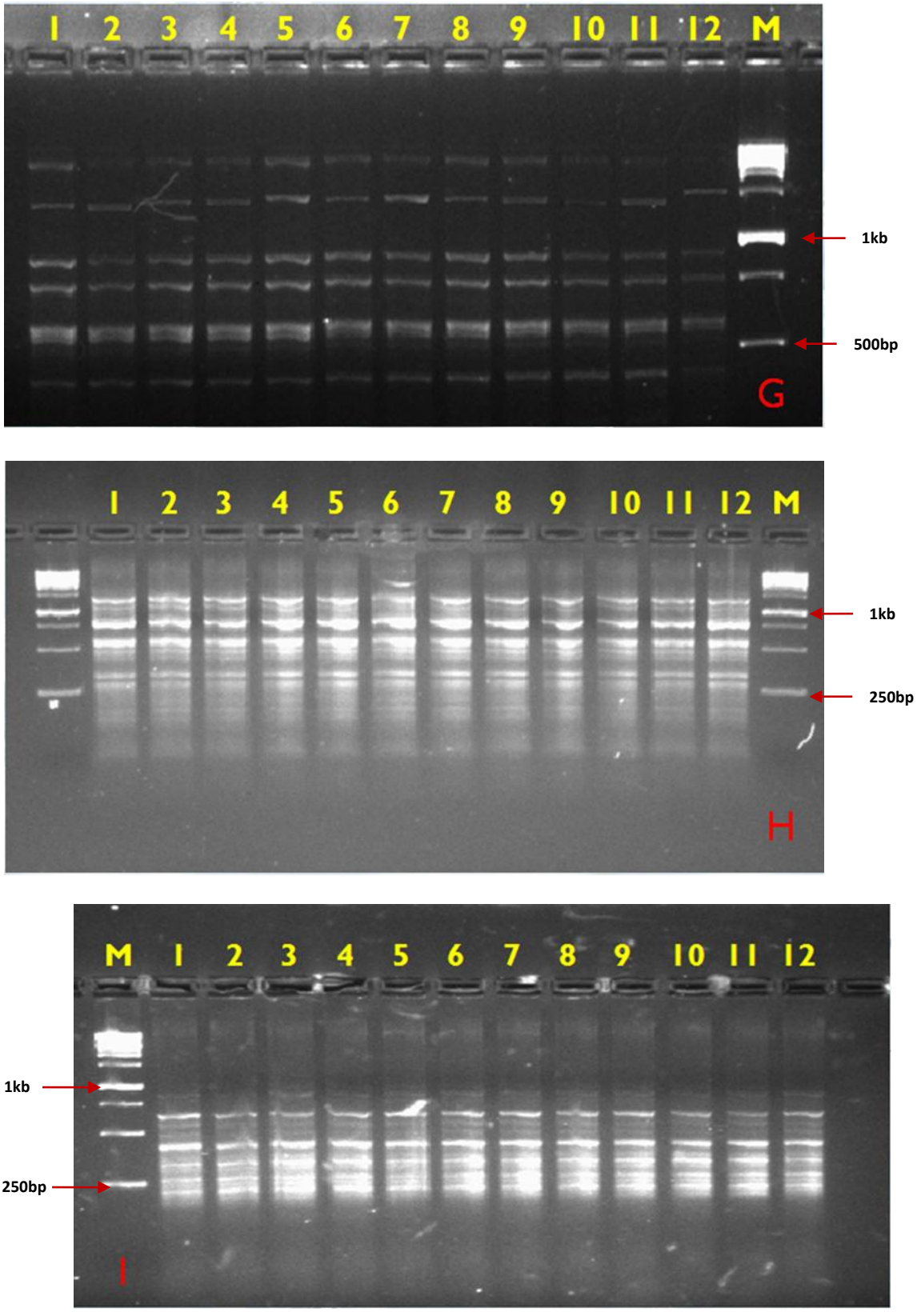

Fig. 4.29: Amplification of Primer TaYSL2-6Di (G), TaYSL2-6Dii (H) & TaYSL2-6Diii (I) in Genotypes CRP7, CRP15, CRP18, CRP21, CRP33, CRP37, CRP45, CRP46, CRP48, CRP50, CRP51 & CRP52 in wells 1-12 respectively. M= 1 Kb DNA ladder

4.3.2 Gene based genome specific Microsatellite (SSR) polymorphism detection within the wheat genome

Microsatellite primers designed from the gene based genome specific sequences were used to amplify the SSR in different contrasting genotypes and compared for the presence of polymorphism based on the size of bands obtained.

Amplification by TaYSL2-S1 primer

The amplification of the SSR primer pairs located on the TaYSL2-6A in all the 12 genotypes taken under study yielded results at the Ta of 58^0C. The band of interest was seen to be present in all the 12 genotypes as a single band with size ranging from approximately 215 bp (CRP 7) to 249 bp (CRP 51) (**Fig. 4.30**). The analysis of bands showed that out of the total 8 alleles observed, 5 were unique and 3 were shared. The polymorphism percentage was calculated as 62.5% and The PIC value was calculated to be 0.848 (**Table 4.11**) . Nonspecific binding was not observed.

Amplification by TaYSL2-S2 primer

The amplification of the SSR primer pairs located on the TaYSL2-6A gene in all the 12 genotypes taken under study yielded results at the Ta of 63^0C. The band of interest was seen to be present in all the 12 genotypes as a single band with size ranging from approximately 174 bp (CRP 37) to 183 bp (CRP 52) (**Fig. 4.30**). The analysis of bands showed that out of the total 8 alleles observed, 5 were unique and 3 were shared. The polymorphism percentage was calculated as 62.5% and The PIC value was calculated to be 0.848 (**Table 4.11**). Two Nonspecific bindings were observed.

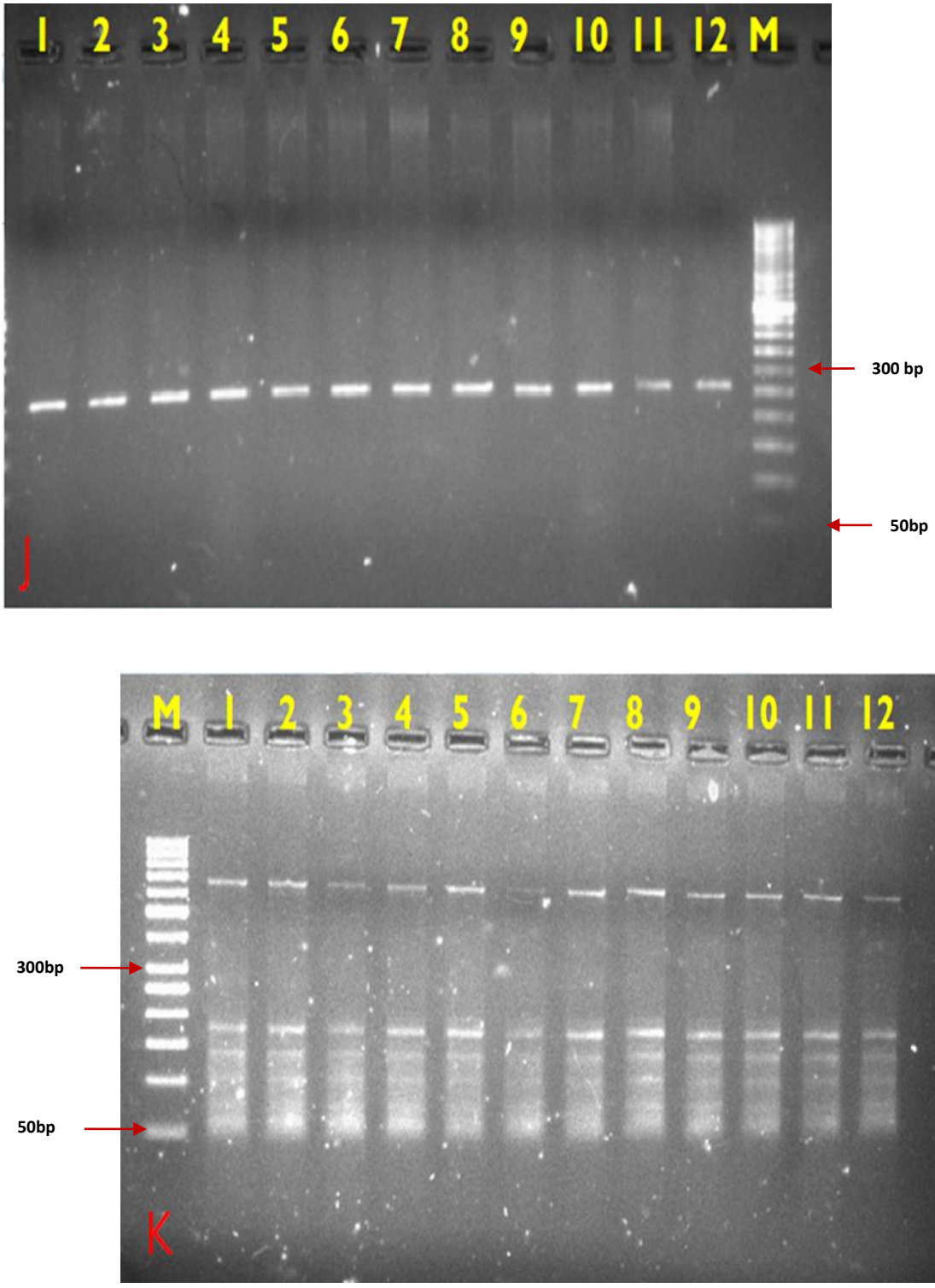

Fig. 4.30: Amplification of Primer TaYSL2-S1 (J) & TaYSL2-S2 (K) in Genotypes CRP7, CRP15, CRP18, CRP21, CRP33, CRP37, CRP45, CRP46, CRP48, CRP50, CRP51 & CRP52 in wells 1-12 respectively. M= 50 bp DNA ladder

Table 4.11: Analysis of primers used for amplification of genomic DNA of 12 genotypes

Sl No.	Primer	Range of bp	Total alleles	Unique alleles	Shared alleles	% of unique alleles	PIC
1	TaYSL2-6Ai	1057 - 1186	6	2	4	33.3	0.793
2	TaYSL2-6Aii	1338 - 1455	8	4	4	50.0	0.862
3	TaYSL2-6Aiii	698 - 828	5	2	3	40.0	0.737
4	TaYSL2-6Bi	1420-1513	5	2	3	40.0	0.75
5	TaYSL2-6Bii	1285 - 1365	7	4	3	57.1	0.82
6	TaYSL2-6Biii	754 - 805	6	2	4	33.3	0.806
7	TaYSL2-6Di	1382 - 1456	7	2	5	28.6	0.904
8	TaYSL2-6Dii	1244 - 1366	4	2	2	50.0	0.625
9	TaYSL2-6Diii	627 - 651	3	1	2	33.3	0.542
10	TaYSL2-S1	215 - 249	8	5	3	62.5	0.848
11	TaYSL2-S2	174 - 183	8	5	3	62.5	0.848

4.3.3 Computation of similarity coefficient

The Dice's similarity coefficients were computed from the primer data and it was observed that the highest similarity was observed to be 0.821 between the genotypes CRP 48 &CRP 50 and CRP 15 & CRP 21 and lowest similarity was observed to be 0.672 between the genotypes CRP 7 & CRP 15, CRP 7 & CRP 33, CRP 7 & CRP 52, CRP 15 & CRP 37, CRP 15 & CRP 46, CRP 15 & CRP 48, CRP 18 & CRP 45, CRP 21 & CRP 37, CRP 21 & CRP 50 and CRP 37 & CRP 51. The table of similarity coefficients has been given in **Fig. 4.31**.

	CRP7	CRP15	CRP18	CRP21	CRP33	CRP37	CRP45	CRP46	CRP48	CRP50	CRP51
CRP15	0.731										
CRP18	0.672	0.791									
CRP21	0.701	0.821	0.761								
CRP33	0.672	0.731	0.791	0.701							
CRP37	0.701	0.672	0.701	0.672	0.761						
CRP45	0.731	0.731	0.672	0.731	0.791	0.791					
CRP46	0.701	0.672	0.701	0.701	0.761	0.761	0.761				
CRP48	0.701	0.672	0.701	0.701	0.731	0.761	0.791	0.761			
CRP50	0.701	0.701	0.701	0.672	0.761	0.761	0.791	0.731	0.821		
CRP51	0.701	0.701	0.701	0.761	0.701	0.672	0.701	0.701	0.701	0.701	
CRP52	0.672	0.701	0.701	0.701	0.701	0.701	0.701	0.761	0.731	0.731	0.791

Fig. 4.31: Table of Similarity coefficients

4.3.4 Clustering of genotypes based on Similarity coefficient

The genotypes were clustered based on the similarity coefficients, and Dendrogram was drawn by the UPGMA method (**Fig. 4.32**). Four genotypic clusters were identified at the phenon level of 25% (0.73) (**Table 4.12**). The obtained clusters were compared with Fe and Zn content data and the types of genotypes in clusters were noted based Fe and Zn accumulation levels. The clusters were labeled based on decreasing order of similarity.

Table 4.12: Cluster analysis of genotypes based on molecular data

Cluster	Genotypes	Type of mineral accumulator
A	CRP 37, CRP 48, CRP 45, CRP 50, CRP 46	High Fe accumulator
B	CRP 15, CRP 21, CRP 18, CRP 33	Average- low Fe accumulator High Zn accumulator
C	CRP 51, CRP 52	Average - low Fe accumulator Average Zn accumulator
D	CRP 7	High Fe accumulator Low Zn accumulator

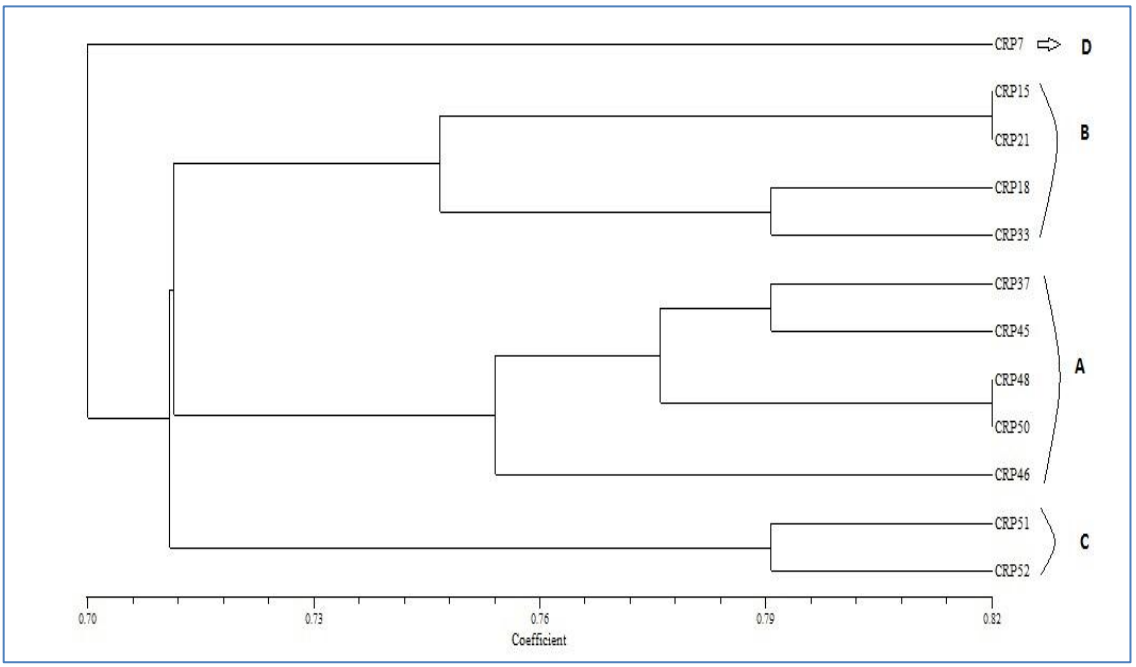

Fig. 4.32: Dendrogram of Genotypes based on Similarity coefficient

CHAPTER - V

DISCUSSION

V DISCUSSION

Wheat is one of the most important staple food crops in the world. The mineral content in wheat is an important aspect of grain quality. The increase in wheat yield leads to a reduction in grain mineral content (Fan *et al.*, 2008; Murphy *et al.*, 2008). Wheat is a hexaploid crop with a total genome size of $1.7*10^{10}$ (Amuruganathan *et al.*, 1991). Various genes and gene families are involved in the uptake and loading of minerals into the seeds. These include NAS gene, ZIP family, YSL family of genes etc. Out of these, the YSL gene family, which codes for transporters, is one of the most important gene families involved in the translocation of minerals, especially Fe and Zn throughout the plant. In rice, OsYSL2 is directly involved in the loading of Fe into the grains. It is closely related to AtYSL3 which is important genes involved in mineral loading into seeds of Arabidopsis. Based on the above criteria, the study, " **In-Silico and Molecular Characterization of YSL1 gene in Wheat** " was carried out. In the present study, the homologue of OsYSL2 in wheat, i.e., the TaYSL2, was identified for in-silico characterization. Furthermore, molecular characterization of the gene was carried out related to the grain Fe and Zn content in various wheat genotypes at different levels of heat stress. Moreover, all the members of the YSL gene family in wheat were identified based on homology with OsYSLs and AtYSLs genes.

5.1 Quantification of Fe and Zn content in wheat

The Fe and Zn content data showed that there were significant differences among the wheat genotypes under study with respect to the accumulation of the minerals in the seeds. The accumulation of Fe in seeds varied from 17.2-56.4 mg/g of seed with an average of 34.3 mg/g. Accumulation of Zn varied from 28.9-44.4 mg/g of seed except for CRP 48 which showed the highest accumulation of Zn (60.4 mg/g) with an average of 36.5 mg/g (Table 4.3). This variation of Fe and Zn content in wheat grains is nearly consistent with the results obtained by Graham *et al.*, 1999; Morgounov *et al.*, 2007; Gomez-Becerra *et al.*, 2009.

The accumulation of Fe on an average reduced drastically from 40.8 mg/g on the first date of sowing to 27.8 mg/g on the second date of sowing. The result shows that the heat stress on the plant led to reduced Fe accumulation in the seeds. The average Zn accumulation in the seeds also reduced from 37.6 mg/g on the 1st date of sowing to 35.4 mg/g on the second date of sowing (Table 4.3). Most of the genotypes showed positive values for HSI based on Fe and Zn content. Out of 25 genotypes, 5 genotypes showed negative HSI values for Fe accumulation in seeds, and 11 genotypes showed negative HSI values based on Zn accumulation. Four of the five genotypes with negative HSI values for Fe content were common with that of genotypes with negative HSI values for Zn accumulation (**Table 4.3**; **Fig 4.1**). This showed that these four genotypes, namely HD2967, CRP 37, CRP 54, and CRP 43, have increased the intake and accumulation of both Fe and Zn in order to alleviate the effect of heat stress. The fact that there is the varied deposition of Fe and Zn in wheat and that the mineral contents may increase or decrease or remain constant has been shown by Peleg *et al.,* 2008 and Singh *et al.,* 2012.

As the OsYSL2 gene transports both Fe and Zn into the seeds, the higher accumulation in these plants may be due to over-expression of this gene under heat stress or presence of superior allele of this gene. The difference among genotypes showing negative HSI values based on Fe and Zn accumulation over two dates of sowing may be due to the fact that Fe and Zn accumulation in the plants follow many pathways, some of which are common for both the minerals and some of which are different. Thus, the entire Fe and Zn accumulation in the seed cannot entirely be correlated to any one gene. Nevertheless, as YSL2 is one of the few genes directly involved in the accumulation of Fe and Zn in the seed, it can be correlated with Fe and Zn content in seeds to a certain extent. The clustering of genotypes according to their Fe content, clearly classified them into 3 classes, i.e., high accumulators, low accumulators, and medium/average accumulators. However, in the case of the clustering of genotypes based on Zn concentration, such clear classification could not be confirmed. This might be because of Zn accumulation in seeds, the ZIP family of genes are actively involved, and hence the contribution of the YSL gene family reduces with respect to the total Zn accumulation in seeds as supported by Curie *et al.* 2009.

5.2 In-silico characterization/ analysis

AtYSL1 is one of the major genes of the YSL family in Arabidopsis responsible for the loading of minerals such as Fe and Zn in the form of metal-PS chelates into the seed. It is also specifically expressed in grains. Thus it was considered as the model gene whose orthologue was to be discovered in wheat. The initial BLAST results failed to find the orthologues of AtYSL1 in wheat. The result might be explained by the fact that, although the YSL gene family is highly conserved in plants, the evolutionary relationship between Arabidopsis and wheat branched off at a very earlier stage as wheat is a monocot plant whereas Arabidopsis is a dicot plant. 18 YSL genes have already been characterized in rice, a monocot belonging to family Poaceae and thus more closely related to wheat. Therefore, YSL genes from rice were taken as reference for finding YSL genes in wheat. Out of the 18 OsYSLs, OsYSL2 is directly involved in the loading of minerals into seed and is closely related to AtYSL1 and AtYSL3. BLASTn of the genomic sequence of OsYSL2 on the wheat genome (IWGSC, 2018) revealed homology on chromosome 6 of genome B, D and A with high alignment and very low e-value leading to identification of three homeologous copy of the gene namely TaYSL2-6A, TaYSL2-6B and TaYSL2-6D as the three genome being homeologous to each other (**Table 4.6**). Mishra *et al.*, 2017 also reported the identification of three homeologous copies of the SSIII gene in wheat by using single orthologs from maize.

The BLASTn of all the OsYSLs, AtYSLs, and ZmYS1 in the wheat genome resulted in a total of 63 genes over the three genomes in wheat. These 63 genes consist of 24 YSL genes and their homeologous copies (**APPENDIX B**). The number of TaYSL genes observed in this study correlated with the results obtained by Kumar *et al.*, 2019 and Pearce *et al.*, 2014. However, the annotation ID and gene nomenclature are different in the present study because the names were given based on homology with YSL genes in rice instead of Brachypodium. The deduced gene structure of the TaYSL2, as well as its homeologous copies on A and B genomes, were not reported in the study by Kumar *et al.*, 2018. The in silico characterization data of the homeologues of the TaYSL2 has been reported for the first time in this study (**Table 4.6**).

The marking of intron-exon boundaries revealed the presence of 6 introns and 7 exons in each of the homeologous copies of the gene. However, in rice 8 exon and 7 introns have been reported. The mismatch indicates towards splitting or merger of exons during the course of evolution. As compared to the exonic region, the intronic region was found more variable (**Table 4.7; 4.8**). It is because the exonic region being subject to high selection pressure by natural selection, as they code for functional products reflected in the phenotype of the organism, and the selection does not allow the undesirable variabilities to get accumulated during the course of evolution. It was also observed that the number of exons and introns varied over different ysl genes, but were conserved for a particular gene and its homeologues. The finding was in line with the studies of Adams *et al.*, 2003, Akhunov *et al.*, 2013, Deol *et al.*, 2013. The maximum variation was found among intronic sequences than exons, similar to results explained by Ramakrishna *et al.*, 2002.

Though the number of exons and introns did not vary between the homeologues, the total length of the transcripts, length of the exons, introns, and total length of gene varied considerably. The variation in the homeologous copies of the gene might have evolved for making them suitably code to efficiently meet the requirements of different developmental stages and tissues in the overall growth and development of wheat crop under different environmental conditions. In-silico expression analysis of the homeologous copies of the gene has indicated their differential expression at different tissues, growth stages and stress conditions.

The expression analysis of all the three homeologues of the TaYSL2 gene revealed that TaYSL2 is expressed mostly in the grains after anthesis, in senescing leaves and spike, TaYSL2-6D in the stem during senescence (**Fig. 4.20; Fig. 4.23**). Gregersen *et al.*, 2007, also found increased expression of YSL genes in senescing leaves. The facts above indicate the role of TaYSL2 in the mobilization of Fe and Zn and their deposition in wheat grain. In all the tissue under study, TaYSL2-6D expressed at a late stage, indicating its a relatively more significant role in remobilization from senescing tissue and deposition in the sink seed. Out of the three homeologues the expression of TaYSL2-6D showed comparatively least fluctuation, implying that protein product of TaYSL2-6D was more tolerant to stress conditions than its other homeologues.

The expression level of TaYSL2-6A increased many folds under prolong drought conditions indicating its draught induced expression (**Fig. 4.24**). Since a longer protein requires more energy for its synthesis, it has been observed that in many organisms, truncated proteins are expressed under stress conditions in order to minimize the energy utilization by sacrificing few amino acids. Similarly, it is thought that in the case of TaYSL2, since TaYSL2-6A has a smaller protein length and is functional, its expression increases by many folds. Under heat stress, the expression of homeologue TaYSL2-6B increased many folds indicating its role under heat stress. The combined stress of heat and drought increases the expression of TaYSL2-6B to many folds and TaYSL2-6D significantly, revealing their important role in mobilization and depositing the nutrients in the severe stress conditions.

The correlation of expression analysis data with that of Fe and Zn content in wheat grains suggests that Fe content in grains is highly correlated with expression of TaYSL2, whereas, it is very little to no correlation between YSL2 and Zn content in grains. This was supported by the studies carried out on OsYSL2 by Koike *et al.*, 2004.

The length and amino acid composition of the TaYSL2 protein is highly similar to that of OsYSL2 (Koike *et al.*, 2004). The variable temporal and tissue specific expression of TaYSL2 in wheat is very similar to that of OsYSL2 in rice. This supports the fact that TaYSL2 is involved in the homeostasis of minerals in plants from senescing leaves to developing grains via phloem transport of metal-NA complex. The probable 3D structure of TaYSL2 proteins revealed that the number of transmembrane domains and features were quite similar among homeologues and contained structure similar to that of ion transporters in case of reported structural proteins in other organisms (**Fig. 4.17 to Fig 4.19**). Schaaf *et al.*, 2004 reported that ZmYS1 functions as an H+ coupled symporter for PS-metal chelates in maize. The presence of structure similar to that of H+ ion channel and ATPase is similar to that of ZmYS1.

The phylogenetic analysis of the TaYSL proteins classified the protein family into 4 major clades. Similar results were observed in the case of OsYSLs and AtYSLs (Koike *et al.*, 2004; Curie *et al.*, 2001). The comparison of the OsYSLs and TaYSLs revealed that TaYSL2 was closest to OsYSL2, followed by AtYSL1 and AtYSL3.

The TaYSL proteins in wheat were observed to lie in the same clades as their homologs in rice.

5.3 Molecular characterization of TaYSL2

Molecular characterization of TaYSl2 genes was carried out among wheat genotypes understudy having a variable accumulation of Fe and Zn content in the seed with respect to heat stress. The gene-based genome-specific primers amplified the TaYSL2 genes present on all the three genomes and the results obtained were analyzed. There was significant variation among different genotypes based on their molecular composition. The gene-based genome-specific primers amplified in all the 12 genotypes and gave different amplicon sizes, corresponding to various alleles. A similar result was obtained from the amplification of SSR primers for the gene. A total of 67 alleles were observed from all the primer pairs, with an average of ~6 alleles per primer pair. The finding is similar to the results obtained by Gorji and Zolnoori, 2011; Schuster *et al.,* 2009 & Iqbal *et al.,* 2009. Contrarily, it is lower than the number of alleles reported by Schuster *et al.,* 2004; Emon *et al.,* 2010 & Zhang *et al.,* 2011. The amplification of both SSR primers resulted in 8 alleles each.

A total of 37 unique alleles were obtained from all of the primers. The polymorphism percentage in products amplified by primers of the B genome was higher than that of A and D genome, which was also reported by Wang *et al.,* 2007. The present study also correlates with the reports of various studies by Cho *et al.,* (2000) in rice, Scott *et al.,* (2000) in grapes and Eujayl *et al.,* (2002) in wheat.

The range of PIC values was observed to lie between, 0.542 to 0.904 (**Table 4.11**). This range of PIC values is more than the range of PIC values reported in the studies by Schuster *et al.,* 2009 & Zhang *et al.,* 2011. The PIC value observed in the SSR primers was 0.848 in both cases. This data is slightly higher than the data observed by Emon *et al.,* 2010, who reported it as 0.776. The highest similarity coefficient was observed to be 0.821 and lowest to be 0.672. The high value of Dice's similarity coefficient was observed between genotypes as the primers were gene-based genome-specific and hence highly conserved. The findings are in line with the findings of Zurabishvili, 1978, Gianibelli *et al.,* 2001and Deol *et al.,* 2013. Similar studies were carried out using SSR markers by Panaud *et al.,*1996 and Chakravarthy and Naravaneni., 2006.

Clustering is done based on common features to classify a set of data into a different group. The representation of hierarchical clustering as a tree is called a dendrogram (Jiang *et al.*, 2004). The dendrogram computed on the basis of the obtained similarity coefficients clustered the genotypes, and the genotypes were found to separate into 4 major clusters (**Table 4.12**). When correlated with the data obtained from the analysis of mineral content in seed, it was observed that the clusters of molecular analysis data coincided with the clusters computed from the Fe content data over two dates of sowing, but not with the clusters obtained from Zn content data. Similar studies have been carried out by various investigators using SSR markers and candidate gene-based markers in various crops (Barakat *et al.*, 2011; Bennett *et al.*, 2012; Sadat *et al.*, 2013, Pandey *et al.*, 2013). The findings of the present study are more relevant for crop improvement as there is evident genetic variation among the genotypes of bread wheat taken in this study with respect to Fe and Zn content under normal and heat stress conditions.

◈◈◈

CHAPTER - VI

SUMMARY AND CONCLUSION

VI SUMMARY AND CONCLUSION

Twenty-five wheat genotypes used for the present study were taken from the wheat germplasm maintained at the Department of Agricultural Biotechnology and Molecular Biology, Dr. R.P.C.A.U., Pusa. The genotypes were planted in the fields of Pusa Farm of Dr. RPCAU, under normal and late sown conditions. The sowing in the late condition was done to impose heat stress. The In-silico and molecular studies were carried out in the Genetic Transformation Laboratory, Department of Agricultural Biotechnology and Molecular Biology, Dr. R.P.C.A.U., Pusa, and the micronutrient estimation was carried out in Department of Soil Science, Dr. R.P.C.A.U., Pusa. The Fe and Zn content in wheat seeds were analyzed using AAS. The results summarised and the conclusions drawn are as follows:

- The variance among the genotypes between the two DOS and the interaction between them, based on their Fe and Zn content, was highly significant
- For Fe, the genotype CRP 7 was the highest accumulator (76 mg/g of seed) under normal sown condition whereas CRP 54 was the highest accumulator (43.9 mg/g of seed) under late sown condition.
- The highest accumulation of Zn was observed in the genotype CRP 48 under both the dates of sowing as 65.6 mg/g (1^{st} DOS) and 55.1 mg/g of seed (2nd DOS).
- Most of the genotypes showed a reduction in mineral content from 1st DOS to 2nd DOS. The average Fe content reduced from 40.813 ppm in 1^{st} DOS to 27.763 ppm in 2^{nd} DOS. The reduction in Zn content over the two dates of sowing was not as drastic (37.6 ppm in 1^{st} DOS to 35.38 ppm in 2^{nd} DOS).
- The HSI for most of the genotypes was positive, i.e., the Fe and Zn accumulation in grains reduced in the late sown conditions from that of the normal sown conditions.
- In few genotypes such as HD 2967, CRP 37, CRP 54, and CRP 43, the HSI for both Fe and Zn content was found negative as the content of two nutrients increased under the late sown conditions.

- The genotypes were divided into 3 clusters concerning Fe content accumulation and 4 clusters based on their performance in Zn accumulation with respect to their sensitivity towards heat stress.
- The in-silico study helped in the identification of a total of 63 TaYSL genes over the three genomes in wheat. Three homeologous copy of the gene TaYSL2 namely TaYSL2-6A, TaYSL2-6B and TaYSL2-6D were identified on the 6^{th} chromosome of each of the three genome.
- The marking of intron-exon boundaries revealed the presence of 6 introns and 7 exons in each of the homeologous copies of the gene.
- The in silico expression analysis data showed that the expression of TaYSL2 was restricted mainly to the grain. TaYSL2-6B and TaYSL2-6D expressed mostly in the endosperm, TaYSL2-6D in senescing leaves and sparsely in spike.
- The expression of TaYSL2 over heat stress condition showed that there is a reduction in the expression level of TaYSL2-6A in heat stress while TaYSL2-6B shows a significant increase.
- Expression studied under stress condition revealed that expression level of TaYSL2-6A increased many folds under prolonged drought conditions, under heat stress, the expression of homeologue TaYSL2-6B increased many folds and combined stress of heat and drought increases the expression of TaYSL2-6B to many folds and TaYSL2-6D significantly.
- Out of the three homeologues the expression of TaYSL2-6D exhibited comparatively least fluctuation, implying that protein product of TaYSL2-6D was more tolerant to stress conditions than its other homeologues. TaYSL2-6A showed increased expression in drought stress, while TaYSL2-6B showed increased expression in heat stress, signifying their importance in the respective stress conditions.
- The field data was correlated to the expression analysis data, and it was hypothesised that either one of the following three conditions or their interaction might cause this contradiction:
    - The late sowing condition causes a heat-induced limited stress condition leading to increased expression of TaYSL2

  - The heat stress condition may reduce the efficiency of the TaYSL2 protein to take up Fe-PS complexes.
  - The pathways of Fe and Zn accumulation in wheat seed, though similar, involves different proteins throughout their overall transport as the metal-PS chelate. The difference in the reduction of Fe and Zn may be due to the difference in the efficiency of these pathways.

- The molecular characterization of TaYSL2 showed that the most informative primer was TaYSL2-6Di (PIC= 0.904) whereas the maximum polymorphism percentage was obtained in the case of SSR primers TaYSL2-S1 and TaYSL2-S2 (62.5%).
- The Dice's similarity coefficient showed that the highest similarity (0.821) was observed between CRP 48 &CRP 50 and CRP 15 & CRP 21 and the lowest similarity was observed to be 0.672.
- The dendrogram was computed based on the similarity coefficient values, and the genotypes were grouped into 4 major clusters. The clusters were labeled based on decreasing order of similarity.
- The comparison of the molecular data with micronutrient data revealed that the clusters A and D formed from molecular similarity data consisted of high Fe accumulators, whereas clusters B and C consisted of average to low Fe accumulators.
- Based on grain Zn content, cluster B consisted of high Zn accumulators, and cluster C consisted of average to high Zn accumulators.

Thus, it can be said that information generated from the current study might be useful in improvement for the bio-fortification in wheat concerning Fe and Zn content in grain. This study will also be helpful in the molecular investigation for identification stress-tolerant SNPs present among YSL genes in wheat for the development of climate-resilient biofortified cultivars of wheat crop.

◈◈◈

BIBLIOGRAPHY

BIBLIOGRAPHY

Adams, K.L., Cronn, R., Percifield, R., Wendel, J.F. (2003) Genes duplicated by polyploidy show unequal contributions to the transcriptome and organ-specific reciprocal silencing. *Proc Natl Acad Sci USA* **100**:4649–4654.

Akhunov, E.D., Sehgal, S., Liang. H., Wang, S., Akhunova, A.R., Kaur, G., Li, W., Forrest, K.L., See, D., Simkova, H., Ma, Y., Hayden, M.J., Luo, M., Faris, J.D., Dolezel, J., Gill, B.S. (2013) Comparative analysis of syntenic genes in grass genomes reveals accelerated rates of gene structure and coding sequence evolution in polyploidy wheat. *Plant Physiol* **161**:252–265

Amuruganathan, E. and Earle E. D. (1991). Nuclear DNA content of some important plants species. *Plant Molecular Biology Report* **9:** 208-218.

Barakat, M. N., Al-Doss A. A., Elshafei, A. A., Moustafa, K. A., (2011).Identification of new microsatellite marker linked to the grain filling rate as indicator for heat tolerance genes in F2 wheat population. *Australian J. Crop Sci*. **5**(**2**):104-110.

Bennett, D., Izanloo A., Reynolds M., Kuchel H., Langridge P, and Schnurbusch T.,(2012) Genetic dissection of grain yield and physical grain quality in bread wheat (*Triticum aestivum* L.) under water-limited environments. *Theoretical and Applied Genetics*, **125**(**2**), 255–271.

Birnbaum, K., Jung, J. W., Wang, J. Y., Lambert, G. M., Hirst, J. A., Galbraith, D. W., & Benfey, P. N. (2005). Cell type–specific expression profiling in plants via cell sorting of protoplasts from fluorescent reporter lines. *Nature methods*, **2**(**8**), 615.

Bughio, N., Yamaguchi, H., Nishizawa, N. K., Nakanishi, H., & Mori, S. (2002). Cloning an iron-regulated metal transporter from rice. *Journal of Experimental Botany*, **53**(**374**), 1677-1682.

Cakmak, I., (2008) Enrichment of cereal grains with zinc: agronomic or genetic biofortification? *Plant Soil,* **302**: 1–17.

Chakravarthi, B. K. and Naravaneni, R. (2006). SSR marker based DNA fingerprinting and diversity study in rice (*Oryza sativa* L.). *Afr. J. Biotechnol*., **8**: 684-688.

Chattopadhyay, M.K. (2006) Mechanism of bacterial adaptation to low temperature. *J. Biosci*. **31**:157-165.

Cho, Y.G., Ishii, T., Temnykh, S., Chen, S., Lipovich, L., Park, W. D., Ayres, Cartinhour, S. and Mc COUCH, S. R (2000). Diversity of microsatellites derivered form genomic libraries and GenBank sequences in rice (*Oryza sativa* L.). *Theor. Appl. Genet*., **100**:713-722.

Choulet, F., Alberti, A., Theil, S., Glover, N., Barbe, V., Daron, J., Pingault, L., Sourdille, P., Couloux, A., Paux, E. and Leroy, P., (2014) Structural and functional partitioning of bread wheat chromosome 3B. *Science*, **345**, 1249721.

Chu, H. H., Chiecko, J., Punshon, T., Lanzirotti, A., Lahner, B., Salt, D. E., Walker, E. L. (2010) Successful reproduction requires the function of Arabidopsis Yellow Stripe-Like1 and Yellow Stripe-Like3 metal-nicotianamine transporters in both vegetative and reproductive structures. *Plant Physiology*. **154**(**1**):197-210.

Colangelo, E. P., & Guerinot, M. L. (2004). The essential basic helix-loop-helix protein FIT1 is required for the iron deficiency response. *The Plant Cell*, **16**(**12**), 3400-3412.

Connolly, E. L., Campbell, N. H., Grotz, N., Prichard, C. L., & Guerinot, M. L. (2003). Overexpression of the FRO2 ferric chelate reductase confers tolerance to growth on low iron and uncovers posttranscriptional control. *Plant Physiology*, **133**(**3**), 1102-1110.

Connolly, E. L., Fett, J. P., & Guerinot, M. L. (2002). Expression of the IRT1 metal transporter is controlled by metals at the levels of transcript and protein accumulation. *The Plant Cell*, **14**(**6**), 1347-1357.

Curie, C. and Briat, J.F. (2003) Iron transport and signaling in plants. *Annu. Rev. Plant Biol*. **54**: 183–206.

Curie, C., Cassin, G., Couch, D., Divol, F., Higuchi, K., Le Jean, M., Misson, J., Schikora, A., Czernic, P. and Mari, S. (2009) Metal movement within the plant: contribution of nicotianamine and yellow stripe 1-like transporters. *Annals of Botany* **103**: 1–11.

Curie, C., Panaviene, Z., Loulergue, C., Dellaporta, S.L., Briat, J.F. and Walker, E.L. (2001) Maize yellow stripe1 encodes a membrane protein directly involved in Fe(III) uptake. *Nature*, **409**: 346–349.

Deol, K.K., Mukherjee, S., Gao, F., Brûlé-Babel, A., Stasolla, C., Ayele, B.T. (2013) Identification and characterization of the three homeologues of a new sucrose transporter in hexaploid wheat (*Triticum aestivum* L.). *BMC Plant Biol* **13**:181–196.

Dice, L.R. (1945). Measures of the amount of ecologic association between species. *Ecology* **26**: 297-302.

Dinneny, J.R., Long, T.A., Wang, J.Y., Jung, J.W., Mace, D., Pointer, S., Barron, C., Brady, S.M., Schiefelbein, J. and Benfey, P.N. (2008). Cell identity mediates the response of Arabidopsis roots to abiotic stress. *Science*, **320**(**5878**), 942-945.

Dipanwita, S., Chattopadhyay, M.K. (2013) Metabolism in bacteria at low temperature: a recent report. *J. Biosci*. **38**(**2**) 409-412.

Directorate of statistics evaluation, Deptt. of agriculture, Govt. of Bihar 2016.

Doyle, J. J. and Doyle, J. L. (1987). A rapid DNA isolation procedure for small quantities of fresh leaf material. Phytochem. Bull, 119: 11-15.

Eckhardt, U., Marques, A. M., & Buckhout, T. J. (2001). Two iron-regulated cation transporters from tomato complement metal uptake-deficient yeast mutants. *Plant molecular biology*, **45**(**4**), 437-448.

Eide, D., Broderius, M., Fett, J., & Guerinot, M. L. (1996). A novel iron-regulated metal transporter from plants identified by functional expression in yeast. *Proceedings of the National Academy of Sciences*, **93**(**11**), 5624-5628.

Emon, R. M., Gustafson, J. P., Nguyen, H., Musket, T., Jahiruddin, M., Islam, M. A., Haque, M. S., Islam, M. M., Begum, S. N. and Hassan, M. M. (2010). Molecular marker-based characterization and genetic diversity of wheat genotypes in relation to Boron use efficiency. *Indian J. Genet.,* **70(4):** 339-348.

Eujayl, I., Sorrells, M.E., Baum, M., Wolters, P. and Powell, W. (2002). Isolation of EST-derived microsatellite markers for genotyping the A and B genomes of wheat. *Theor. Appl. Genet*. **104:** 399–407.

Fageria, N.K., Baligar, V.C., Clark, R.B. (2002) Micronutrients in crop production. *Adv. Agron*. **77**:185-250.

Fan, M.S., Zhao, F.J., Fairweather-Tait, S.J., Poulton, P.R., Dunham, S.J., McGrath, S.P. (2008) Evidence of decreasing mineral density in wheat grain over the last 160 years. *J Trace Elem Med Biol*. **22**(**4**):315-24.

Fischer, R. A., & Maurer, R. (1978). Drought resistance in spring wheat cultivars. I. Grain yield responses. *Australian Journal of Agricultural Research*, **29**(**5**), 897-912.

Fiser, A., Do, R.K., Sali, A. (2000) Modeling of loops in protein structures. *Protein Sci*. **9**(**9**):1753-73.

Fiser, A., Sali, A. (2003) ModLoop: automated modeling of loops in protein structures. *Bioinformatics*. **19**(**18**):2500-1.

Garcia, W., Hodgson, R., Blessin, C., Inglett, G. (1977) Preparation of corn products endogenously labeled with zinc-65 for use in bioavailability studies, *J. Agric. Food Chem*. **25**: 1290–1295

Garnett, T.P., Graham, R.D. (2005) Distribution and remobilization of iron and copper in wheat, *Ann. Bot*. **95**: 817–826.

Gorji, A. H and Zolnoori, M. (2011). Genetic diversity in Hexaploid wheat genotypes using Microsatellite markers, *Asian J. Biotechnol*., **3** : 368-377.

Gross, J., Stein, R. J., Fett-Neto, A. G., & Fett, J. P. (2003). Iron homeostasis related genes in rice. *Genetics and Molecular Biology*, **26**(**4**), 477-497.

Hansen, N.C., Jolley, V.D., Berg, W.A., Hodges, M.E., Krenzer, E.G. (1996) Phytosiderophore release related to susceptibility of wheat to iron deficiency. *Crop Sci.* **36**: 1473-1476.

Henriques, R., Jásik, J., Klein, M., Martinoia, E., Feller, U., Schell, J., ... & Koncz, C. (2002). Knock-out of Arabidopsis metal transporter gene IRT1 results in iron deficiency accompanied by cell differentiation defects. *Plant molecular biology*, **50**(**4-5**), 587-597.

Herren, T., Feller, U. (1994) Transfer of zinc from xylem to phloem in the peduncle of wheat. *J. Plant Nutr*. **17**: 1587–1598.

Herren, T., Feller, U. (1996) Effect of locally increased zinc contents on zinc transport from the flag leaf lamina to the maturing grains of wheat, *J. Plant Nutr*. **19**: 379–387.

Hill, J. (1980) The remobilization of nutrients from leaves. *J. Plant Nutr*. **2**: 407–444.

Hocking, P.J., (1994) Dry-matter production, mineral nutrient concentrations, and nutrient distribution and redistribution in irrigated spring wheat. *J. Plant Nutr*. **17**: 1289–1308.

Hu, B., Jin, J., Guo, A., Zhang, H., Luo, J., Gao, G. (2015). GSDS 2.0: an upgraded gene feature visualization server. *Bioinformatics*. **31**(8):1296-1297.

Iqbal, N., Tabasum, A., Sayed, H. and Hameed, A.(2009). Evaluation of genetic diversity among bread wheat varieties and landraces of Pakistan by SSR markers. *Cereal Res. Commun*. **37(4):** 489-498.

Ishimaru, Y., Kim, S., Tsukamoto, T., Oki, H., Kobayashi, T., Watanabe, S., Matsuhashi, S., Takahashi, M., Nakanishi, H., Mori, S. and Nishizawa, N.K. (2007). Mutational reconstructed ferric chelate reductase confers enhanced tolerance in rice to iron deficiency in calcareous soil. *Proceedings of the National Academy of Sciences*, **104**(**18**), 7373-7378.

Ishimaru, Y., Masuda, H., Bashir, K., Inoue, H., Tsukamoto, T., Takahashi, M., Nakanishi, H., Aoki, N., Hirose, T., Ohsugi, R., Nishizawa, N.K. (2010) Rice metal–nicotianamine transporter, OsYSL2, is required for the long-distance transport of iron and manganese. *Plant J*. **62**: 379–390.

Ishimaru, Y., Suzuki, M., Tsukamoto, T., Suzuki, K., Nakazono, M., Kobayashi, T., Wada, Y., Watanabe, S., Matsuhashi, S., Takahashi, M., Nakanishi, H., Mori, S., Nishizawa, N.K. (2006) Rice plants take up iron as an Fe^{3+}-phytosiderophore and as Fe^{2+}. *Plant J.* **45**: 335–346.

Jean, M. L., Schikora, A., Mari, S., Briat, J. F., & Curie, C. (2005). A loss-of-function mutation in AtYSL1 reveals its role in iron and nicotianamine seed loading. *The Plant Journal*, **44**(**5**), 769-782.

Jiang, D., Tang, C., & Zhang, A. (2004). Cluster analysis for gene expression data: a survey. *IEEE Transactions on Knowledge & Data Engineering* (**11**), 1370-1386.

Knight, A. (1977) Long term culture methods for the production of isotopically labelled plant material. *New Phytol*. **79**: 573–582.

Kole, C. (Ed.). (2006). Cereals and millets (Vol. **1**). *Springer Science & Business Media*.

Korshunova, Y. O., Eide, D., Clark, W. G., Guerinot, M. L., & Pakrasi, H. B. (1999). The IRT1 protein from Arabidopsis thaliana is a metal transporter with a broad substrate range. *Plant molecular biology*, **40**(**1**), 37-44.

Li, Y., Dhankher, O. P., Carreira, L., Lee, D., Chen, A., Schroeder, J. I., Balish, R.S. and Meagher, R.B. (2004). Overexpression of phytochelatin synthase in Arabidopsis leads to enhanced arsenic tolerance and cadmium hypersensitivity. *Plant and Cell Physiology*, **45**(**12**), 1787-1797.

Liu, Y., Zhang, J., Li, W., Guo, C., Shu, Y. (2016) *In-silico* identification, phylogeny and expression analysis of expansin superfamily in *Medicago truncatula*. *Biotechnology & Biotechnological Equipment*, **30**:1, 197-203.

Liu, Z., Xin, M., Qin, J., Peng, H., Ni, Z., Yao, Y. and Sun, Q. (2015) Temporal transcriptome profiling reveals expression partitioning of homeologous genes contributing to heat and drought acclimation in wheat (*Triticum aestivum* L.). *BMC Plant Biology* **15**:153.

Lovell, S.C., Davis, I.W., Arendall III, W.B., de Bakker, P.I.W., Word, J.M., Prisant, M.G., Richardson, J.S., Richardson D.C. (2002) Structure validation by Calpha geometry: phi,psi and Cbeta deviation. *Proteins: Structure, Function & Genetics*. **50**: 437-450.

Malviya, N., Gupta, S., Singh, V. K., Yadav, M. K., Bisht, N. C., Sarangi, B. K., & Yadav, D. (2015). Genome wide in silico characterization of Dof gene families of pigeonpea (*Cajanus cajan* (L) Millsp.). *Molecular biology reports*, **42**(**2**), 535-552.

Marchler-Bauer, A., Bo, Y., Han, L., He, J., Lanczycki, C.J., Lu, S., Chitsaz, F., Derbyshire, M.K., Geer, R.C., Gonzales, N.R. and Gwadz, M. (2016). CDD/SPARCLE: functional classification of proteins via subfamily domain architectures. *Nucleic acids research*, **45**(**D1**), D200-D203.

Marchler-Bauer, A., Bryant, S.H. (2004) CD-Search: protein domain annotations on the fly. *Nucleic Acids Res*.**32**(**W**)327-331.

Marchler-Bauer, A., Derbyshire, M. K., Gonzales, N. R., Lu, S., Chitsaz, F., Geer, L. Y., Geer, R.C., He, J., Gwadz, M., Hurwitz, D.I. and Lanczycki, C.J. (2014). CDD: NCBI's conserved domain database. *Nucleic acids research*, **43**(**D1**), D222-D226.

Marchler-Bauer, A., Lu, S., Anderson, J. B., Chitsaz, F., Derbyshire, M. K., DeWeese-Scott, C., Fong, J.H., Geer, L.Y., Geer, R.C., Gonzales, N.R. and Gwadz, M. (2010). CDD: a Conserved Domain Database for the functional annotation of proteins. *Nucleic acids research*, **39**(**suppl_1**), D225-D229.

Marschner, H. (1995) Mineral Nutrition of Higher Plants. Vol. **2nd** ed.. Boston: Academic Press.

Marschner, H., Romheld, V., Kissel, M. (1986) Different strategies in higher plants in mobilization and uptake of iron. *J. Plant Nutr*. **9**: 695-713.

Mihashi, S., & Mori, S. (1989). Characterization of mugineic-acid-Fe transporter in Fe-deficient barley roots using the multi-compartment transport box method. *Biology of Metals*, **2**(**3**), 146-154.

Mishra, B. P., Kumar, R., Mohan, A., Gill, K. S. (2017) Conservation and divergence of Starch Synthase III genes of monocots and dicots. *PLoS ONE* **12**(**12**): e0189303

Morgounov, A., Gómez-Becerra, H.F., Abugalieva, A., Dzhunusova, M., Yessimbekova, M., Muminjanov, H., Zelenskiy, Y., Ozturk, L. and Cakmak, I. (2007). Iron and zinc grain density in common wheat grown in Central Asia. *Euphytica*, **155**(**1-2**), 193-203.

Mori S, Nishizawa N (1987). Methionine as a dominant precursor of phytosiderophores in Graminaceae plants. *Plant Cell Physiol*. **28**:1081-1092.

Mori, S. (1999). Iron acquisition by plants. *Current opinion in plant biology*, **2**(**3**), 250-253.

Murphy K.M., Reeves P.G., Jones S.S. (2008) Relationship between yield and mineral nutrient concentrations in historical and modern spring wheat cultivars. *Euphytica*. **163**:381–390.

Oki, H., Kim, S., Nakanishi, H., Takahashi, M., Yamaguchi, H., Mori, S., & Nishizawa, N. K. (2004). Directed evolution of yeast ferric reductase to produce plants with tolerance to iron deficiency in alkaline soils. *Soil science and plant nutrition*, **50**(**7**), 1159-1165.

Panaud, O., Chen, X. and Mc Couch, S. R. (1996). Development of microsatellite markers and characterization of simple sequence length polymorphism (SSLP) in rice (*Oryza sativa* L.) *Mol. Gen. Genet*.,**252**: 597-607.

Pandey, G. C., Rane, J., Sareen, S., Siwach, P., Singh, N. K., & Tiwari, R. (2013). Molecular investigations on grain filling rate under terminal heat stress in bread wheat (*Triticum aestivum* L.). *African Journal of Biotechnology*, ***12***(**28**).

Pearce, S., Huttly, A.K., Prosser, I.M., Li, Y.D., Vaughan, S.P., Gallova, B., Patil, A., Coghill, J.A., Dubcovsky, J., Hedden, P., Phillips, A.L. (2015) Heterologous expression and transcript analysis of gibberellin biosynthetic genes of grasses reveals novel functionality in the GA3ox family. *BMC Plant Biology*,**15**: 130.

Pearce, S., Tabbita, F., Cantu, D., Buffalo, V., Avni, R., Vazquez-Gross, H., Zhao, R., Conley, C. J., Distelfeld, A., Dubcovksy, J. (2014) Regulation of Zn and Fe transporters by the GPC1 gene during early wheat monocarpic senescence. *BMC Plant Biol*. **14**:368.

Pearson, J.N., Rengel, Z. (1994) Distribution and remobilization of Zn and Mn during grain development in wheat, *J. Exp. Bot*. **45**: 1829–1835.

Peleg, Z., Cakmak, I., Ozturk, L., Yazici, A., Jun, Y., Budak, H., Korol, A.B., Fahima, T., Saranga, Y. (2009) Quantitative trait loci conferring grain mineral nutrient concentrations in durum wheat×wild emmer wheat RIL population, *Theor. Appl. Genet*. **119**: 353–369.

Pfeifer M., Kugler K.G., Sandve S. R., Zhan B. J., Rudi H., Hvidsten T. R., IWGSC, Mayer K. F. and Olsen O. A. (2014) Genome interplay in the grain transcriptome of hexaploid bread wheat. *Science*, **345**: 1250091

Pfeiffer W. H., McClafferty B., (2007) HarvestPlus: breeding crops for better nutrition, *Crop Sci*. **47**: S88–S105.

Ramakrishna W, Dubcovsky J, Park YJ, Busso C, Emberton J, SanMiguel P, Bennetzen JL (2002). Different types and rates of genome evolution detected by comparative sequence analysis of orthologous segments from four cereal genomes. *Genetics*.**162**(**3**):1389-400.

Ramesh, S. A., Shin, R., Eide, D. J., & Schachtman, D. P. (2003). Differential metal selectivity and gene expression of two zinc transporters from rice. *Plant Physiology*, **133**(**1**), 126-134.

Robinson, N. J., Procter, C. M., Connolly, E. L., & Guerinot, M. L. (1999). A ferric-chelate reductase for iron uptake from soils. *Nature*, **397**(**6721**), 694.

Römheld, V., & Marschner, H. (1983). Mechanism of iron uptake by peanut plants: I. FeIII reduction, chelate splitting, and release of phenolics. *Plant Physiology*, **71**(**4**), 949-954.

Sadat, S., Saeid, K. A., Bihamta, M. R., Torabi, S., Salekdeh, S. G. H., & Ayeneh, G. A. L. (2013). Marker assisted selection for heat tolerance in bread wheat. *World Appl. Sci. J*, **21**(**8**), 1181-1189.

Sambrook, J. and Russell, D.W. (2001). Molecular Cloning: A Laboratory Manual, 3rd edn. CSHL Press, Cold Spring Harbour, NY.

Santi, S., & Schmidt, W. (2009). Dissecting iron deficiency-induced proton extrusion in Arabidopsis roots. *New Phytologist*, **183**(**4**), 1072-1084.

Santi, S., Cesco, S., Varanini, Z., & Pinton, R. (2005). Two plasma membrane H+-ATPase genes are differentially expressed in iron-deficient cucumber plants. *Plant Physiology and Biochemistry*, **43**(**3**), 287-292.

Schaaf, G., Erenoglu, B. E., & von Wirén, N. (2004). Physiological and biochemical characterization of metal-phytosiderophore transport in graminaceous species. *Soil Science and Plant Nutrition*, **50**(**7**), 989-995.

Schaaf, G., Honsbein, A., Meda, A. R., Kirchner, S., Wipf, D., & von Wirén, N. (2006). AtIREG2 encodes a tonoplast transport protein involved in iron-dependent nickel detoxification in *Arabidopsis thaliana* roots. *Journal of Biological Chemistry*, **281**(**35**), 25532-25540.

Schmidt, W., Michalke, W., & Schikora, A. (2003). Proton pumping by tomato roots. Effect of Fe deficiency and hormones on the activity and distribution of plasma membrane H+-ATPase in rhizodermal cells. *Plant, Cell & Environment*, **26**(**3**), 361-370.

Schuster, I., Vieira, E. S. N., Silva, G.J., Franco, F. A. and Marchioro, V. S. (2009).Genetic variability in Brazilian wheat cultivars assessed by microsatellite markers. *Genet. Mol. Biol*., **32(3)**: 557-563.

Scott, K. D., Eggler, P., Seaton, G., Rossetto, M., Ablett, E. M., Lee, L. S., & Henry, R. J. (2000). Analysis of SSRs derived from grape ESTs. *Theoretical and applied genetics*, **100**(**5**), 723-726.

Sheoran, O. P, Tonk, D. S., Kaushik, L. S., Hasija, R. C. and Pannu, R. S. (1998). Statistical Software Package for Agricultural Research Workers. *Recent Advances in information theory, Statistics & Computer Applications* by D.S. Hooda & R.C. Hasija Department of Mathematics Statistics, CCS HAU, Hisar (139-143). Available online at http://14.139.232.166/opstat/default.asp.

Starks, T.L., Johnson, P.E. (1985) Techniques for intrinsically labeling wheat with Zn-65, *J. Agric. Food Chem*. **33**: 691–698.

Starks, T.L., Johnson, P.E. (1986) Evaluation of foliar application and stem injection as techniques for intrinsically labeling wheat with copper-65, *J. Agric. Food Chem*. **34**: 23–26.

Suzuki, M., Takahashi, M., Tsukamoto, T., Watanabe, S., Matsuhashi, S., Yazaki, J., Kishimoto, N., Kikuchi, S., Nakanishi, H., Mori, S., Nishizawa, N.K. (2006) Biosynthesis and secretion of mugineic acid family phytosiderophores in zinc-deficient barley, *Plant J*. **48**: 85–97.

Suzuki, M., Tsukamoto, T., Inoue, H., Watanabe, S., Matsuhashi, S., Takahashi, M., Nakanishi, H., Mori, S., Nishizawa, N.K. (2008) Deoxymugineic acid increases Zn translocation in Zn-deficient rice plants, *Plant Mol. Biol*. **66**: 609–617.

Takagi, S. I. (1976). Naturally occurring iron-chelating compounds in oat-and rice-root washings: I. Activity measurement and preliminary characterization. *Soil science and plant nutrition*, **22**(**4**), 423-433.

Takagi, S., Nomoto, K., Takemoto, T. (1984) Physiological aspect of mugineic acid, a possible phytosiderophore of graminaceous plants. *J. Plant Nutr*. **7**: 469-477.

Takahashi, M., Nakanishi, H., Kawasaki, S., Nishizawa, N. K., & Mori, S. (2001). Enhanced tolerance of rice to low iron availability in alkaline soils using barley nicotianamine aminotransferase genes. *Nature biotechnology*, **19**(**5**), 466.

Ueno, D., Rombola, A.D., Iwashita, T., Nomoto, K., Ma, J.F. (2007). Identification of two novel phytosiderophores secreted by perennial grasses. *New Phytol*. **174**:304-310.

Varotto, C., Maiwald, D., Pesaresi, P., Jahns, P., Salamini, F., & Leister, D. (2002). The metal ion transporter IRT1 is necessary for iron homeostasis and efficient photosynthesis in *Arabidopsis thaliana*. *The Plant Journal*, **31**(**5**), 589-599.

Vasconcelos, M., Eckert, H., Arahana, V., Graef, G., Grusak, M. A., & Clemente, T. (2006). Molecular and phenotypic characterization of transgenic soybean expressing the Arabidopsis ferric chelate reductase gene, FRO2. *Planta*, **224**(**5**), 1116-1128.

Vert, G., Grotz, N., Dédaldéchamp, F., Gaymard, F., Guerinot, M. L., Briat, J. F., & Curie, C. (2002). IRT1, an Arabidopsis transporter essential for iron uptake from the soil and for plant growth. *The Plant Cell*, **14**(**6**), 1223-1233.

Walker, E. L., Connolly, E. L. (2008) Time to pump iron: iron-deficiency-signaling mechanisms of higher plants, *Curr. Opin. Plant Biol*. **11**: 530–535.

Wallace, A. (1991) Rational approaches to control of iron deficiency other than plant breeding and choice of resistant cultivars. *Plant Soil* **130**:281-288.

Wang, H. Y., Wei Y. M., Yan Z. H. and Zheng Y. L. (2007). EST-SSR DNA polymorphism in durum wheat (*Triticum durum* L.) collections. *J. Appl. Genet*. **40**: 365-369.

Ward, J. H., Jr. (1963). Hierarchical Grouping to Optimize an Objective Function. *Journal of the American Statistical Association*, **58:** 236–244.

Wass, M. N., Kelley, L. A., & Sternberg, M. J. (2010). 3DLigandSite: predicting ligand-binding sites using similar structures. *Nucleic acids research*, **38**(**suppl_2**), W469-W473.

Waters B. M., Sankaran R. P. (2011) Moving micronutrients from the soil to the seeds: Genes and physiological processes from a biofortification perspective. *Plant Science*, **180**: 562–574.

Waters, B. M., Chu, H. H., DiDonato, R. J., Roberts, L. A., Eisley, R. B., Lahner, B., Salt, D.E. and Walker, E.L. (2006). Mutations in Arabidopsis yellow stripe-like1 and yellow stripe-like3 reveal their roles in metal ion homeostasis and loading of metal ions in seeds. *Plant Physiology*, **141**(**4**), 1446-1458.

Waters, B. M., Lucena, C., Romera, F. J., Jester, G. G., Wynn, A. N., Rojas, C. L., Alcántara, E. and Pérez-Vicente, R. (2007). Ethylene involvement in the regulation of the H+-ATPase CsHA1 gene and of the new isolated ferric

reductase CsFRO1 and iron transporter CsIRT1 genes in cucumber plants. *Plant Physiology and Biochemistry*, **45**(**5**), 293-301.

White, P.J., Broadley M.R. (2009) Biofortification of crops with seven mineral elements often lacking in human diets: iron, zinc, copper, calcium, magnesium, selenium and iodine, *New Phytol*. **182**: 49–84.

Yordem, B. K., Conte, S. S., Ma, J. F., Yokosho, K., Vasques, K. A., Gopalsamy, S. N., & Walker, E. L. (2011). *Brachypodium distachyon* as a new model system for understanding iron homeostasis in grasses: phylogenetic and expression analysis of Yellow Stripe-Like (YSL) transporters. *Annals of botany*, **108**(**5**), 821-833.

Zadoks, J.C., Chang, T.T., Konzak, C.F. (1974) A decimal code for the growth stages of cereals. *Weed Research* **14**: 415-21.

Zhang, X., Liu, D., Jiang, W., Guo, X., Yang, W., Sun, J., Ling, H. and Zhang, A. (2011). PCR-based isolation and identification of full-length low-molecular-weight glutenin subunit genes in bread wheat (*Triticum aestivum* L.). *Theoretical and Applied Genetics*, **123**(**8**), 1293-1305.

◈◈◈

APPENDICES

APPENDIX A

Table A.1: Developmental Timecourse In Five Tissues Expression Data Table

Gene	Grain			Leaf			Root			Spike			Stem		
	Z71	**Z75**	**Z85**	**Z10**	**Z23**	**Z71**	**Z10**	**Z13**	**Z39**	**Z32**	**Z39**	**Z65**	**Z30**	**Z32**	**Z65**
TaYSL2-6A	0.38	0.37	1.66	0.41	0.38	0.25	0.19	0.52	0.39	0.65	0.62	0.59	0.5	0.41	0.57
TaYSL2-6B	1.69	4.19	2.93	0.47	0.33	0.28	0.09	0.29	0.23	0.17	0.24	1.11	0.36	0.34	0.25
TaYSL2-6D	1.06	0.5	6.62	0.25	0.86	2.15	1.39	1.31	1.34	1.04	0.8	1.58	0.48	1.01	3.46
TaYSL2-6A SE	0.02	0.02	0	0.08	0.13	0.04	0.02	0.12	0.04	0.09	0.06	0.02	0.02	0.1	0.11
TaYSL2-6B SE	0.08	0.11	0.24	0.04	0.05	0.04	0.02	0.16	0.21	0.05	0	0.04	0.08	0.17	0.1
TaYSL2-6D SE	0.08	0	0.07	0.07	0.08	0.04	0.04	0.04	0.35	0.13	0.02	0.14	0.07	0.01	0.26

Table A.2: Grain Layers Expression Data Table

Gene	Endosperm	Inner Pericarp	Outer Pericarp
TaYSL2-6A	0.33	1.94	0.22
TaYSL2-6B	10.57	7.13	7.03
TaYSL2-6D	2.23	2.31	0.89
TaYSL2-6A SE	0.33	0.34	0.22
TaYSL2-6B SE	1.41	0.46	1.46
TaYSL2-6D SE	0.3	0.27	0.31

Table A.3: Grain Layer Developmental Timecourse Expression Data Table

Gene	10DPA	20DPA				30DPA	
	Whole Endosperm	Whole Endosperm	Starchy Endosperm	Transfer Cells	Aleurone	Starchy Endosperm	Aleurone + Endosperm
TaYSL2-6A	0.64	1.31	0.62	0.91	1.26	0.84	0.98
TaYSL2-6B	4.52	4.94	4.99	4.96	2.82	3.36	4
TaYSL2-6D	0.92	0.74	0.32	2.17	0.52	0.48	1.34
TaYSL2-6A SE	0.05	0.23	0.17	0.14	0.16	0.08	0.2
TaYSL2-6B SE	0.75	0.56	0.11	0.17	0.19	0.27	0.95
TaYSL2-6D SE	0.17	0.15	0.06	0.31	0.09	0.12	0.39

Table A.4: Senescing Leaves Timecourse Expression Data Table

Gene	HD	12DAA	22DAA
TaYSL2-6A	1.71	2.76	1.96
TaYSL2-6B	2.35	3.19	2.07
TaYSL2-6D	No Data	No Data	No Data
TaYSL2-6A SE	0.15	0.45	0.22
TaYSL2-6B SE	0.41	0.71	0.35
TaYSL2-6D SE	No Data	No Data	No Data

Table A.5: Drought And Heat Expression Data Table

Gene	Control	Drought		Heat		Drought + heat	
		1hr	6hr	1hr	6hr	1hr	6hr
TaYSL2-6A	0.4	0.48	2.48	0.19	0.15	0.2	0.23
TaYSL2-6B	0.21	0.22	0.58	0.68	1.04	1.41	0.27
TaYSL2-6D	1.58	1.69	2.25	1.61	1.66	2.86	1.24
TaYSL2-6A SE	0.11	0.01	0.54	0.09	0.06	0.03	0.11
TaYSL2-6B SE	0	0.05	0.08	0.11	0.01	0.11	0.05
TaYSL2-6D SE	0.15	0.11	0.09	0.22	0.09	0.11	0.06

APPENDIX B

TaYSL genes	IWGSC annotation ID	Location	Orientation	mRNA Length	Length of Protein
TaYSL1	TraesCS3B02G191300	**3B** : 204281977-204282260	Forward	2494	759aa
	TraesCS3A02G160700	**3A** : 161,446,234-161,448,924	Forward	2331	706aa
	TraesCS3D02G167900	**3D** : 142,476,504-142,479,067	Forward	2192	704aa
TaYSL2	TraesCS6D02G223000	**6D** : 315,175,504-315,178,824	Reverse	2459	673aa
	TraesCS6A02G240800	**6A** : 452,097,169-452,099,442	Reverse	1425	474aa
	TraesCS6B02G283900	**6B** : 512,234,269-512,237,479	Forward	2381	673aa
TaYSL3	TraesCS1A02G415700	**1A** : 574,472,319-574,483,821	Reverse	2349	782aa
	TraesCS1D02G423000	**1D** : 478,226,005-478,229,457	Reverse	2458	676aa
	TraesCS1B02G445700	**1B** : 665,794,896-665,798,459	Reverse	2551	679aa
TaYSL4	TraesCS5B02G453100	**5B** : 626,009,702-626,038,394	Forward	1548	515aa
TaYSL5	TraesCS2D02G283600	**2D** : 357,702,680-357,707,848	Forward	2569	690aa
	TraesCS2A02G284900	**2A** : 478,763,438-478,768,168	Forward	2774	482aa
	TraesCS2B02G302000	**2B** : 425,354,199-425,360,724	Forward	1893	630aa
TaYSL6	TraesCS2A02G083400	**2A** : 38,309,364-38,314,205	Reverse	2031	676aa
	TraesCS2B02G097400	**2B** : 57,664,450-57,670,210	Reverse	2322	699aa
	TraesCS2D02G081000	**2D** : 34,988,005-34,992,393	Reverse	2283	670aa
TaYSL7	TraesCS6A02G042900	**6A** : 22,546,879-22,549,307	Forward	2429	692aa
	TraesCS6D02G049500	**6D** : 24,022,336-24,024,657	Forward	2322	692aa
	TraesCS6B02G058700	**6B** : 38,925,480-38,927,813	Forward	2334	692aa
TaYSL8	TraesCS6A02G043100	**6A** : 22,642,270-22,644,707	Forward	2353	703aa
	TraesCS6B02G059100	**6B** : 39,061,733-39,064,522	Reverse	2683	704aa
	TraesCS6D02G049900	**6D** : 24,198,018-24,200,818	Reverse	2676	703aa

TaYSL genes	IWGSC annotation ID	Location	Orientation	mRNA Length	Length of Protein
TaYSL9	TraesCS2D02G387700	**2D** : 493,077,613-493,082,231	Reverse	2082	693aa
	TraesCS2A02G391000	**2A** : 640,706,410-640,710,776	Forward	2274	691aa
	TraesCS2B02G408000	**2B** : 579,685,736-579,690,421	Reverse	2128	644aa
TaYSL10	TraesCS5A02G531800	**5A** : 689,896,911-689,912,314	Forward	2001	666aa
TaYSL11	TraesCS7A02G420300	**7A** : 611,728,599-611,734,540	Forward	1796	511aa
TaYSL12	TraesCS2A02G553300	**2A** : 758,880,869-758,883,546	Forward	2142	687aa
	TraesCS2D02G554800	**2D** : 629,074,075-629,080,289	Forward	2147	687aa
	TraesCS2B02G585300	**2B** : 772,115,726-772,121,977	Reverse	2201	687aa
TaYSL13	TraesCS2A02G376700	**2A** : 619,201,967-619,206,852	Reverse	2381	710aa
	TraesCS2B02G393600	**2B** : 557,990,059-557,993,624	Forward	2352	711aa
	TraesCS2D02G373100	**2D** : 476,837,236-476,840,831	Reverse	2305	706aa
TaYSL14	TraesCS2B02G394400	**2B** : 559,188,330-559,193,538	Reverse	2699	718aa
	TraesCS2D02G373800	**2D** : 477,259,990-477,265,004	Reverse	2655	721aa
	TraesCS2A02G377200	**2A** : 619,624,164-619,628,174	Reverse	2032	592aa
TaYSL15	TraesCS6A02G221100	**6A** : 410,866,184-410,868,847	Forward	2350	673aa
	TraesCS6D02G214100	**6D** : 304,294,879-304,297,213	Reverse	2037	678aa
TaYSL16	TraesCS2A02G377400	**2A** : 619,756,474-619,758,222	Forward	1383	460aa
	TraesCS2B02G394500	**2B** : 559,306,002-559,310,070	Forward	2628	720aa
	TraesCS2D02G373900	**2D** : 477,269,782-477,273,859	Forward	2654	717aa
TaYSL17	TraesCS2B02G394600	**2B** : 559,415,984-559,419,253	Forward	2628	723aa
	TraesCS2D02G374000	**2D** : 477,393,890-477,397,124	Forward	2447	723aa
	TraesCS2A02G377600	**2A** : 619,764,872-619,768,327	Forward	2689	724aa

TaYSL genes	IWGSC annotation ID	Location	Orientation	mRNA Length	Length of Protein
TaYSL18	TraesCS6B02G262400	**6B** : 472,609,626-472,614,350	Reverse	2684	713aa
	TraesCS6A02G220900	**6A** : 410,579,641-410,584,143	Reverse	2555	711aa
	TraesCS6D02G214300	**6D** : 304,735,344-304,740,069	Forward	2770	711aa
TaYSL19	TraesCS6D02G223100	**6D** : 315,190,693-315,194,094	Reverse	2423	675aa
	TraesCS6A02G240900	**6A** : 452,264,023-452,267,427	Reverse	2386	678aa
	TraesCS6B02G283800	**6B** : 512,213,571-512,219,278	Forward	2498	678aa
TaYSL20	TraesCS7A02G420700	**7A** : 611,910,850-611,918,357	Forward	1716	571aa
TaYSL21	TraesCS2A02G390800	**2A** : 640,269,702-640,273,246	Reverse	2514	702aa
	TraesCS2B02G408500	**2B** : 581,467,942-581,471,391	Reverse	2494	705aa
	TraesCS2D02G387800	**2D** : 493,173,893-493,177,351	Reverse	2400	702aa
TaYSL22	TraesCS6A02G042900	**6A** : 22,546,879-22,549,307	Forward	2429	692aa
	TraesCS6B02G058700	**6B** : 38,925,480-38,927,813	Forward	2334	692aa
	TraesCS6D02G049500	**6D** : 24,022,336-24,024,657	Forward	2322	692aa
TaYSL23	TraesCS3A02G349500	**3A** : 598,548,699-598,551,792	Reverse	2552	681aa
	TraesCS3B02G382100	**3B** : 602,302,204-602,305,152	Reverse	2411	681aa
	TraesCS3D02G343500	**3D** : 455,863,900-455,866,801	Reverse	2390	681aa
TaYSL24	TraesCS2A02G427400	**2A** : 680,261,404-680,263,818	Forward	2334	696aa
	TraesCS2B02G447900	**2B** : 640,599,009-640,608,487	Forward	2138	677aa
	TraesCS2D02G425500	**2D** : 537,928,523-537,930,921	Forward	2322	693aa

APPENDIX C

Fig. C.1: Un-rooted Phyllogenetic tree of TaYSL and OsYSL proteins

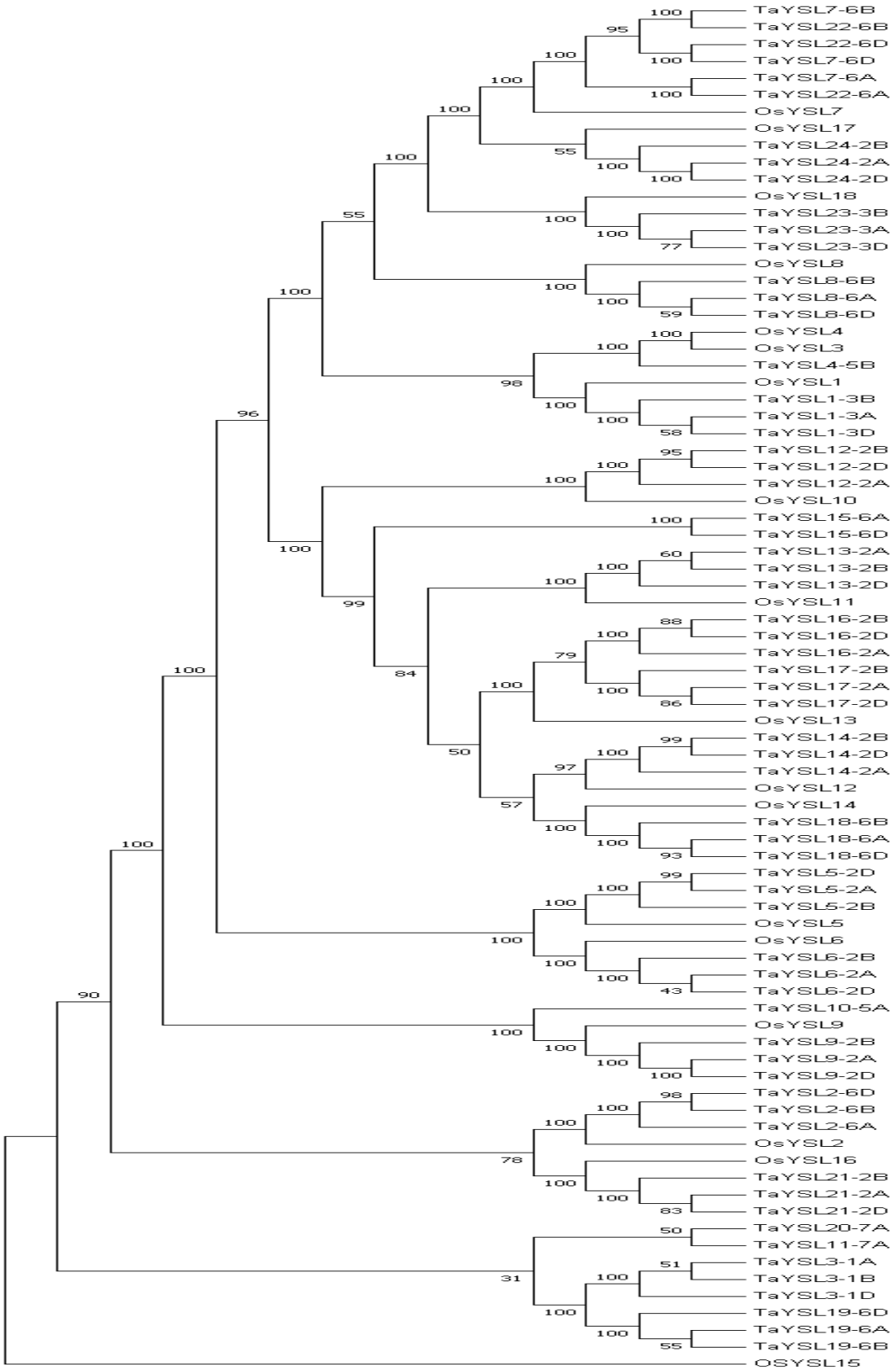

Fig. C.2: Phyllogenetic tree of TaYSL and OsYSL proteins in form of radiation

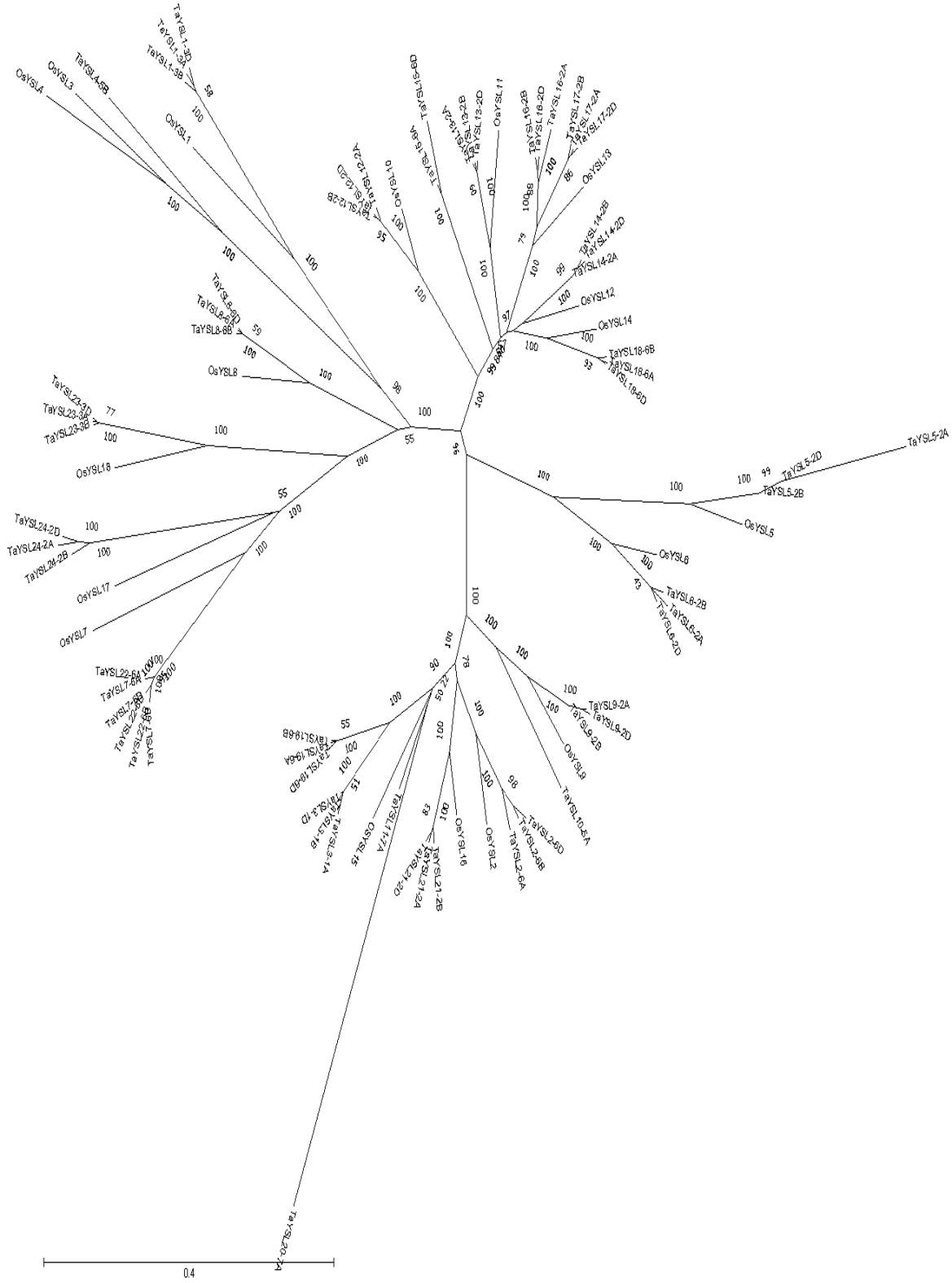

tree.

Note: The Neighbour-joining phyllogenetic tree was computed using MEGA 7.0 software UPGMA method with poisson correction and pair wise deletion using 1000 bootstraps.

Appendix D

Primer TaYSL2-6Ai		
Sl. No.	Genotypes	length
M	1 Kb ladder	
1	CRP 7	1156.5
2	CRP 15	1156.5
3	CRP 18	1164.22
4	CRP 21	1186.38
5	CRP 33	1164.22
6	CRP 37	1164.22
7	CRP 45	1114.20
8	CRP 46	1164.22
9	CRP 48	1171.86
10	CRP 50	1114.20
11	CRP 51	1056.5
12	CRP 52	1056.5

Primer TaYSL2-6Ai		
Sl. No.	Genotypes	Length
M	1 Kb ladder	
1	CRP 7	1346.66
2	CRP 15	1337.90
3	CRP 18	1372.54
4	CRP 21	1337.90
5	CRP 33	1372.54
6	CRP 37	1363.68
7	CRP 45	1390.19
8	CRP 46	1399.14
9	CRP 48	1390.19
10	CRP 50	1426.50
11	CRP 51	1454.65
12	CRP 52	1454.65

Primer TaYSL2-6Aiii		
Sl. No.	Genotypes	Length
M	1 Kb ladder	
1	CRP 7	698.43
2	CRP 15	768.80
3	CRP 18	768.80
4	CRP 21	768.80
5	CRP 33	814.29
6	CRP 37	800.81
7	CRP 45	814.29
8	CRP 46	800.81
9	CRP 48	814.29
10	CRP 50	814.29
11	CRP 51	828.10
12	CRP 52	768.80

Primer TaYSL2-6Bi		
Sl. No.	Genotypes	Length
M	1 Kb ladder	
1	CRP 7	1465.32
2	CRP 15	1513.12
3	CRP 18	1480.05
4	CRP 21	1420
5	CRP 33	1420
6	CRP 37	1465.32
7	CRP 45	1465.32
8	CRP 46	1435
9	CRP 48	1435
10	CRP 50	1465.32
11	CRP 51	1420
12	CRP 52	1435

Primer TaYSL2-6Bii		
Sl. No.	Genotypes	Length
M	1 Kb ladder	
1	CRP 7	1302.6
2	CRP 15	1364.82
3	CRP 18	1411.26
4	CRP 21	1364.82
5	CRP 33	1328.71
6	CRP 37	1319.54
7	CRP 45	1364.82
8	CRP 46	1328.71
9	CRP 48	1319.54
10	CRP 50	1319.54
11	CRP 51	1355.55
12	CRP 52	1284.49

Primer TaYSL2-6Biii		
Sl. No.	Genotypes	Length
M	1 Kb ladder	
1	CRP 7	753.84
2	CRP 15	786.07
3	CRP 18	786.07
4	CRP 21	786.07
5	CRP 33	799.13
6	CRP 37	791.81
7	CRP 45	805.10
8	CRP 46	805.10
9	CRP 48	797.68
10	CRP 50	797.68
11	CRP 51	797.68
12	CRP 52	797.68

Primer TaYSL2-6Di		
Sl. No.	Genotypes	Length
M	1 Kb ladder	
1	CRP 7	1381.83
2	CRP 15	1381.83
3	CRP 18	1428.55
4	CRP 21	1399.72
5	CRP 33	1428.55
6	CRP 37	1441.09
7	CRP 45	1441.09
8	CRP 46	1417.96
9	CRP 48	1389.14
10	CRP 50	1389.14
11	CRP 51	1455.53
12	CRP 52	1455.53

Primer TaYSL2-6Dii		
Sl. No.	Genotypes	Length
M	1 Kb ladder	
1	CRP 7	1283.41
2	CRP 15	1324.06
3	CRP 18	1324.06
4	CRP 21	1283.41
5	CRP 33	1324.06
6	CRP 37	1366.01
7	CRP 45	1283.41
8	CRP 46	1283.41
9	CRP 48	1283.41
10	CRP 50	1324.06
11	CRP 51	1283.41
12	CRP 52	1243.99

Primer TaYSL2-6Diii		
Sl. No.	Genotypes	Length
M	1 Kb ladder	
1	CRP 7	628.78
2	CRP 15	639.96
3	CRP 18	639.96
4	CRP 21	639.96
5	CRP 33	651.35
6	CRP 37	651.35
7	CRP 45	651.35
8	CRP 46	651.35
9	CRP 48	651.35
10	CRP 50	651.35
11	CRP 51	639.96
12	CRP 52	651.35

Primer TaYSL2-S1		
Sl. No.	Genotypes	Length
M	50 bp ladder	
1	CRP 7	215
2	CRP 15	221
3	CRP 18	232
4	CRP 21	242
5	CRP 33	244
6	CRP 37	244
7	CRP 45	244
8	CRP 46	246
9	CRP 48	238.5
10	CRP 50	238.5
11	CRP 51	248.5
12	CRP 52	246

Primer TaYSL2-S2		
Sl. No.	Genotypes	Length
M	50 bp ladder	
1	CRP 7	178
2	CRP 15	176
3	CRP 18	179
4	CRP 21	177
5	CRP 33	176
6	CRP 37	174
7	CRP 45	176
8	CRP 46	180
9	CRP 48	179
10	CRP 50	180
11	CRP 51	182
12	CRP 52	183